Bethe Lattice Spin Glass: The Effects of a Ferromagnetic Bias and External Fields. I. Bifurcation Analysis

J. M. Carlson,[1] **J. T. Chayes,**[2] **L. Chayes,**[2] **J. P. Sethna,**[3] **and D. J. Thouless**[4]

We present a rigorous analysis of the $\pm J$ Ising spin-glass model on the Bethe lattice with fixed uncorrelated boundary conditions. Phase diagrams are derived as a function of temperature vs. concentration of ferromagnetic bonds and, for a symmetric distribution of bonds, external field vs. temperature. In this part we characterize the bulk ordered phases using bifurcation theory: we prove the existence of a distribution of single-site magnetizations far inside the lattice which is stable with respect to changes in the boundary conditions.

1. INTRODUCTION

In this and the companion paper[1] we analyze the $\pm J$ Ising spin-glass problem on the Bethe lattice with fixed uncorrelated boundary conditions. The symmetric case (i.e., when half of the bonds are ferromagnetic) in zero field was analyzed previously in ref. 2, where it was shown that there is a spin-glass transition at temperature T_G above which the system is paramagnetic and below which the Edwards–Anderson order parameter is strictly positive. In this work we extend the phase diagram to include varying fractions λ of ferromagnetic bonds, and, in the symmetric case ($\lambda = 1/2$), finite external fields. Our principal results are illustrated in Figs. 1 and 2.

---

[1] Institute for Theoretical Physics, University of California, Santa Barbara, California 93106.
[2] Department of Mathematics, University of California, Los Angeles, California 90024.
[3] Department of Physics, Cornell University, Ithaca, New York 14853.
[4] Department of Physics, University of Washington, Seattle, Washington 98195.
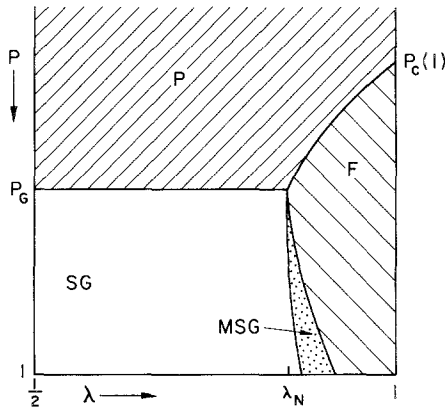
Fig. 1.   Phase diagram for the Bethe lattice spin glass, plotted as a function of $p = \tanh(J/kT)$ and the fraction λ of ferromagnetic bonds. At high temperatures, the system is paramagnetic. As the temperature decreases, there is a transition to either a spin-glass or a ferromagnetic phase, depending on λ. Between these phases there is an intermediate magnetized spin-glass phase (MSG). Like the ferromagnet, the MSG phase has nonzero net magnetization, but it also has glassy susceptibilities. The phase diagram for $\lambda < 1/2$ can be obtained by reflection across the line $\lambda = 1/2$, replacing F and MSG with phases which have long-range antiferromagnetic order.

1.1. Historical Background

Spin glasses are magnetic systems characterized by randomness and frustration: see ref. 3 for a review of theoretical and experimental progress. The Hamiltonian typically used to describe spin glasses is the Edwards–Anderson Hamiltonian[4]

$$H_{EA} = - \sum_{\langle i, j \rangle} J_{i,j} \sigma_i \sigma_j \tag{1}$$
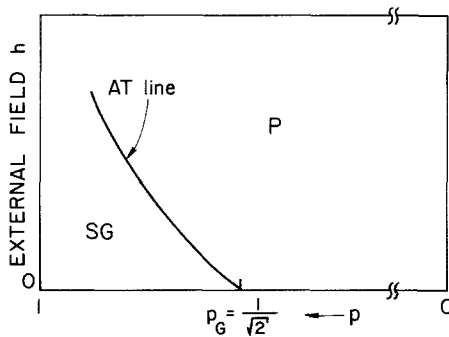

Fig. 2.   De Almeida–Thouless line. On the Bethe lattice the spin-glass transition persists in the presence of an external field. The asymptotic form of the AT line is $h(T) \sim |p - p_G|^{3/2}$, and the critical exponent for the Edwards–Anderson susceptibility is $\gamma = 1$.
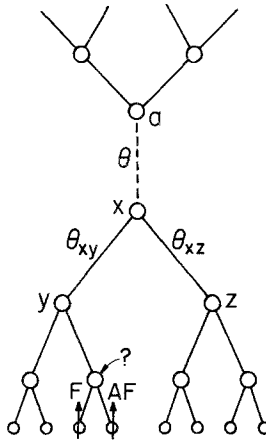
Fig. 3. A Bethe lattice with forward branching ratio 2. Frustration is associated with the fixed spins on the boundary. In the full-space lattice the dashed bond connecting x and a is present, whereas in the half-space lattice it is removed, and x is the origin.

where the bonds $J_{i,j}$ are quenched and independently distributed, and the sum is over nearest neighbor pairs on a regular lattice. Frustration (i.e., the fact that all interaction energies cannot be minimized simultaneously) makes this problem extremely difficult to analyze in finite dimensions. In an effort to develop an understanding of some of the basic properties of this model, many people have turned to mean field theory.

To obtain mean field results for spin systems, there are two special models which are often studied, and for which certain exact results can be obtained. The first model corresponds to an infinite-range interaction, and the second corresponds to an infinite-dimensional lattice,[5] the Bethe lattice illustrated in Fig. 3. For many other systems (e.g., ferromagnets) the phase structures of these two models agree with each other[6] and with those of other mean field approaches.

The infinite-range model was introduced for spin glasses by Sherrington and Kirkpatrick (SK).[5] In that model every spin interacts equally with every other spin. Using the replica method, Sherrington and Kirkpatrick obtained a solution. Later work by de Almeida and Thouless[6] revealed that the SK solution was unstable, and that the

[5] The identification of the Bethe lattice with an infinite-dimensional lattice is geometric. The Bethe lattice cannot be embedded in a finite-dimensional lattice; alternatively, the number of steps that can be reached in an N-step walk ($\sim N^d$ in d dimensions) grows exponentially with N.

[6] Specifically, the phase diagrams and critical exponents agree, although the numbers of states clearly do not.

correct solution should have a spin-glass phase in the presence of an external magnetic field. The presumably correct solution to the SK model (the "replica-symmetry-broken" solution) was obtained by Parisi.[7] However, the methods which were used were quite unconventional, and the relationship to finite-dimensional spin glasses remains unclear.

Compared to the infinite-range model, analysis on the Bethe lattice is more straightforward. In particular, the Bethe lattice has two main advantages over the SK model: (1) the interactions are short range; (2) the distribution of single-site magnetizations can be described by exact recursion relations. On the other hand, the spin-glass model is more difficult to formulate on the Bethe lattice because the boundary spins are a finite fraction of the lattice. Consequently, different boundary conditions can lead to different behaviors. For example, free boundary conditions lead to uninteresting behavior. Because there are no loops on the Bethe lattice, with free boundary conditions it is possible to start at the center of the lattice and minimize every interaction energy simultaneously. In contrast, when the boundary conditions are fixed, the above scheme results in an energy cost which scales with the volume due to "broken bonds" at the boundary. Thus, in the Bethe lattice spin glass, fixed boundary conditions are responsible for frustration. For a more detailed discussion of the role of boundary conditions see Section 2.

Early work on spin glass models on the Bethe lattice was done by groups in Tohoku[8] and Tokyo,[9] who derived recursion relations for the Ising spin-glass model and found a spin-glass transition temperature. Neither group directly addressed the question of boundary conditions. Nonetheless, using a self-consistent probabilistic approach, the Tohoku group obtained paramagnetic, ferromagnetic, and (nonmagnetized) spin-glass phases in accord with those established here. On the other hand, the Tokyo group of Ueno and Oguchi concluded that for the same model the spin-glass phase and the ferromagnetic phase were preempted by a random ordered phase, which is now understood to be the consequence of "unfrustrating" boundary conditions.

Bowman and Levin[10] examined the entropy of the spin-glass state. At low temperatures they found that when the boundary was included (i.e., a Cayley tree) the entropy was nonnegative at low temperatures, whereas when the boundary was ignored, the entropy became negative at low temperatures for sufficiently large coordination number. (The fact that the replica-symmetric solution to the infinite-range model had negative entropy was the signal that it was an unphysical saddle-point self-consistent solution. On the Bethe lattice, the effects of the boundary make the analogous solution correct.)

Finally, there is the work of ref. 11 and of ref. 2, of which this work is

a continuation, and ref. 12, which summarizes some of the results which will be presented here. In ref. 2 the recursion relation was derived and analyzed rigorously for a symmetric distribution of bonds. More recently, Kwon and Thouless[13] studied the zero-temperature recursion relation for symmetric and asymmetric bond distributions. We incorporate their results in our phase diagram (Fig. 1).

The results described above and those obtained in this work are in qualitative agreement with certain experiments.[7] For our work, the most relevant aspects of the temperature vs. concentration phase diagrams are reentrance (i.e., at certain fixed concentrations, as the temperature is lowered, there is a series of phase transitions from a disordered paramagnetic phase, to a ferromagnetic phase which has long-range magnetic ordering, to a spin glass which has no long-range magnetic order),[14–16] and the existence of an intermediate magnetized spin-glass phase.[17,18] The most relevant aspect of the temperature vs. field phase diagram is the existence of a phase transition in nonzero external field.[19,20] For a general discussion of experiments see ref. 3; for a discussion of experiments specifically related to this work see ref. 21.

1.2. Methods, Results, and Organization

In Section 2 we introduce the recursion relation for single-site magnetizations, which was derived rigorously (but rather incomprehensibly) in ref. 2. (A simpler, but equally rigorous derivation is given in Appendix A.) Most of the rest of this paper is devoted to the study of the solutions of this recursion relation as a function of temperature and fraction λ of ferromagnetic bonds. We use probabilistic methods and bifurcation theory to derive the phase boundaries illustrated in Fig. 1. The results we obtain are rigorous throughout the paramagnetic phase and in a neighborhood below the critical line.

In Section 3 we determine the paramagnetic phase boundaries; a proof of global stability of the paramagnetic fixed point is relegated to Appendix B. Properties of the spin-glass phase are studied in Section 4. Somewhat surprisingly, we find that in a neighborhood of the phase boundary the character of the spin-glass phase remains the same as in the symmetric case. For example, the distribution of single-site magnetizations is independent of λ. The ferromagnetic phase is analyzed in Section 5. While this phase is less controversial, the bifurcation analysis is more challenging here than at the spin-glass transition. In order to describe the ferromagnetic state, we construct a continuous family of complete sets of

---

[7] We caution the reader that the results described here are not found in all experiments.

analytic functions, which, unlike the spin-glass solution, varies with the thermodynamic parameters.

In Section 6 we analyze the multicritical point (p_G, λ_N) where the spin-glass and ferromagnetic phase boundaries intersect. While the spin-glass and ferromagnetic transitions are regular critical points with a single degree of freedom giving rise to a codimension-one bifurcation, at the multicritical point there are two degrees of freedom, giving rise to a codimension-two bifurcation.

The magnetized spin-glass (MSG) phase is discussed in Sections 6 of this paper and Section 2 of the companion paper. The phase boundary between the spin-glass phase and the neighboring magnetized phase (Section 6) is determined by the instability of the symmetric spin-glass density with respect to small perturbations in the mean. Because this phase boundary bends to the right of the line $\lambda = \lambda_N$, the spin-glass phase is reentrant. The ferromagnetic–MSG phase boundary (ref. 1, Section 2) is determined by divergence of the Edwards–Anderson susceptibility

$$\chi_{\mathrm{EA}} = \frac{1}{N^2} \sum_{i,j} \overline{\langle \sigma_i \sigma_j \rangle^2 - \langle \sigma_i \rangle^2 \langle \sigma_j \rangle^2}$$

where angle brackets denote the thermal average, the overbar denotes the average over quenched bonds (i.e., the disorder average), and N is the number of spins in the system. The fact that χ_{EA} diverges before we cross the zero-magnetization phase boundary establishes the existence of an intermediate magnetized spin-glass phase.

In Section 3 of the companion paper we calculate χ_{EA} for a symmetric distribution of couplings and a nonzero external field. We find that χ_{EA} diverges crossing a curve $h(T)$ which is the de Almeida–Thouless line (see Fig. 2). Thus the spin-glass transition persists in the presence of an external field.

Finally, in Section 4 of the companion paper we end with a summary of our results, and a discussion of the relationship between the Bethe lattice spin glass and the infinite-range model. We show that in the formal limit where the coordination number of the lattice tends to infinity, the recursion relation becomes the so-called SK equation.[5] The solution of this equation is the replica-symmetric solution of the SK model. Thus, at least in a formal sense, the correct solution on the Bethe lattice is analogous to the (unphysical) replica-symmetric solution of the infinite-range model.

2. THE RECURSION RELATION AND BOUNDARY CONDITIONS

The treelike structure of the Bethe lattice allows us to derive a recursion relation which gives properties on a given level $n + 1$ in terms of the

same properties on level n. Here we will work on the half-space tree; a simple formula given in Appendix A relates half-space quantities to the corresponding quantities on the full tree. The lattice with forward branching ratio two is illustrated in Fig. 3. As previously stated, the Hamiltonian for this model is the Edwards–Anderson Hamiltonian,[4]

$$H_{\mathrm{EA}} = -\sum_{\langle i,j \rangle} J_{i,j} \sigma_i \sigma_j - \sum_i H_i \sigma_i \tag{2}$$

where the first sum is over nearest neighbor pairs, and the second sum is over sites. The bonds are of equal strength, and distributed, independently, according to $J_{i,j} = \theta_{i,j} J$, where

$$\theta_{i,j} = \begin{cases} +1 & \text{with prob. } \lambda \\ -1 & \text{with prob. } 1 - \lambda \end{cases} \tag{3}$$

The external fields H_i may or may not be uniform.

Our recursion relation is an equation relating the single-site magnetizations $\langle \sigma_x \rangle_u$ on different levels of the tree. Here $\langle \sigma_x \rangle_u$ is the thermal expectation of the Ising spin σ_x in the *uncoupled* system in which x is viewed as the root of its own tree—i.e., the bond connecting x to the site above it on the isotropic tree has been severed. (See Fig. 3.) Occasionally we will refer to $\langle \sigma_x \rangle_u$ as a "half-space" magnetization, since x is uncoupled from the upper portion of the full lattice. Note that for fixed boundary conditions, $\langle \sigma_x \rangle_u$ is a function (i.e., a random variable) depending on the coupling realization. In our formulation, the thermal expectation is taken in a system in which each site is viewed as the root of its own tree.

In ref. 2 it was shown that in the absence of external fields, if $\langle \sigma_x \rangle_u$ is the value of the magnetization at the origin, then

$$\langle \sigma_x \rangle_u = \frac{p(\theta_{x,y} \langle \sigma_y \rangle_u + \theta_{x,z} \langle \sigma_z \rangle_u)}{1 + p^2 \theta_{x,y} \theta_{x,y} \langle \sigma_y \rangle_u \langle \sigma_z \rangle_u} \tag{4}$$

where $p = \tanh(J/k_{\mathrm{B}} T)$, and $\langle \sigma_y \rangle_u$ and $\langle \sigma_z \rangle_u$ are the magnetizations of the decoupled systems (i.e., the magnetizations that would be calculated were these taken to be the origin). An alternate derivation of this recursion relation is given in Appendix A, along with the generalization of (4) to nonzero external fields.

Since the $\langle \sigma_i \rangle_u$ are random variables, we are led to study the distributional equation

$$X =_d \frac{p(\theta_{x,y} Y + \theta_{x,z} Z)}{1 + p^2 \theta_{x,y} \theta_{x,y} YZ} = F^*(Y, Z; \theta_{x,y}, \theta_{x,z}) \tag{5}$$

where Y and Z are independent and identically distributed (i.i.d.) random variables, and the subscript d indicates that this an equality in distribution.

The equivalent equation for the density of single-site magnetizations on level $n + 1$, $\rho_{n+1}(X)$ of X, is given in terms of a convolution of the density on level n, $\rho_n(Y)$ of Y and $\rho_n(Z)$ of Z, by

$$\rho_{n+1}(X) = \int_{-1}^{+1} \int_{-1}^{+1} \rho_n(Y) \rho_n(Z) E[\delta(X - F^*(Y, Z; \theta_{x,y}, \theta_{x,z}))] \, dY \, dZ \quad (6)$$

where E denotes the expectation over the bond distribution (3), i.e., $E[f(\theta)] = \lambda f(1) + (1 - \lambda) f(-1)$.

Equation (6) can be viewed as a discrete-time dynamical system in the function space of probability measures. Boundary conditions on the tree correspond to initial conditions for the dynamical system. Iteration of the equation corresponds to moving from one level to the next, away from the boundary toward the center of the tree. We study the stable self-consistent fixed points of (5), that is, the existence of X, Y, and Z satisfying (5) with

$$Y =_d Z \quad (7)$$

These solutions describe half-space properties deep inside the tree. In Fig. 4 we illustrate how the iteration scheme evolves when the system is almost completely ferromagnetic.

This recursion relation was analyzed in the symmetric case ($\lambda = 1/2$) by Chayes *et al.*[2] They showed that there is a spin-glass transition at a temperature determined by $p_G = 1/\sqrt{2}$, above which the system is paramagnetic, and below which the Edwards–Anderson order parameter

$$q_{EA} = E(X^2) \quad (8)$$

is strictly positive.

Before we begin our analysis of the asymmetric case, we simplify our notation by making a change of variables. It follows from the Fortuin–Kasteleyn–Ginibre (FKG) inequality[22] that no limiting distribution can have support outside $[-\mu^\infty, \mu^\infty]$, where μ^∞ is the magnetization of the purely ferromagnetic system ($\lambda = 1$) at a given value of p,

$$\mu^\infty(p) = \frac{(2p - 1)^{1/2}}{p} \quad (9)$$

Therefore, if we rescale the random variables according to

$$X^\dagger = X/\mu^\infty, \qquad Y^\dagger = Y/\mu^\infty, \qquad Z^\dagger = Z/\mu^\infty \quad (10)$$

and define $\mu^2 = 2p - 1$, then the recursion relation (5) takes the form

$$X^\dagger =_d \frac{p(\theta_{x,y} Y^\dagger + \theta_{x,z} Z^\dagger)}{1 + \mu^2 \theta_{x,y} \theta_{x,z} Y^\dagger Z^\dagger} \equiv F^\dagger(Y^\dagger, Z^\dagger; \theta_{x,y}, \theta_{x,z}) \quad (11)$$
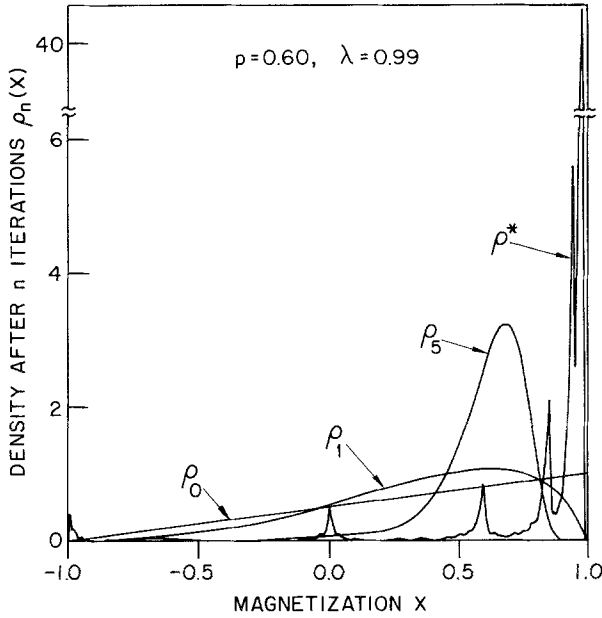
Fig. 4. Iteration of the recursion relation corresponds to a dynamical system in a function space. The results illustrated here were obtained numerically by integrating (6), with $F^*(Y, Z; \theta_{x,y}, \theta_{x,y})$ replaced by $F(Y, Z; \theta)$ [Eq. (12)]. Boundary conditions $\rho_0(X)$ are initial conditions for the dynamical system. In this case we have specified that $\rho_0(X)$ varies linearly from $\rho_0(-1) = 0$ to $\rho_0(1) = 1$. After one iteration ρ_1 begins to develop some structure. After five iterations (ρ_5) this structure becomes more pronounced. Deep inside the tree $\rho_n(X)$ approaches the fixed point ρ^*, which is sharply peaked near $X = +1$. [$\rho(X) = \delta(X - 1)$ is the corresponding fixed point for the fully ferromagnetic system].

where the distributions are supported on the temperature-independent interval $[-1, 1]$.

At times it will be convenient to make an additional simplification. Letting $X^{\ddagger} = \theta X^{\dagger}$, $Y^{\ddagger} = \theta_{x,y} Y^{\dagger}$, and $Z^{\ddagger} = \theta_{x,z} Z^{\dagger}$, where θ is the sign of the bond connecting X to the rest of the full-space lattice, Eq. (11) becomes

$$X^{\ddagger} =_d \frac{p\theta(Y^{\ddagger} + Z^{\ddagger})}{1 + \mu^2 Y^{\ddagger} Z^{\ddagger}} \equiv F(Y^{\ddagger}, Z^{\ddagger}; \theta) \tag{12}$$

We can obtain $X^{\dagger}$ from $Y^{\ddagger}$ by a single application of the recursion relation, with the θ's removed:

$$X^{\dagger} =_d \frac{p(Y^{\ddagger} + Z^{\ddagger})}{1 + \mu^2 Y^{\ddagger} Z^{\ddagger}} \tag{13}$$

When our calculations involve moment analysis, it will be more convenient to use (11), because certain terms in the moment expansions will have smaller coefficients, whereas when we consider the scaling solutions and perform bifurcation analysis, Eq. (12) will prove to be more tractable. To simplify notation, we will now drop the superscripts on the random variables, the subscript x on $\theta_{x,y}$ and $\theta_{x,z}$, and the subscript d on the distributional equality.

3. THE PARAMAGNETIC PHASE BOUNDARIES

The first step in our analysis of the magnetic recursion relation is to determine the critical lines which separate the paramagnetic phase from the other phases which exhibit long-range order (spin glass or ferromagnet). These transitions are second order and are marked by a nonzero value of the order parameter which describes the phase. These order parameters, $m = E(X) \equiv \int X\rho(X)\, dX$, the magnetization of the ferromagnet, and $q = E(X^2) \equiv \int X^2\rho(X)\, dX$, the Edwards–Anderson order parameter for the spin glass, are given by the first and second moments of the fixed-point density ρ of the recursion relation.

The paramagnetic solution is the degenerate distribution, $\rho(X) = \delta(X)$, or equivalently $X = Y = Z \equiv 0$, corresponding to no long-range order. This solution is seen to be a fixed point of the recursion relation for all values of p and λ. The paramagnetic phase boundary is the locus of points at which this solution becomes unstable. As one crosses these curves there are bifurcations in the solution of the recursion relation, yielding nontrivial solutions $\rho(X)$. We begin with a few simple statements regarding the stability of the paramagnetic solution with respect to small perturbations in the single-site magnetization. These arguments are relatively easy to follow and they also give the right phase boundary. In Appendix B we prove the corresponding global stability. The global result rules out the possibility of an ordered phase in this region of the phase diagram.

Proposition 1. The paramagnetic solution is stable with respect to small variations in the single-site magnetization when both of the following conditions hold:

1. $2p(2\lambda - 1) < 1$.
2. $2p^2 < 1$.

Remark. In the limiting case of equality, condition 1 gives the phase boundary with the ferromagnetic phase, while condition 2 gives the phase boundary with the spin-glass phase.

Proof. Assume that Y is not identically zero, but that $\text{Prob}[Y > \varepsilon] = 0$ for some small ε. This corresponds to a small perturbation of the paramagnetic distribution $Y = 0$ in function space. Hence the distribution has a small first moment, say $E(Y) = \varepsilon m$, where m is of order one. To avoid any ambiguity in the sign, we consider the absolute value of the magnetization. To prove condition 1, we define $|m_n| = \varepsilon^{-1} |E(Y)|$ and $|m_{n+1}| = \varepsilon^{-1} |E(X)|$. Taking the expectation of the recursion relation (11) yields

$$|m_{n+1}| = 2p(2\lambda - 1) |m_n| [1 + O(\varepsilon^2)] \tag{14}$$

It follows that the absolute value of the first moment contracts if $2p(2\lambda - 1) < 1$ and grows if $2p(2\lambda - 1) > 1$.

Now consider the behavior of the second moment, independent of the first (i.e., set the first moment equal to zero). Squaring the recursion relation, we obtain

$$X^2 = \frac{p^2(Y^2 + Y^2 + 2\theta_y \theta_z YZ)}{(1 + \mu^2 \theta_y \theta_z YZ)^2} \tag{15}$$

Upon defining $q_n = \varepsilon^{-2} E(Y^2)$ and $q_{n+1} = \varepsilon^{-2} E(X^2)$, we find that

$$q_{n+1} = 2p^2 q_n [1 + O(\varepsilon^2)] \tag{16}$$

indicating that the second moment contracts if $2p^2 < 1$ and grows if $2p^2 > 1$. The paramagnetic solution is stable if and only if both q_n and $|m_n|$ contract. ∎

In addition, we have the following theorem.

Theorem 2. The paramagnetic solution is globally stable when both of the following conditions hold:

$$\begin{aligned} &1. \quad 2p(2\lambda - 1) \leqslant 1 \\ &2. \quad 2p^2 \leqslant 1 \end{aligned} \tag{17}$$

Remark on Proof. The complete proof is given in Appendix B. The method used is moment analysis, where we show that any initial condition leads to a solution of the recursion relation (11) deep inside the tree which has first and second moments arbitrarily close to zero. Consequently, $\rho(X) = \delta(X)$ is the unique globally attracting fixed point of (6). ∎

These curves dtermine the paramagnetic phase boundary, and are illustrated in Fig. 1. They intersect at the multicritical point (λ_N, p_G). The boundaries between distinct ordered phases also branch from this point.

4. THE SPIN-GLASS PHASE

In this section, we characterize the spin-glass phase in a variety of ways. First, in Section 4.1 and Appendix C we show that the Edwards–Anderson order parameter q_{EA} is positive, indicating the onset of some sort of long-range order in the system. While the onset of positive q_{EA} proves that a phase transition has occurred, it does not give us any explicit information about the nature of the phase. In order to obtain more information, we study properties of the stable fixed point $\rho(X)$ (see Fig. 5), which is symmetric in the spin-glass phase. The width of $\rho(X)$ is proportional to $q_{EA}^{1/2}$ and we obtain $\rho(X)$ using bifurcation theory (Sections 4.2 and 4.3). One noteworthy feature is that, at fixed temperature in the spin-glass phase near the paramagnetic phase boundary, $\rho(X)$ does not change when the fraction of ferromagnetic bonds is varied. Finally, it is worth mentioning that in experimental systems, the spin-glass transition can be characterized by divergence of a nonlinear (quadratic) susceptibility. In ref. 1, Sections 2 and 3 we calculate a different quadratic susceptibility, the Edwards–Anderson susceptibility, and show that it diverges at the spin-glass phase boundary.
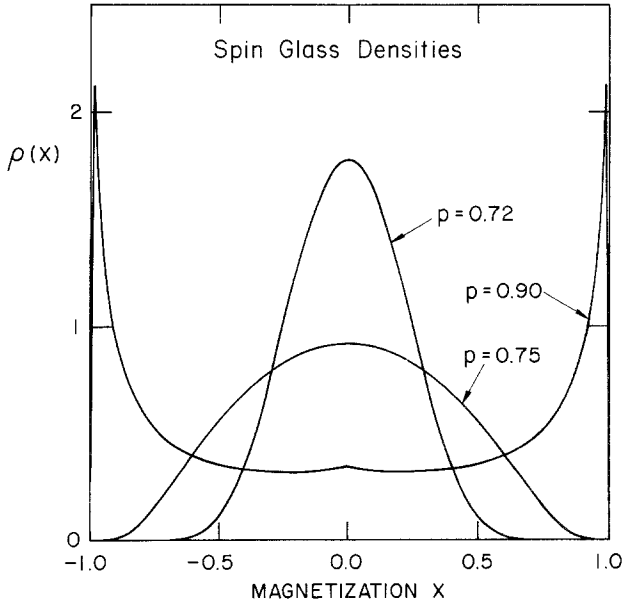

Fig. 5.   The fixed-point density of single-site magnetizations in the spin-glass phase for various values of p. In every case the density is symmetric about $X = 0$, and as p increases (T decreases) the width, which is proportional to $q_{EA}^{1/2}$, increases. These results were obtained numerically by iteration of the recursion relation as in Fig. 4.

4.1. Bounds on the Edwards–Anderson Order Parameter

In the paramagnetic phase (Section 2 and Appendix B), moment analysis indicates that the unique globally attracting fixed point of the recursion relation has second moment $q = 0$, or, equivalently, $\rho(X) = \delta(X)$. In this section and Appendix C we show how similar moment analysis of the recursion relation [Eq. (11)] leads to positive upper and (more importantly) lower bounds on the second moment $q_L \leqslant q \leqslant q_U$ near the spin-glass phase boundary (see Fig. 6). Here q is the Edwards–Anderson order parameter q_{EA}, and the onset of positive q marks the phase transition.

Moment analysis allows us to prove global results. Using the moment inequalities, we obtain bounds in a manner analogous to those used to determine stable fixed points for dynamical systems. However, because we have inequalities rather than equalities, instead of determining a fixed point $\rho(X)$, we obtain a stable range of allowed values for particular moment(s) of $\rho(X)$.

In the symmetric case ($\lambda = 1/2$) our analysis was greatly simplified by the fact that we could a priori ignore all odd moments. In the asymmetric case, a separate argument shows that we can ignore these terms for $\lambda < 3/4$; however, in general, these terms must be retained. As a consequence the analysis is much more tedious; the details are provided in Appendix C.

Theorem 3. In a finite neighborhood of the phase boundary, $p \gtrsim p_G = 1/\sqrt{2}$ and $1/2 < \lambda < \lambda_N$, iterates of the second moment q_n eventually obey the bounds $q_L < q_n < q_U$, with

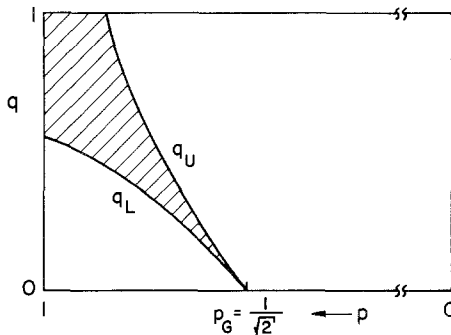$$q_L = V(p, \lambda) \, |p - p_G| \tag{18}$$

Fig. 6. Upper and lower bounds on q_{EA} obtained by moment analysis. Because these bounds have the same power law asymptotically at the transition, we can extract the critical exponent $\beta = 1$. As described in Theorems 2 and 3, these bounds hold throughout the paramagnetic phase, and in a neighborhood of the phase boundary in the spin-glass phase.

and

$$q_U = W(p, \lambda) \, |p - p_G| \tag{19}$$

with $0 < V(p, \lambda) < W(p, \lambda) < \infty$. Furthermore, for $\lambda < 3/4$, $V(p, \lambda) = V(p, 1/2)$ and $W(p, \lambda) = W(p, 1/2)$, and $\lim_{p \to p_G} V(p, 1/2) = \lim_{p \to p_G} W(p, 1/2) = 1/p_G \mu_G^2$.

Both the upper and lower bounds on q in the spin-glass phase are asymptotically of the form $q \sim |2p^2 - 1| \sim |p - p_G|$. Hence, we obtain the critical exponent $\beta = 1$.

Corollary. For $\lambda < \lambda_N$, in a finite neighborhood of the spin-glass critical point $p \gtrsim p_G = 1/\sqrt{2}$, the leading behavior of the Edwards–Anderson order parameter is linear in the sense of upper and lower bounds, i.e.,

$$q_{EA} \sim |p - p_G|^\beta$$

where $\beta = 1$. Furthermore, for $\lambda < 3/4$ the coefficients of the asymptotic forms of the upper and lower bounds agree in the sense that

$$\lim_{p \to p_G} \frac{q_{EA}}{|p - p_G|} = \frac{1}{p_G \mu_G^2}$$

Remark. The restriction $\lambda < 3/4$ arises for technical reasons. Indeed, the bifurcation results obtained later in this section indicate that as $p \to p_G$, $q_{EA}/|p - p_G|$ should approach $1/p_G \mu_G^2$ whenever $\lambda < \lambda_N$.

4.2. The Spin-Glass Scaling Solution

To obtain the spin-glass $\rho(X)$, we must return to the full recursion relation (6), regarded as an infinite-dimensional dynamical system acting in function space. Recall that the paramagnetic solution $\rho(X) = \delta(X)$ is the unique globally attracting solution of the recursion relation (6) up to the critical line (Section 2 and Appendix B). Only inside the phase boundary does $\rho(X)$ have any nontrivial structure. In the previous section we proved that approaching the phase boundary, q approaches 0, indicating that the solution continuously approaches the paramagnetic fixed point. In this section we rescale the magnetizations to keep q finite as $p \to p_G$, and determine the limiting solution for the rescaled variables along the phase boundary. Before rescaling, the solution along the phase boundary $\rho(X) = \delta(X)$ cannot reveal any of the structure of the spin-glass solution.

Define $\Delta = p - p_G$. From our results on the asymptotic form of the

second moment near the phase boundary (i.e., the corollary to Theorem 3 in Section 4.1) we find that, to keep q finite as we approach the phase boundary, the magnetizations should be rescaled according to

$$X^* = \frac{X}{\sqrt{\Delta}}, \qquad Y^* = \frac{Y}{\sqrt{\Delta}}, \qquad Z^* = \frac{Z}{\sqrt{\Delta}} \tag{20}$$

We rewrite the recursion relation (12) in terms of these variables,

$$X^* = \frac{p\theta(Y^* + Z^*)}{1 + \mu^2 \, \Delta Y^* Z^*} = F_\Delta(Y^*, Z^*; \theta) \tag{21}$$

where $\mu^2 = 2p - 1$ and the random variables take values only in the interval $[-1/\sqrt{\Delta}, 1/\sqrt{\Delta}]$. We denote the density of the rescaled random variable X^* by $\rho_\Delta(X^*)$.

When $\Delta = 0$ the recursion relation takes the particularly simple linear[8] form

$$X^* = p_G \theta(Y^* + Z^*) \tag{22}$$

where the rescaled variables take values in $(-\infty, +\infty)$. It is, however, worth emphasizing that the solutions to (22)—the scaling solutions—are not *a priori* the $\Delta \to 0$ limit of the positive Δ solutions of (21) (should such solutions exist). in the following proposition we show that the solutions ρ_0 of (22) are Gaussians of arbitrary width, whereas in the next section we will find that there is only one solution as $\Delta \to 0$.

Proposition 4. Let X^*, Y^*, and Z^* be random variables which satisfy (22), where Y^* and Z^* are i.i.d., $p_G = 1/\sqrt{2}$, and $\theta = \pm 1$. Then the fixed-point density $\rho_0(X^*)$ is a Gaussian, with mean zero and arbitrary variance:

$$\rho_0(X^*) = \mathscr{G}_0^\sigma(X^*) \equiv (\pi\sigma^2)^{-1/2} \exp[-x^2/\sigma^2]$$

Proof. Our results from moment analysis indicate that after rescaling, the second moment α_2 must be nonzero and finite. Squaring (22) and taking the expectation, our equation for the first moment, $\alpha_1 = E(X^*)$, becomes $2p_G^2 \alpha_1 = (1 - 2p_G^2) \alpha_2 = 0$. Now raising (22) to any odd power n and solving for α_n in terms of all preceding moments establishes that all odd moments are proportional to α_1, and are consequently also equal to zero. Hence $\rho(X^*)$ is symmetric. Therefore, the θ can be dropped, and (22)

---

[8] Note that while this recursion relation is linear in the random variables, the corresponding integral equation for the distribution of the random variables is quadratic.

is simply the stable law $X^* = (Y^* + Z^*)/\sqrt{2}$, for which a Gaussian is the unique solution of finite width. ∎

We suggest that the reader pause for a moment to appreciate the simplicity of the spin-glass scaling solution. As we will see, the corresponding analysis along the ferromagnetic phase boundary is much more complicated, because the scaling solution $\rho_0(X^*)$ is not a well-known function of X^*. In addition, it is worth pointing out that the spin-glass scaling solution remains the same along the entire phase boundary. This is the first hint that despite large bond asymmetry, in the spin-glass phase $\rho_\Delta(X^*)$ [or equivalently $\rho(X)$ of the original variables] is the same as when $\lambda = 1/2$. In Section 5 we show that this is not the case in the ferromagnetic phase.

4.3. Existence of a Spin-Glass Solution

Loosely speaking, the transition from the paramagnetic phase to the spin-glass phase is like a pitchfork bifurcation, except there is only one spin-glass solution instead of two (see Fig. 7a). For $p \leqslant p_G$ the unique globally attracting solution of the recursion relation is $\rho(X) = \delta(X)$, the paramagnetic solution. At p_G, $\delta(X)$ becomes unstable, and a new spin-glass solution $\rho(X)$ emerges. The width of $\rho(X)$ is proportional to $q_{EA}^{1/2}$ and as the transition is approached from the spin-glass phase, more and more of the mass of $\rho(X)$ is concentrated near the origin ($q_{EA} \to 0$). The limiting solution $\rho(X)$ at the phase transition is $\delta(X)$, which exhibits none of the properties of $\rho(X)$ within the ordered phase. Consequently, we cannot perform a bifurcation analysis directly using $\delta(X)$. We overcome this problem

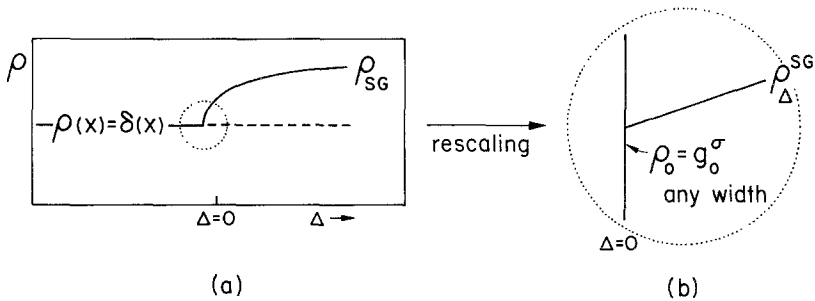(a)   (b)

Fig. 7. (a) The P → SG transition is like a pitchfork bifurcation, except only one new solution emerges at the transition instead of two. When $\Delta \leqslant 0$ the unique globally attracting solution of the recursion relation is $\rho(X) = \delta(X)$. At $\Delta = 0$ a new spin-glass solution emerges, and $\delta(X)$ becomes unstable. (b) At $\Delta = 0$ rescaling replaces the paramagnetic fixed point $\delta(X)$ with a continuum of scaling solutions $\mathscr{G}_0^\sigma$. The scaling solution with the correct variance σ bifurcates, giving rise to the spin-glass solution for $\Delta > 0$.

by the rescaling (20), which gives rise to a continuum of scaling solutions along the phase boundary (Fig. 7b).

The transformation which leads to the scaling solution is singular along the phase boundary. Thus, there is no *a priori* reason to believe that the solutions we found (Proposition 4) are related to the distribution of magnetizations inside the phase boundary. On the other hand, the instability of the paramagnetic solution $\delta(X)$ at this point suggests that new solutions may bifurcate from some (or in this case a particular one) of these Gaussians. In this section we show how the spin-glass transition is associated with such a bifurcation.

Instead of simply calculating q_{EA} inside the phase boundary, we look for the magnetization *density* which satisfies the full nonlinear recursion relation

$$\rho_{\Delta}(x) = \int_{-1/\sqrt{\Delta}}^{1/\sqrt{\Delta}} \int_{-1/\sqrt{\Delta}}^{1/\sqrt{\Delta}} \rho_{\Delta}(y)\, \rho_{\Delta}(z)\, E[\delta(x - F_{\Delta}(y, z; \theta))]\, dy\, dz \quad (23)$$

where $-1/\sqrt{\Delta} \leqslant x, y, z \leqslant +1/\sqrt{\Delta}$, and

$$F_{\Delta}(y, z; \theta) = \frac{p\theta(y + z)}{1 + \Delta\mu^2 yz} \quad (24)$$

For future reference, note that Eq. (24) can be written in the form

$$\rho_{\Delta} = B_{\Delta}[\rho_{\Delta}, \rho_{\Delta}] \quad (25)$$

where B_{Δ} is the bilinear operator

$$B_{\Delta}[f, g] = \int_{-1/\sqrt{\Delta}}^{1/\sqrt{\Delta}} \int_{-1/\sqrt{\Delta}}^{1/\sqrt{\Delta}} f(y)\, g(z)\, E[\delta(x - F_{\Delta}(y, z; \theta))]\, dy\, dz \quad (26)$$

From the above form, it is clear that B_{Δ} has an "integral-preserving" property, i.e., if $f, g \in L^1$, then

$$\int B_{\Delta}[f, g] = \int f \int g \quad (27)$$

We also define the operator $\mathscr{H}_{\Delta}$ according to

$$\mathscr{H}_{\Delta}(f) = B_{\Delta}[f, f] \quad (28)$$

Because of the presence of the δ-function, the integrals in (23) and (26) may seem to be poorly defined. However, without loss of generality, these

can be interpreted in the usual way, leading, for example, to the rather complicated formula

$$\mathcal{H}_{\varDelta}(\rho_{\varDelta}) = p\lambda \int_{-1/\sqrt{\varDelta}}^{+1/\sqrt{\varDelta}} \rho_{\varDelta}(y) \, \rho_{\varDelta}\left(\frac{x-py}{p-\varDelta\mu^2 xy}\right)\left[\frac{1-\varDelta\mu^2 y^2}{(p-\mu^2\varDelta xy)^2}\right] dy$$

$$+ p(1-\lambda) \int_{-1/\sqrt{\varDelta}}^{+1/\sqrt{\varDelta}} \rho_{\varDelta}(y) \, \rho_{\varDelta}\left(\frac{x+py}{-p-\varDelta\mu^2 xy}\right) \frac{(1-\varDelta\mu^2 y^2)}{(-p-\mu^2\varDelta xy)^2} \, dy$$

$$(29)$$

where in the above equation we have also explicitly written out the result of the expectation over the bond distribution [the E in Eq. (23)].

If we define

$$\mathcal{R}_{\varDelta}(\rho_{\varDelta}) = \mathcal{H}_{\varDelta}(\rho_{\varDelta}) - \rho_{\varDelta} \tag{30}$$

then zeros of $\mathcal{R}_{\varDelta}$ correspond to fixed points of the recursion relation. To obtain a solution ρ_1 at a given point $\varDelta_1$ in terms of a known solution ρ_0 at $\varDelta_0$, we linearize the operator as follows:

$$\mathcal{R}_{\varDelta_1}(\rho_{\varDelta_1}) = \mathcal{R}_{\varDelta_0 + \kappa}(\rho_{\varDelta_0} + \varepsilon\phi)$$

$$= \mathcal{R}_{\varDelta_0}(\rho_{\varDelta_0}) + \kappa \left(\frac{\partial\mathcal{R}_{\varDelta}}{\partial\varDelta}\right)_{\varDelta = \varDelta_0} (\rho_{\varDelta_0}) + \varepsilon \left(\frac{\partial\mathcal{R}_{\varDelta_0}}{\partial\rho}\right)_{\rho = \rho_0} (\phi)$$

$$+ O(\kappa^2, \varepsilon^2, \varepsilon\kappa) \tag{31}$$

where the first term in the expansion corresponds to the known fixed point, and therefore is equal to zero, the second term is obtained by straightforward differentiation of (29) with respect to $\varDelta$, and the third term is Frechet derivative of the operator evaluated at the known solution.

At the phase transition, the linear operator $\partial R_0/\partial\rho$ is not invertible: there is a zero mode (zero eigenvalue) associated with the indeterminacy in the width of the scaling solution. Thus, to find a solution for $\varDelta > 0$, we must restrict to the subspace orthogonal to this mode. As is standard in such situations, we accomplish this by using a version of the center manifold theorem. (See Fig. 8.) The main result in this section will be a proof of the existence of a density which satisfies (29) for small positive values of $\varDelta$. The nonlinearities of our function select the width of the bifurcating scaling solution, so that in terms of the rescaled variables, our density converges to the Gaussian fixed point $\mathcal{G}_0^\sigma(X^*)$ with the correct variance σ^2.

To ensure that the final solution has no support outside the compact interval $[-1/\sqrt{\varDelta}, 1/\sqrt{\varDelta}]$, we make a simple transformation which allows
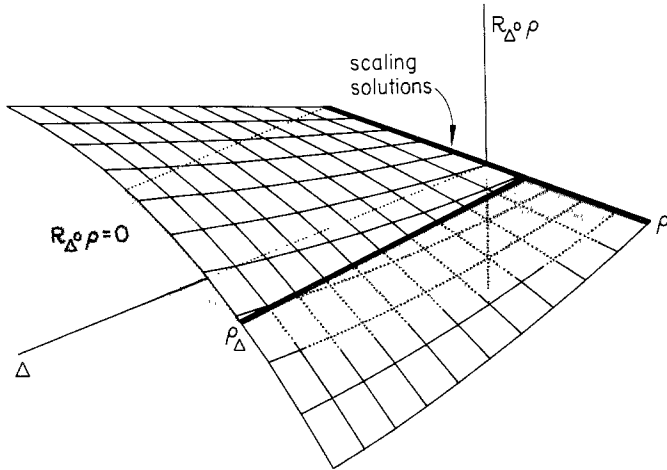
Fig. 8. At a phase transition we apply the center manifold theorem to find new solutions. This theorem reduces the problem of searching all of function space for a solution to that of searching a restricted space with one dimension per zero mode.

us to work in $\mathbb{R}$. We define $\Phi_\Delta(x) = \Phi(x\sqrt{\Delta})$, so that $\Phi_\Delta(x)$: $[-1/\sqrt{\Delta}, 1/\sqrt{\Delta}] \to \mathbb{R}$, where $\Phi_\Delta(x)$ is the identity in a neighborhood of the origin. This transformation is discussed in detail in ref. 2, Section IV.a. The transformation has two important properties. First, it is invertible, so that we can work on all of $\mathbb{R}$ and then transform back to the compact interval. Additionally, $\Phi_\Delta(x)$ rapidly approaches the identity as Δ approaches zero. It is this second feature which allows us to proceed with our calculations, ignoring the transformation. In particular, at times it will be necessary to differentiate the full recursion relation with respect to Δ, and evaluate the result at $\Delta = 0$. Because $\Phi_\Delta(x)$ is the identity in a neighborhood of the origin, the derivative has the same form as the function one would calculate in the absence of $\Phi_\Delta(x)$. However, by using this transformation, we know our solution is contained in the desired interval.

4.3.1. The Linear Operator and its Eigenfunctions.

To apply the center manifold theorem, we begin by linearizing the operator $\mathscr{R}_0$ [Eq. (30) evaluated at $\Delta = 0$] about any one of the scaling fixed points $\rho_0(X^*) = \mathscr{G}_0^\sigma(X^*)$. Next we calculate the eigenfunctions and eigenvalues of this operator. The eigenfunctions span the function space for the bifurcation, which in this case may be taken as $L^2([\mathscr{G}_0^\sigma(x)]^{-1} dx) \subset L^1(dx)$.[9]

[9] Although we are interested in positive solutions in $L^1(dx)$, i.e., densities, it is easily seen that $L^2([\mathscr{G}_0^\sigma(x)]^{-1} dx) \subset L^1(dx)$. However, the spectral questions are better addressed in the more restrictive spaces. This latter point, although taken into account, was not stated explicitly in ref. 2.

When the recursion relation is linearized about the scaling fixed point $\rho_0(X^*)$ we obtain the following linear operator:

$$L \circ f(x) = \left(\frac{\partial \mathscr{R}_{\Delta_0}}{\partial \rho}\right)_{\rho = \rho_0} (f(x))$$

$$= 2\lambda \int \rho_0(y) f\left(\frac{x}{p} - y\right) \frac{dy}{p} + 2(1 - \lambda)$$

$$\times \int \rho_0(y) f\left(-\frac{x}{p} - y\right) \frac{dy}{p} - f(x) \tag{32}$$

To study the properties of this operator, we first look for its eigenfunctions, which satisfy

$$L \circ f_n(x) = v_n f_n(x) \tag{33}$$

where v_n is the associated eigenvalue. For the spin glass, $\rho_0(y)$ in Eq. (32) is replaced by $\mathscr{G}_0^\sigma(y)$; however, here we write the equation in a more general form which will apply at the ferromagnetic transition as well.

The eigenfunctions of (33) were determined in ref. 2, and by direct substitution are easily seen to be

$$\mathscr{G}_n^\sigma(x) = \sigma^n(-1)^n \, d^n/dx^n \mathscr{G}_0^\sigma(x) = H_n(x/\sigma) \, \mathscr{G}_0^\sigma(x) \tag{34}$$

where σ^2 is the variance of the Gaussian $\mathscr{G}_0^\sigma$, and H_n is the nth Hermite polynomial. The associated eigenvalues are

$$v_n = \begin{cases} 2p^n - 1, & n \text{ even} \\ 2p^n(2\lambda - 1) - 1, & n \text{ odd} \end{cases} \tag{35}$$

A plot of the point spectrum as a function of λ appears in Fig. 9.

With the exception of $\mathscr{G}_0^\sigma$, and $\mathscr{G}_2^\sigma$, with eigenvalues 1 and 0, respectively, the eigenfunctions have negative eigenvalues. The first eigenfunction $\mathscr{G}_0^\sigma$ is simply the Gaussian fixed-point density. The associated eigenvalue is 1, and $\mathscr{G}_0^\sigma$ is a trivial "growth mode," which can easily can be removed by redefining the operator as shown in ref. 2, Eq. (5.15). On the other hand, along the spin-glass phase boundary, $\mathscr{G}_2^\sigma$ has eigenvalue zero, which prevents the linear operator from being invertible. Perturbations in the $\mathscr{G}_2^\sigma$ direction correspond to moving from one of the Gaussian scaling solutions $\mathscr{G}_0^\sigma(X^*)$ to another $\mathscr{G}_0^{\sigma/c}(X^*) = c\mathscr{G}_0^\sigma(cX^*)$, since

$$\mathscr{G}_2^\sigma(X^*) = \frac{d}{dc} \, \mathscr{G}_0^{\sigma/c}(X^*)]_{c=1} \tag{36}$$

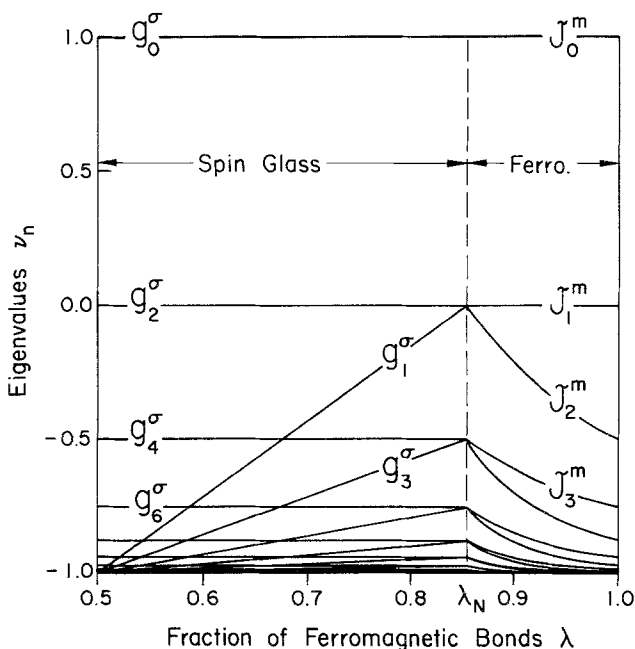Fig. 9.   Point spectrum plotted as a function of λ. The spin-glass eigenfunctions correspond to $\lambda < \lambda_N$, and the ferromagnetic eigenfunctions correspond to $\lambda > \lambda_N$. Note that the eigenvalues are doubly degenerate at $\lambda = \lambda_N$.

The linear convolution operator (32) may be viewed as the bilinear operator B_Δ [Eq. (26)] evaluated at $\Delta = 0$:

$$B_0[f, g] = \lambda \int_{-\infty}^{\infty} g(y) f\left(\frac{x}{p} - y\right) \frac{dy}{p} + (1 - \lambda) \int_{-\infty}^{\infty} g(y) f\left(-\frac{x}{p} - y\right) \frac{dy}{p}$$

$$(37)$$

In the bifurcation analysis it is necessary to know how the bilinear operator acts on pairs of eigenfunctions. From the calculations of this section, we have

$$B_0[\mathscr{G}_n^\sigma, \mathscr{G}_m^\sigma] = \begin{cases} p^{n+m} \mathscr{G}_{n+m}^\sigma, & n + m \text{ even} \\ p^{n+m}(2\lambda - 1)\, \mathscr{G}_{n+m}^\sigma, & n + m \text{ odd.} \end{cases} \qquad (38)$$

Again the reader should pause and appreciate the remarkable simplicity of the relation above. In the ferromagnetic phase, life is not so simple; pairs of eigenfunctions do not always combine to yield another eigenfunction under the action of B_0.

4.3.2. Bifurcation of the Spin-Glass Solution. The bifurcation of the spin-glass solution is illustrated in Fig. 8. In this section, armed with the eigenfunctions of the linear operator, we are ready to prove the results illustrated in this figure. We begin with a precise statement of the relevant version of the center manifold theorem.

Center Manifold Theorem. Let X, Y denote Banach spaces, and $\mathscr{R}_\Delta: X \to Y$ be a $\mathscr{C}^2$ map defined in some neighborhood of $(\Delta = 0,\ \rho = \rho_0)$, satisfying $\mathscr{R}_\Delta(\rho_0) = 0$. Furthermore, suppose $\delta\mathscr{R}_0/\delta\rho \equiv (\delta/\delta\rho)\,\mathscr{R}_0(\rho_0; \cdot)$ is a linear Fredholm operator, with $\dim \ker(\delta\mathscr{R}_0/\delta\rho) < \infty$ and $\dim \operatorname{coker}(\delta\mathscr{R}_0/\delta\rho) < \infty$. If $\psi \in \ker(\delta\mathscr{R}_0/\delta\rho)$ and Δ is small enough, then for ε sufficiently small, there is a function $g_{\varepsilon,\Delta}(\psi) \in X \backslash \ker(\delta\mathscr{R}_0/\delta\rho)$ such that

$$\mathscr{R}_\Delta(\rho_0 + \varepsilon\psi + g_{\varepsilon,\Delta}) \in \operatorname{coker}(\delta\mathscr{R}_0/\delta\rho)$$

Moreover, for fixed ψ, $g_{\varepsilon,\Delta}$ is unique.

Remark. This is a standard result in Liapunov–Schmitt theory. A proof of the theorem and a discussion of related matters are given in ref. 23.

At the spin-glass transition, the relevant Banach space is $L^2([\mathscr{G}_0^\sigma(x)]^{-1}\,dx)$, which is spanned by the eigenfunctions $\{\mathscr{G}_n^\sigma\}$. The map $\mathscr{R}_\Delta$ given in Eq. (30) is the convolution operator less the identity, and the linear operator $\delta\mathscr{R}_0/\delta\rho \equiv \delta/\delta\rho\mathscr{R}_0(\rho_0; \cdot)$ is given in Eq. (32). The kernel and the cokernel both contain only the zero mode, $\mathscr{G}_2^\sigma$.

Zeros of $\mathscr{R}_\Delta$ are fixed points of the recursion relation. At $\Delta = 0$ these are the scaling solutions $\rho_0 = \mathscr{G}_0^\sigma$. The above theorem tells us that

$$\mathscr{R}_\Delta(\mathscr{G}_0^\sigma + \varepsilon\mathscr{G}_2^\sigma + g_{\varepsilon,\Delta}^\sigma) = h^\sigma(\varepsilon, \Delta)\,\mathscr{G}_2^\sigma \tag{39}$$

The function $g_{\varepsilon,\Delta}^\sigma$ can be expressed as a linear combination of the even eigenfunctions $\{\mathscr{G}_{2n}^\sigma\}$ starting at $\mathscr{G}_4^\sigma$. The function $h^\sigma(\varepsilon, \Delta)$ can be expressed as a Taylor series in ε and Δ. A fixed point of the recursion relation corresponds to a zero of $h^\sigma(\varepsilon, \Delta)$. To obtain the fixed point for $\Delta > 0$, we expand the map $\mathscr{R}_\Delta$ for small, positive Δ. Equating powers of ε and Δ on the opposite sides of Eq. (39), we choose σ so that $h^\sigma(\varepsilon, \Delta) = 0$. This leads to an explicit proof of the existence of a fixed point.

Details of the how the center manifold theorem is applied at the spin-glass transition are given in ref. 2, the main result appearing as Theorem 4.1, which we restate here. A related theorem, giving the same results in a different Banach space, follows as a special case of the results which we obtain at the multicritical point in Section 6.2.

Theorem 5. Provided that Δ is sufficiently small, there is a unique

one-parameter family of positive, symmetric L^1 functions ρ_Δ with $\|\rho_\Delta\|_1 = 1$, satisfying

$$\mathscr{R}_\Delta(\rho_\Delta) = 0$$

The family has the property that

$$\lim_{\Delta \to 0} \rho_\Delta = \mathscr{G}_0^{\sigma^G}$$

where $\mathscr{G}_0^\sigma$ is a normalized Gaussian of variance σ^2:

$$\mathscr{G}_0^\sigma = (\pi\sigma^2)^{-1} \exp(-x^2/\sigma^2)$$

and $(\sigma^G)^2 = 2/[p_G(2p_G - 1)]$.

This guarantees the existence of a spin-glass solution for small, positive Δ. The method of proof is analogous to the method we will be using for the ferromagnet. Linear stability of the spin-glass solution is demonstrated in ref. 2, Section V, where the leading non-Gaussian correction to $\rho(X)$ is also explicitly calculated.

Note that the spin-glass solution is symmetric, and at fixed temperature is exactly the same for the whole range of λ along the spin-glass phase boundary. This is consistent with our results from moment analysis (Section 4.1 and Appendix C), but much more explicit.

5. THE FERROMAGNETIC PHASE

The ferromagnetic Ising model on the Bethe lattice is well understood. It is easily shown that at high temperatures the system is paramagnetic: $\rho(X) = \delta(X)$. As the temperature is lowered, there is a transition at $p_c = 1/2$, below which the system develops ferromagnetic solutions: $\rho(X) = \delta(X - 1)$ or $\rho(X) = \delta(X + 1)$. The state the system ultimately chooses depends on boundary conditions.

It is natural to ask how the character of the ferromagnetic phase is altered by the inclusion of a finite fraction of antiferromagnetic bonds. The phase diagram (Fig. 1) illustrates that on the Bethe lattice, as in experimental systems, ferromagnetism persists for a wide range of concentrations of antiferromagnetic bonds. We study $\rho(X)$ near the paramagnetic phase boundary. (See Fig. 10.) There are two solutions, corresponding to positive and negative magnetization. When nearly all of the bonds are ferromagnetic, $\rho(X)$ has a great deal of structure. One of the solutions has a strong peak near $X = 1$, indicating that the system is mostly ferromagnetic, and a tiny peak near $X = -1$, reflecting the small but finite
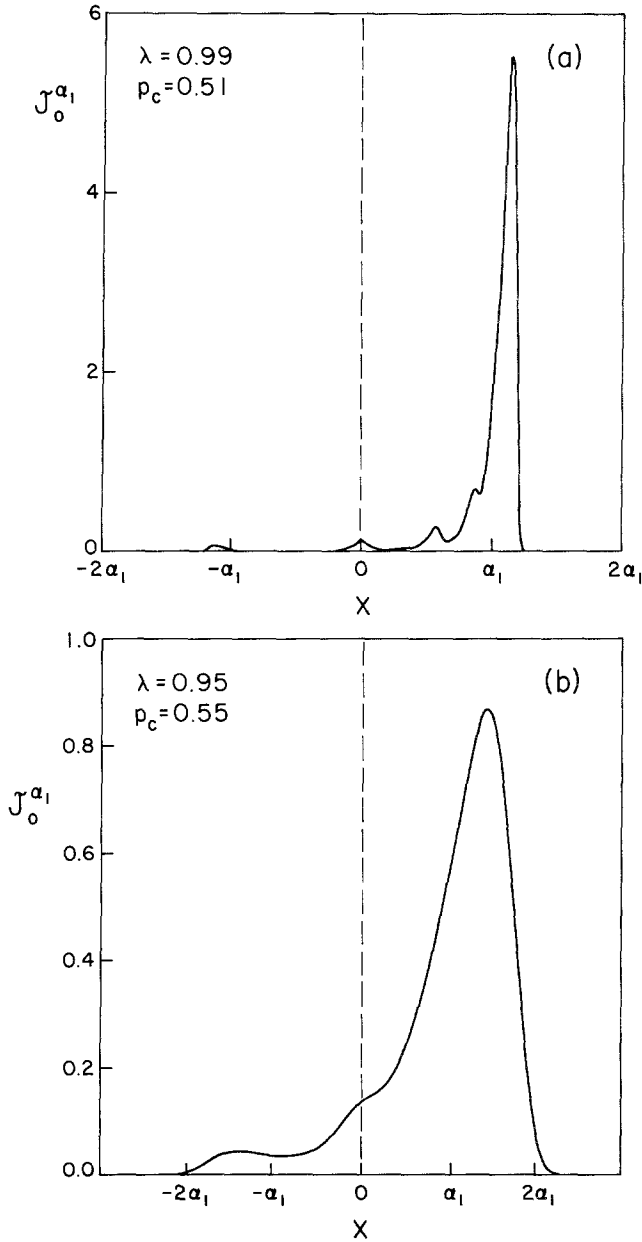
Fig. 10. The scaled form of the fixed-point density $\mathscr{J}_0^{\alpha_1}$ along the ferromagnetic phase boundary for increasing values of p_c. (a) The result for a nearly fully ferromagnetic system, (b) the result for an intermediate value of p_c, and (c) the result near the multicritical point. These results were obtained using Eq. (51), which gives a relationship between the function $\hat{\rho}_0$ at the two different arguments: k and $k' = p_c k$. Numerically we generated these densities by specifying $\hat{\rho}(k)$ in a small interval near the origin in k space, which essientially corresponds to choosing the value of α_1. To obtain $\hat{\rho}(k)$ for any k outside the specified interval, it is sufficient to iterate Eq. (51) until we return to the small interval.
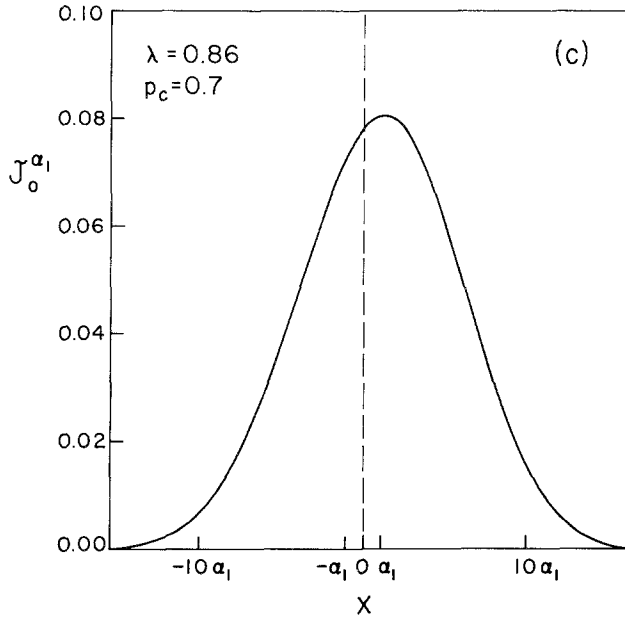
Fig. 10.   (*Continued*)

probability that the origin is antiferromagnetically connected to the site above it. There is also an intermediate peak at $X = 0$ representing the possibility that the origin is connected to one of the sites below it with a ferromagnetic bond, and to the other with an antiferromagnetic bond. Moving toward the spin-glass phase, $\rho(X)$ becomes more smooth in appearance, until finally, approaching the spin-glass phase boundary, $\rho(X)$ approaches the symmetric spin-glass solution. While the ferromagnetic phase is generally thought to be less exciting than glassy behavior, we find that mathematically it presents many interesting problems on the Bethe lattice.

5.1. The Ferromagnetic Solution in the Scaling Limit

We obtain explicit information about the ferromagnetic phase by studying the density of single-site magnetizations $\rho(X)$. For each value of λ we define $\Delta = p - p_c(\lambda)$, where $2p_c(\lambda)(2\lambda - 1) = 1$. As we did in Section 4.2 for the spin glass, we rescale the magnetizations $X \to X^* = X/\sqrt{\Delta}$ (and Y and Z accordingly) to see the limiting behavior. The rescaled

recursion relation is given in Eq. (21). In the scaling limit $(\Delta = 0)$ we are left with the linear scaled form of the recursion relation

$$X^* = p_c \theta(Y^* + Z^*) \tag{40}$$

Equation (40) has the expected solutions at the two extreme points of the ferromagnetic phase boundary. At $p_c = 1/2$, (40) is satisfied by $\delta(X - m)$, for arbitrary m, which is the anticipated solution for the pure ferromagnet. At $p_c = p_G = 1/\sqrt{2}$, where the spin-glass and ferromagnetic phase boundaries meet, (40) is satisfied by a Gaussian of arbitrary width, as discussed in Section 4.2. For the intermediate values $1/2 < p_c < 1/\sqrt{2}$, (40) is not satisfied by any well-known function. However, we can still prove the existence and uniqueness (up to the mean) of the scaling solution. We find that the ferromagnetic scaling solutions $\rho_0(X^*) = \mathscr{I}_0^m(X^*)$ vary analytically as a function of the ferromagnetic bias λ, and that they have a lot of interesting structure (see Fig. 10).

Because Eq. (40) is linear, iteration of any initial distribution preserves the first moment

$$E(X) = E(p_c \theta(Y + Z)) = 2p_c(2\lambda - 1) E(Y) = E(Y) \tag{41}$$

Therefore, the first moment $m = E(X) \equiv \alpha_1$ of a fixed-point distributions satisfying (40) will be arbitrary. On the other hand, when a nonzero mean α_1 is specified, (40) allows us to inductively determine all other moments. Raising (40) to the nth power, taking the expectation, and solving for α_n $(n \geqslant 2)$, we obtain

$$\alpha_n = \frac{E(\theta^n) \, p_c^n}{1 - 2E(\theta^n) \, p_c^n} \sum_{k=1}^{n-1} \binom{n}{k} \alpha_k \alpha_{n-k} \tag{42}$$

where

$$E(\theta^n) = \begin{cases} 1 & \text{if } n \text{ is even} \\ (2\lambda - 1) & \text{if } n \text{ is odd} \end{cases} \tag{43}$$

When $p_c < 1/\sqrt{2}$, α_n is finite for all finite n, whereas when $p_c = p_G = 1/\sqrt{2}$, α_2 is infinite because the denominator in (42) is zero. To obtain a finite width at the multicritical point and along the spin-glass phase boundary, the mean α_1 must be zero, which leads to the Gaussian spin-glass scaling solutions.

As we show below, when $p_c < 1/\sqrt{2}$ the set of moments (42) describe a probability distribution, which we call $\mathscr{I}_0^{\alpha_1}$, which is unique up to the scale of the mean α_1. Our proof is accomplished using the Hamburger moment theorems (see, e.g., Reed and Simon[24]), which specify conditions

on the growth of the moments which must be satisfied in order for the moments to uniquely describe a probability distribution. In the following proposition we verify that these conditions are satisfied.

Proposition 6. Let $1/2 < p_c < 1/\sqrt{2}$ and $2p_c(2\lambda - 1) = 1$. Define $\{\alpha_n\}$ to be the set of moments given in Eq. (42). Then $\{\alpha_n\}$ are the moments of a probability density $\mathscr{I}_0^{\alpha_1}$ satisfying (40), which, for a specified finite mean α_1, is unique.

Proof. We begin with the existence proof, followed by the uniqueness proof. According to the (existence) Hamburger moment theorem, a set of moments $\{\alpha_i\}$ are the moments of a probability distribution if and only if $\forall N$, the $(N+1) \times (N+1)$ matrix A_N, with elements $(A_N)_{i,j} = \alpha_{i-1+j-1}$, is nonnegative definite. Let us verify this for the moments given by (42). To this end, let us approximate the $\{\alpha_i\}$ by the moments $\{\alpha_i^m\}$ obtained after m iterations of some probability distribution. Explicitly, starting with any initial distribution with mean α_1, iteration of the linear recursion relation (40) m times results in a probability distribution at the mth level, with moments $\{\alpha_i^m\}$. Below, we will show that these moments converge (exponentially fast in m) to the $\{\alpha_i\}$. However, because the distribution after any finite number of iterations is still a probability distribution, the $(N+1) \times (N+1)$ matrix A_N^m, with elements $(A_N^m)_{i,j} = \alpha_{i-1+j-1}^m$, is nonnegative definite. For any fixed N, this, together with the (exponential) convergence, implies that A_N must also be positive definite, as desired.

It remains to show that the $\{\alpha_i^m\}$ converge exponentially fast to the $\{\alpha_i\}$. Indeed, defining $\psi_n^m \equiv \alpha_{n+1} - \alpha_{n+1}^m$, it is found that $\psi_2^m = 2p_c^2 \psi_2^{m-1}$. Using this and formula (42) for α_{n+1} (as well as the corresponding formula for α_{n+1}^m), it is easy to verify inductively that, for each n, there is an $H(n)$ such that, for large m,

$$\psi_n^m \leqslant H(n)[2p_c^2]^{m+2-n} \tag{44}$$

which completes the existence proof.

Next, we show that once the mean is specified, this distribution is unique. According to the (uniqueness) Hamburger moment theorem, a probability distribution with moments $\{\alpha_i\}$ is unique if and only if there are finite constants C and D such that, $\forall n$, $|\alpha_n| \leqslant CD^n n!$. Here we will establish the stronger result that the moments $\{\alpha_i\}$ of $\mathscr{I}_0^{\alpha_1}(x)$ satisfy

$$|\alpha_n| \leqslant Cn^{n/a} e^{\kappa n} \tag{45}$$

where C and $\kappa = \kappa(\alpha_1)$ are finite constants and a is a number satisfying

$$a < a_0 \equiv -\log(2)/\log(p_c) \tag{46}$$

We will need this stronger result for our proof of completeness in Appendix D.

We will establish (45) by induction on n. We first note that for $n > 2$,

$$|\alpha_n| \leqslant D p_c^n \sum_{k=1}^{n-1} \binom{n}{k} |\alpha_k| \, |a_{n-k}| \tag{47}$$

where D is a finite constant. Next, in Eq. (47) we substitute the upper bound on $|\alpha_k|$ and $|\alpha_{n-k}|$ given by the inductive hypothesis. We bound the product $|\alpha_k| \, |\alpha_{n-k}|$ by the largest term in the sum, which occurs for $k = n/2$. Explicitly using the trivial relation $\sum \binom{n}{k} = 2^n$, we see that Eq. (47) becomes

$$|\alpha_n| \leqslant D C^2 e^{\kappa n} [(\tfrac{1}{2})^{1/a} \, 2p_c]^n \, n^{n/a} \tag{48}$$

Noting that $a < a_0$, we find that (48) is sufficient to verify (45), and thus completes the proof. ∎

The following corollary is an immediate consequence of the uniqueness proof.

Corollary. The density $\mathscr{I}_0^{\alpha_1}(x)$ defined in Proposition 6 is entire.

Proof. Equation (45) implies that the Fourier transform $\hat{\mathscr{I}}_0^{\alpha_1}(k)$ satisfies

$$|\hat{\mathscr{I}}_0^{\alpha_1}(k)| < C_1 \exp(-C_2 \, |k|^a) \tag{49}$$

for some constants $C_1 < \infty$ and $C_2 > 0$, and a satisfying (46). Thus, $\hat{\mathscr{I}}_0^{\alpha_1}(k)$ and $\mathscr{I}_0^{\alpha_1}(x)$ are entire. ∎

It is important to note that, although (40) is a linear relation for the random variables, it corresponds to a convolution for the densities

$$\rho_0(x) = \lambda \int_{-\infty}^{\infty} \rho_0(y) \, \rho_0\left(\frac{x}{p_c} - y\right) \frac{dy}{p_c} + (1 - \lambda) \int_{-\infty}^{\infty} \rho_0(y) \, \rho_0\left(-\frac{x}{p_c} - y\right) \frac{dy}{p_c} \tag{50}$$

This leads to the following equation for the Fourier transform:

$$\hat{\rho}_0(k) \equiv \int e^{ikx} \rho_0(x) \, dx = \lambda \hat{\rho}_0^2(p_c k) + (1 - \lambda) \, \hat{\rho}_0^2(-p_c k) \tag{51}$$

We use Eq. (51) to obtain the numerical results illustrated in Fig. 10.

5.2. Existence of a Ferromagnetic Solution

The ferromagnetic transition is like a pitchfork bifurcation, illustrated schematically in Fig. 11. When $\Delta \leqslant 0$ the unique globally attracting fixed point of the recursion relation is the paramagnetic solution $\rho(X) = \delta(X)$. At $\Delta = 0$, the paramagnetic solution becomes unstable, and two new ferromagnetic solutions emerge. The two ferromagnetic solutions are related by a change in sign of the magnetization; the one the system ultimately chooses depends on the boundary conditions.

Like the spin-glass transition, the ferromagnetic transition is a regular critical point, with only one degree of freedom. This degree of freedom is related to the indeterminacy in the mean of the scaling density $\mathscr{J}_0^m(X^*)$, and gives rise to a zero mode. In Section 5.2.1 we begin by considering the effects of small perturbations to the scaling fixed-point density $\mathscr{J}_0^m$ when $\Delta = 0$. From this we obtain a linear operator for which we compute the eigenfunctions and eigenvalues. These eigenfunctions are defined in terms of the scaling fixed-point density $\mathscr{J}_0^m$, and pose interesting mathematical problems which are discussed in Appendix D. In Section 5.2.2 we prove the existence of the ferromagnetic fixed points.

5.2.1. The Ferromagnetic Eigenfunctions. Recall that in Section 4.3 we introduced an operator $\mathscr{R}_\Delta(\rho_\Delta)$ [Eq. (30)], with zeros ρ_Δ of $\mathscr{R}_\Delta(\rho_\Delta)$ being fixed points of the recursion relation. The first step in applying the center manifold theorem is to linearize the operator $\mathscr{R}_0(\rho)$ [Eq. (30)] about the scaling fixed point, which is $\mathscr{J}_0^m$ for the ferromagnet.

In this section we obtain the eigenfunctions and eigenvalues of the linear operator. The eigenfunctions are expressed in terms of $\mathscr{J}_0^m(X^*)$, and in Appendix D we show that they form a complete set in, e.g.,

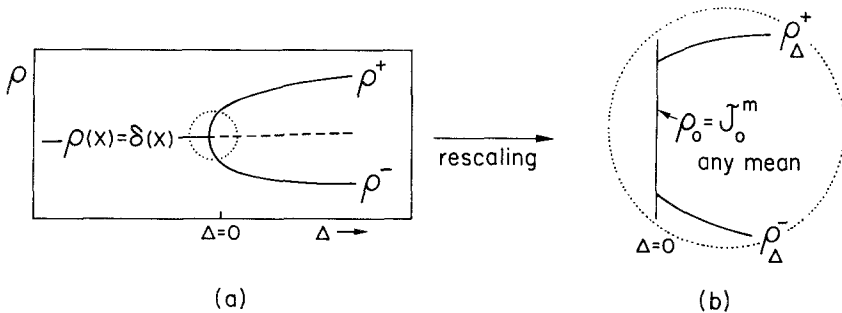(a)   (b)

Fig. 11. (a) The ferromagnetic transition is like a pitchfork bifurcation. At the transition two new solutions emerge which are related by a change in sign of the magnetization. (b) After rescaling, we obtain a continuum of solutions along the phase boundary. Two of these bifurcate, giving rise to nontrivial ferromagnetic densities.

$L^2(\cosh x\, dx)$. Here we use $L^2(\cosh x\, dx)$ for our bifurcation analysis, because convergence in this space [which is stronger than convergence in $L^2(dx)$] will allow us to make uniform convergence statements about the Fourier transforms of sequences of functions.

When the operator $\mathscr{R}_0(\rho)$ is linearized about the scaling fixed point $\mathscr{J}_0^m$, we obtain the linear operator given in Eq. (32), with $\rho_0(y)$ replaced by $\mathscr{J}_0^m(y)$. For the ferromagnet we will work with the Fourier transform of (32),

$$\hat{L} \circ \hat{f}(k) = 2\lambda \hat{\rho}_0(pk)\, \hat{f}(pk) + 2(1-\lambda)\, \hat{\rho}_0(-pk)\, \hat{f}(-pk) - \hat{f}(k) \quad (52)$$

where $\hat{\rho}_0(k) = \hat{\mathscr{J}}_0^m(k)$. To study the properties of this operator, we must first look for eigenfunctions

$$\hat{L} \circ \hat{f}_n(k) = v_n \hat{f}_n(k) \quad (53)$$

with v_n the associated eigenvalues.

First we obtain two sets of generalized eigenfunctions; from these we then select a complete set in $L^2(\cosh x\, dx)$. If we compare Eq. (52) with the scaling form of the recursion relation in k space (51), we note that when we multiply the fixed-point density by $|k^n|$ it satisfies the eigenvalue equation, with eigenvalue $v_n = 2p^n - 1$. Therefore,

$$\mathscr{A}_n = |k^n|\, \hat{\rho}_0(k) \quad (54)$$

are generalized eigenfunctions. Differentiating the scaling form of the recursion relation (51) once with respect to k, we obtain

$$\hat{\rho}_0'(k) = 2p\lambda \hat{\rho}_0(pk)\, \hat{\rho}_0'(pk) - 2p(1-\lambda)\, \hat{\rho}_0(-pk)\, \hat{\rho}_0'(-pk) \quad (55)$$

Comparing this with the eigenfunction equation, we deduce that

$$\hat{\mathscr{B}}_n = \operatorname{sign}(k)\, |k^n|\, \hat{\rho}_0'(k) \quad (56)$$

are also generalized eigenfunctions, with eigenvalue $v_n = 2p^n(2\lambda - 1) - 1 = p^{n-1} - 1$. When we inverse Fourier transform these functions to obtain their x-space counterparts, we find that, except for the even-integer $\mathscr{A}_n(x)$ and the odd-integer $\mathscr{B}_n(x)$, the functions behave poorly at infinity. This means that, with an appropriate definition of the relevant measure (e.g., $\cosh x\, dx$), these functions are not summable. However, the remaining functions [the even-integer $\mathscr{A}_n(x)$ functions and the odd-integer $\mathscr{B}_n(x)$ functions] form a complete set in $L^2(\cosh x\, dx)$; the proof of this is given in Appendix D. Thus, our k-space eigenfunctions are

$$\hat{\mathscr{J}}_n^m(k) = \begin{cases} k^n \hat{\rho}_0(k), & n \text{ even} \\ k^n \hat{\rho}_0'(k), & n \text{ odd} \end{cases} \quad (57)$$

where $\hat{\rho}_0(k) = \hat{\mathscr{J}}_0^m(k)$. This gives the following (complete) set of x-space eigenfunctions:

$$\mathscr{J}_n^m(x) = \begin{cases} d^n \mathscr{J}_0^m(x)/dx^n, & n \text{ even} \\ d^n(x \mathscr{J}_0^m(x))/dx^n, & n \text{ odd} \end{cases} \tag{58}$$

with associated eigenvalues (independent of m)

$$v_n = \begin{cases} 2p^n - 1, & n \text{ even} \\ 2p^n(2\lambda - 1) - 1, & n \text{ odd} \end{cases} \tag{59}$$

The point spectrum is plotted as a function of λ in Fig. 9. Note that the eigenvalues have the same functional form as the corresponding eigenvalues along the spin-glass phase boundary. However, since p_c is a function of λ along the ferromagnetic phase boundary, the curves look quite different.

With the exceptions of $\mathscr{J}_0^m$ and $\mathscr{J}_1^m$ with eigenvalues 1 and 0, respectively, the eigenfunctions have negative eigenvalues. The first eigenfunction $\mathscr{J}_0^m$ corresponds to the trivial "growth mode," analogous to the Gaussian solution $\mathscr{G}_0^\sigma$ in the spin-glass case. Here we focus on the marginal eigenfunction $\mathscr{J}_1^m$, which prevents the linear operator from being invertible. In accord with physical intuition, in this case the zero mode is associated with the mean of the distribution (whereas in the spin-glass case the zero mode is associated with the width), i.e., $\mathscr{J}_0^{m/c}(x) = c\mathscr{J}_0^m(xc)$, with

$$\mathscr{J}_1^m(x) = \frac{d}{dc}\mathscr{J}_0^{m/c}(x)\big|_{c=1} \tag{60}$$

Note that the low-momentum behavior is the same for the ferromagnetic eigenfunctions as it is for the spin-glass eigenfunctions, $\hat{\mathscr{J}}_n^m(k) \sim \hat{\mathscr{G}}_n^\sigma(k) \sim k^n$. However, unlike the Gaussian case, we have been unable to write the ferromagnetic eigenfunctions in terms of a single generating function as in Eq. (34), nor can we show that they are orthogonal with respect to some weight function.

The relative complexity of the ferromagnetic eigenfunctions is also apparent when we consider how the eigenfunctions combine under action of the bilinear operator (37), which will be important in the bifurcation analysis. Working with the transform of (37),

$$B_0[\hat{f}, \hat{g}] = \lambda \hat{f}(p_c k) \hat{g}(p_c k) + (1 - \lambda) \hat{f}(-p_c k) \hat{g}(-p_c k) \tag{61}$$

we find that

$$B_0[\hat{\mathscr{J}}_s^m, \hat{\mathscr{J}}_t^m] = \begin{cases} p^{s+t} \hat{\mathscr{J}}_{s+t}^m, & s, t \text{ even} \\ \frac{1}{2} p^{s+t-1} \hat{\mathscr{J}}_{s+t}^m, & s \text{ odd}, t \text{ even} \\ \sum\limits_{i=s+t}^\infty c_i \hat{\mathscr{J}}_i^m, & s, t \text{ odd} \end{cases} \tag{62}$$

In spite of the fact that when both s and t are odd, the eigenfunctions $\hat{\mathscr{J}}_s^m$ and $\hat{\mathscr{J}}_t^m$ do not combine in a simple way, we will be able to use the small-k behavior and the completeness of the eigenfunctions to conclude that the expansion of the resulting function in terms of the eigenfunctions begins with $\hat{\mathscr{J}}_{s+t}^m$ with coefficient $c_{s+t} = -p^{s+t}/m^2$.

5.2.2. Bifurcation of the Ferromagnetic Solution.

Now we are ready to use what we know about the linear operator to establish the existence of a ferromagnetic solution inside the phase boundary. The relevant bifurcation (illustrated in Fig. 12) is slightly different from the corresponding bifurcation (Fig. 8) for the spin glass, since at the ferromagnetic transition two solutions emerge instead of one. However (after rescaling) these solutions bifurcate from distinct points in function space, so that locally each of the two ferromagnetic bifurcations resembles the situation in Fig. 8. Of course, the two ferromagnetic solutions are related by a change in the sign of the magnetization.

In the remainder of this section we prove the following theorem, which verifies the existence of a nontrivial fixed point $\rho(X)$ in the ferromagnetic phase.

Theorem 7. Let $\Delta = p - p_c(\lambda)$ and let $\mathscr{R}_\Delta(\rho_\Delta)$ be defined as in (30), so that zeros of $\mathscr{R}_\Delta$ are fixed points of the recursion relation. For Δ
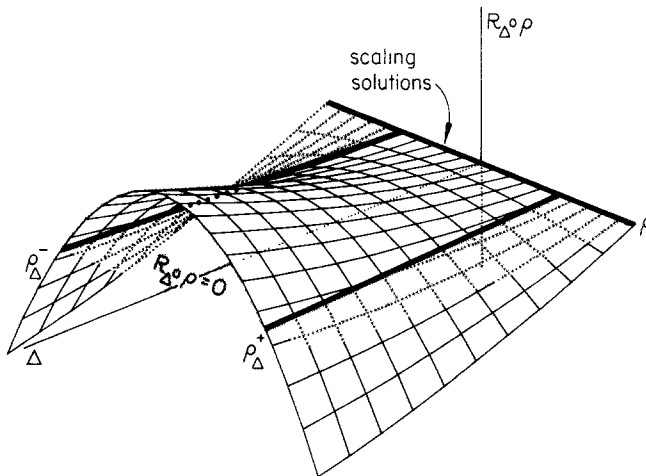

Fig. 12. At the ferromagnetic transition we apply the center manifold theorem to show how new solutions bifurcate from two of the scaling solutions.

sufficiently small, there are two distinct one-parameter families of densities $\rho_\Delta^\pm$ which satisfy the equation

$$\mathscr{R}_\Delta(\rho_\Delta^\pm) = 0$$

The functions ρ_Δ^+ and ρ_Δ^- are simply related by a change in sign of their antisymmetric part. Their limiting behavior is given by

$$\lim_{\Delta \to 0} \rho_\Delta^\pm = \mathscr{J}_0^{\pm m^*}$$

where $\mathscr{J}_0^{\pm m}$ is as given in Proposition 6 and $m^* = \pm[(1 - 2p^2)/\mu^2 p^3]^{1/2}$.

To analyze the bifurcation of the ferromagnetic solution, we work in the Banach space $L^2(\cosh x \, dx)$ (for which $\{\mathscr{J}_n^m\}$ form a complete set, as proved in Appendix D). By the calculations of the previous section, it is clear that the kernel and the cokernel of the linear operator $\delta\mathscr{R}_0/\delta\rho_\Delta$ both have dimension one; both can be identified with the eigenfunction $\mathscr{J}_1^m$. Since these spaces are finite dimensional, we can apply the center manifold theorem (Section 4.3.2), which guarantees that when ε and Δ are sufficiently small, there are functions $g_{\varepsilon,\Delta}^m$ and $h^m(\varepsilon, \Delta)$ which satisfy

$$\mathscr{R}_\Delta(\mathscr{J}_0^m + \varepsilon\mathscr{J}_1^m + g_{\varepsilon,\Delta}^m) = h^m(\varepsilon, \Delta)\,\mathscr{J}_1^m \tag{63}$$

For each value of m, $h^m(\varepsilon, \Delta)$ is the amplitude of the $\mathscr{J}_1^m$ component of the left-hand side of (63). The function $g_{\varepsilon,\Delta}^m$ is selected to make all other components zero.

For given values of m, ε, and Δ, the argument of $\mathscr{R}_\Delta$ in (63) is a fixed point of the recursion relation if $h^m(\varepsilon, \Delta) = 0$. For example, at $\Delta = 0$, $h^m(\varepsilon, 0) = 0$ for a large range of ε, due to the fact that there is a continuum of scaling solutions, and that moving in the $\mathscr{J}_1^m$ direction [i.e., when $\varepsilon \neq 0$ in Eq. (63)] is essentially moving from one scaling solution to another. We prove the existence of nontrivial fixed points for $\Delta \neq 0$ by showing that there exist distinct curves along which $h^m(\varepsilon, \Delta) = 0$ emanating from two of the scaling solutions. Because they emerge from distinct points in the function space, they can be treated separately. Two conditions are sufficient to verify the existence of these curves: (1) particular scaling functions must correspond to critical points for $h^m(\varepsilon, \Delta)$, i.e., the gradient of $h^m(\varepsilon, \Delta)$ must be zero at the scaling functions with the right mean m^*; (2) these scaling functions must be saddle points. The second condition verifies that a distinct curve emerges from each $\mathscr{J}_0^{m^*}$. The proof of Theorem 7 is preceded by two lemmas. In the first we explore properties of $g_{\varepsilon,\Delta}^m$, and in the second we verify conditions 1 and 2 stated above. Together these prove the existence of a solution to the fixed-point equation. In the proof of the theorem, we

show that this solution is pointwise nonnegative and of norm one, and is therefore a probability density.

The eigenfunctions $\{\mathscr{I}_n^m\}$ are complete for any m; consequently, any m can be chosen and Eq. (63) will still hold. Of course, $g_{\varepsilon, \Delta}^m$ and $h^m(\varepsilon, \Delta)$ will depend on the chosen value of m. For simplicity, we choose $m = m^*$, the value of the mean for one of the bifurcating solutions. For $m = m^*$, the bifurcating scaling function corresponds to the origin in ε, Δ space ($\varepsilon = \Delta = 0$).

From the center manifold theorem we know that the $g_{\varepsilon, \Delta}^m \in L^2(\cosh x \, dx) \backslash \mathscr{I}_1^m$. However, in the first lemma we see that for our problem we can obtain somewhat stronger results.

Lemma 8. Let $g_{\varepsilon, \Delta}^m$ and $h^m(\varepsilon, \Delta)$ be the functions described in the center manifold theorem, which satisfy Eq. (63). Then, at $\Delta = 0$:

1. $g_{\varepsilon, 0}^m$ has no component along $\mathscr{I}_0^m$ or $\mathscr{I}_1^m$.
2. $\| g_{\varepsilon, 0}^m \| = O(\varepsilon)$.
3. $h^m(\varepsilon, 0) = 0$ for all $|\varepsilon| < 1$.

Proof. When $\Delta = 0$ the operator $\mathscr{R}_\Delta$ reduces to the linear convolution operator minus the identity operator [Eq. (50)]. By Proposition 6 (Section 5.1), we know that up to the mean, $\mathscr{I}_0^m$ is a unique fixed point of the linearized recursion relation. Therefore, the argument of the operator in Eq. (63) at $\Delta = 0$ must simply be an expansion of $\mathscr{I}_0^{m^\dagger}$ with the different mean $m^\dagger$. Evidently,

$$\mathscr{I}_0^m + \varepsilon \mathscr{I}_1^m + g_{\varepsilon, 0}^m = \mathscr{I}_0^{m^\dagger} \tag{64}$$

where $m^\dagger$ is determined by ε.

Fourier transforming Eq. (64) leads to an identical equation in k space. Solving this equation for $\hat{g}_{\varepsilon, 0}^m$, we obtain

$$\hat{g}_{\varepsilon, 0}^m = \hat{\mathscr{I}}_0^{m^\dagger} - \hat{\mathscr{I}}_0^m - \varepsilon \hat{\mathscr{I}}_1^m \tag{65}$$

Using the small-k behavior of the eigenfunctions (Lemma D.5), we find that to zeroth order in k, the right-hand side vanishes, indicating that $\hat{g}_{\varepsilon, 0}^m$ has no component along $\hat{\mathscr{I}}_0^m$. By the center manifold theorem we know that $\hat{g}_{\varepsilon, 0}^m$ has no component along $\hat{\mathscr{I}}_1^m$. This proves condition 1, and as a result we find that

$$m^\dagger = (1 + \varepsilon) \, m \tag{66}$$

Next we let $\mathscr{I}_0^{m^\dagger} = \mathscr{I}_0^m(x/w(\varepsilon))$ for some function $w(\varepsilon)$. (Recall that

scaling solutions of different means are simply related to one another.) Equation (66) implies that

$$\int \mathscr{J}_0^m(x/w(\varepsilon))\, x\, dx = (1+\varepsilon)\, m \tag{67}$$

However, we can make the change of variables $u = x/w(\varepsilon)$, so that Eq. (67) becomes

$$w^2(\varepsilon)\, m = (1+\varepsilon)\, m \tag{68}$$

because the first moment of $\mathscr{J}_0^m(x)$ is m. Thus, we have $w(\varepsilon) = (1+\varepsilon)^{1/2}$. This, together with the small-k behavior of the functions $\{\mathscr{J}_n^m\}$, indicates that $\|g_{\varepsilon,0}^m\| = O(\varepsilon)$. Finally, condition 3 follows from the fact that the Taylor expansion of $(1+\varepsilon)^{1/2}$ converges for $|\varepsilon| < 1$. ∎

Next we show that the fixed-point equation has a nontrivial solution for positive values of $\varDelta$.

Lemma 9. Let $h^m(\varepsilon, \varDelta)$ be the function described in the center manifold theorem and Lemma 8. Then the origin is a critical point if the mean is given by

$$m = \pm m^* = \pm \left(\frac{1 - 2p_c^2}{2p_c^3 \mu_c^2} \right)^{1/2} \tag{69}$$

Furthermore, for these values of the mean, the origin is a saddle point.

Remark. The bifurcating solutions are illustrated schematically in Fig. 12. The fact that the magnetization has the form (69) implies that the critical exponent of the transition is $\beta = 1/2$, consistent with other mean field theories of ferromagnetic transitions.

Proof. Sufficient conditions for the origin to be a critical point are:

1. $\dfrac{\partial h^m}{\partial \varepsilon}(0, 0) = 0.$

2. $\dfrac{\partial h^m}{\partial \varDelta}(0, 0) = 0.$

Condition 1 follows from the previous lemma. In order to prove condition 2, we have to do a little work. Note that condition 1 is satisfied at points other than $(0, 0)$, while condition 2 is satisfied only at a single point, which, by our choice $m = m^*$, turns out to be the origin.

Expanding both sides of (63) and matching terms of order $\varDelta$ indicates

that $(\partial h^m/\partial\Delta)(0,0)$ can be identified with the $\mathcal{J}_1^m$ component of $(d/d\Delta)[\mathcal{R}_\Delta(\mathcal{J}_0^m)]_{\Delta=0}$. Using (29) and (30), this is given by the sum of two terms,

$$\frac{d}{d\Delta}[\mathcal{R}_\Delta(\mathcal{J}_0^m)]_{\Delta=0} = I_1 + I_2 \tag{70}$$

where

$$I_1 = \lambda \int \mathcal{J}_0(y)\,\mathcal{J}_0\left(\frac{x}{p_c} - y\right)[2\mu_c^2 xy - 1 - \mu_c^2 p_c\,y^2]\frac{dy}{p_c^2}$$

$$+ (1-\lambda)\int \mathcal{J}_0(y)\,\mathcal{J}_0\left(-\frac{x}{p_c} - y\right)[-2\mu_c^2 xy - 1 - \mu_c^2 p_c\,y^2]\frac{dy}{p_c^2} \tag{71}$$

$$I_2 = \lambda \int \mathcal{J}_0(y)\,\mathcal{J}_0'\left(\frac{x}{p_c} - y\right)\left[-y - \left(\frac{x}{p_c} - y\right)(1 - \mu_c^2 xy)\right]\frac{dy}{p_c^2}$$

$$+ (1-\lambda)\int \mathcal{J}_0(y)\,\mathcal{J}_0'\left(-\frac{x}{p_c} - y\right)\left[-y - \left(-\frac{x}{p_c} - y\right)(1 + \mu_c^2 xy)\right]\frac{dy}{p_c^2}$$

In the above equation the prime denotes a derivative with respect to the argument, and, to simplify notation, we have dropped the superscript m on the scaling fixed point $\mathcal{J}_0^m$. We see that the integrals are convolutions; hence, the Fourier transforms are easy to calculate:

$$\hat{I}_1 = -2\mu_c^2 B_0[\hat{\mathcal{J}}_0', \hat{\mathcal{J}}_0'] - \mu_c^2 B_0[\hat{\mathcal{J}}_0, \hat{\mathcal{J}}_0''] - \frac{1}{p_c}B_0[\hat{\mathcal{J}}_0, \hat{\mathcal{J}}_0]$$

$$\hat{I}_2 = \frac{1}{p_c}B_0[\hat{\mathcal{J}}_0', (k\hat{\mathcal{J}}_0)] + \frac{1}{p_c}B_0[\hat{\mathcal{J}}_0, (k\hat{\mathcal{J}}_0)'] \tag{72}$$

$$+ \mu_c^2 B_0[\hat{\mathcal{J}}_0', (k\hat{\mathcal{J}}_0)''] + \mu_c^2 B_0[\hat{\mathcal{J}}_0'', (k\hat{\mathcal{J}}_0)']$$

where B_0 is the k-space bilinear operator given in Eq. (61), and the primes denote derivatives with respect to k.

Now, using the small-k behavior (Lemma D.5), we can calculate the $\hat{\mathcal{J}}_1^m$ component of these integrals, which is associated with the coefficient of k in the Taylor expansion of the integrals about the origin. We find that, to leading order in k,

$$I_1 + I_2 = imk\left(\frac{1}{p_c} - \mu_c^2 q\right) + O(k^2) \tag{73}$$

where q is the second moment of $\mathscr{J}_0^m$. The leading behavior of $\hat{\mathscr{J}}_1^m$ is given by $imk + O(k^2)$. Therefore

$$I_1 + I_2 = \left(\frac{1}{p_c} - \mu_c^2 q \right) \hat{\mathscr{J}}_1^m + O(\hat{\mathscr{J}}_2^m) \tag{74}$$

which implies that

$$\frac{\partial h^m}{\partial \Delta}(0, 0) = \left(\frac{1}{p_c} - \mu_c^2 q \right) \tag{75}$$

Consequently, the origin is a critical point if and only if the second moment has the special value

$$q^* = \frac{1}{\mu_c^2 p_c} \tag{76}$$

It is interesting to note that the second moment is given by the same function of p_c as is found for the symmetric spin glass.

Our moment equations (42) for the scaling form of the distribution indicate that

$$q = \frac{2p_c^2 m^2}{1 - 2p_c^2} \tag{77}$$

Therefore, when q has the value specified in (76), the first moment has the form given in (69). Note also that the sign of m^* is arbitrary.

It remains to be shown that when $m = \pm m^*$, the origin is actually a saddle point. To do this we show that the Hessian

$$H = h_{\varepsilon\varepsilon}^m h_{\Delta\Delta}^m - h_{\varepsilon\Delta}^m h_{\Delta\varepsilon}^m$$

is negative. By Lemma I.8, $h_{\varepsilon\varepsilon}^m(0, 0) = \partial^2/\partial\varepsilon^2[h^m(\varepsilon, 0)]_{\varepsilon=0} = 0$. Therefore, it suffices to show

$$h_{\varepsilon\Delta}^m(0, 0) = \frac{\partial^2 h^m(\varepsilon, \Delta)}{\partial\Delta \, \partial\varepsilon}\bigg|_{\varepsilon=0, \Delta=0} \neq 0 \tag{78}$$

when $m = \pm m^*$.

Note that $h_{\varepsilon\Delta}^m(0, 0)$ is the component of

$$\frac{\partial}{\partial\Delta}\left[\frac{\partial}{\partial\varepsilon} \mathscr{R}_\Delta(\mathscr{J}_0^m + \varepsilon\mathscr{J}_1^m + g_{\varepsilon,\Delta}^m) \right]_{\Delta=0, \varepsilon=0} \tag{79}$$

along $\mathscr{J}_1^m$. In order to compute this operator, we first take the functional

derivative of $\mathcal{R}_\Delta$ evaluated at $\mathcal{J}_0^m$, and then differentiate with respect to Δ, and finally evaluate the result at $\Delta = 0$. The result is

$$\frac{\partial}{\partial \Delta}\left[\frac{\partial}{\partial \varepsilon}\, \mathcal{R}_\Delta(\mathcal{J}_0^m + \varepsilon \mathcal{J}_1^m + g_{\varepsilon,\Delta}^m)\right]$$

$$= 2[K_1(\mathcal{J}_0^m, \mathcal{J}_1^m) + K_2(\mathcal{J}_0^m, \mathcal{J}_1^m)]$$

$$\equiv 2C_0[\mathcal{J}_0^m, \mathcal{J}_1^m] \tag{80}$$

where K_1 and K_2 are the bilinear operators I_1 and I_2 used in our previous calculation (71), with $\mathcal{J}_0^m(y)$ replaced by $\mathcal{J}_1^m(y)$, and C_0 is defined here for future reference. Upon Fourier transforming these integrals, we obtain

$$\hat{K}_1 = -2\mu_c^2 B_0[\hat{\mathcal{J}}_1', \hat{\mathcal{J}}_0'] - \mu_c^2 B_0[\hat{\mathcal{J}}_1'', \hat{\mathcal{J}}_0] - \frac{1}{p_c} B_0[\hat{\mathcal{J}}_1, \hat{\mathcal{J}}_0]$$

$$\hat{K}_2 = \frac{1}{p_c} B_0[\hat{\mathcal{J}}_1', (k\hat{\mathcal{J}}_0)] + \frac{1}{p_c} B_0[\hat{\mathcal{J}}_1, (k\hat{\mathcal{J}}_0)'] \tag{81}$$

$$+ \mu_c^2 B_0[\hat{\mathcal{J}}_1', (k\hat{\mathcal{J}}_0)''] + \mu_c^2 B_0[\hat{\mathcal{J}}_1'', (k\hat{\mathcal{J}}_0)']$$

where again B_0 is the k-space bilinear operator given in Eq. (61), and we have dropped the superscript m on the eigenfunctions to simplify notation.

As before, we use the small-k behavior to find the $\hat{\mathcal{J}}_1^m$ component of these integrals. We find that, near the origin,

$$\hat{K}_1 + \hat{K}_2 = imk\left(\frac{1}{2p_c} - \frac{3}{2}q\mu_c^2\right) + O(k^2) \tag{82}$$

so the $\hat{\mathcal{J}}_1^m$ component is given by

$$\hat{K}_1 + \hat{K}_2 = \left(\frac{1}{2p_c} - \frac{3}{2}q\mu_c^2\right)\hat{\mathcal{J}}_1^m + O(\hat{\mathcal{J}}_2^m) \tag{83}$$

Thus, when $q = 1/p_c\mu_c^2$ we find that

$$h_{\varepsilon\Delta}^m(0, 0) = -\frac{2}{p_c} \neq 0 \tag{84}$$

From this we may conclude that the origin is a saddle point when $m = \pm m^*$. ∎

The existence of fixed-point solutions follows from Lemmas 8 and 9.

Corollary. For Δ sufficiently small, there a two distinct one-parameter families of functions $f_\Delta^\pm(x) \in L^1(dx)$ which satisfy the fixed-point equation $R_\Delta(f_\Delta^\pm) = 0$.

Proof of Theorem 7. Given the above corollary, all that remains to be shown is that the $f_\Delta^\pm$ are pointwise nonnegative and of L^1 unit norm. To this end, we follow the strategy of ref. 2 and introduce the auxiliary nonlinear operator $\tilde{\mathscr{R}}_\Delta$ given by

$$\tilde{\mathscr{R}}_\Delta(f) = \mathscr{R}_\Delta(|f|) \tag{85}$$

for $f \in L^1(dx)$.

First we claim that for Δ sufficiently small, there are two distinct one-parameter families of densities $\tilde{f}_\Delta^\pm \in L^1(dx)$ satisfying the equation

$$\tilde{\mathscr{R}}_\Delta(\tilde{f}_\Delta^\pm) = 0 \tag{86}$$

As in the proof of Proposition 4.6 of ref. 2, this follows by verifying that the linear operators of the new fixed-point problem are identical to their analogues computed previously. It turns out that this is a simple consequence of the nonnegativity of $\mathscr{J}_0^m$.

Clearly the new fixed-point solutions are pointwise nonnegative: $\tilde{f}_\Delta^\pm \geq 0$. Next we show that the $\tilde{f}_\Delta^\pm$ are of unit norm. For this we define the analogue of the bilinear operator B_Δ of Eq. (26):

$$\tilde{B}_\Delta[f, g] = B_\Delta[|f|, |g|] \tag{87}$$

Here, rather than the integral-preserving property, we have

$$\int \tilde{B}_\Delta[f, g] = \|f\|_1 \|g\|_1 \tag{88}$$

for $f, g \in L^1(dx)$. However, the fixed-point equation (86) is equivalent to

$$\tilde{B}_\Delta[\tilde{f}_\Delta^\pm, \tilde{f}_\Delta^\pm] = \tilde{f}_\Delta^\pm \tag{89}$$

Equations (88) and (89) imply $\|\tilde{f}_\Delta^\pm\|_1 = \|\tilde{f}_\Delta^\pm\|_1^2$, so that $\|\tilde{f}_\Delta^\pm\|_1 = 1$. Finally, we claim that solutions $f_\Delta^\pm$ of the original problem are equal to those of the auxiliary problem, Indeed, by nonnegativity,

$$\tilde{B}_\Delta[\tilde{f}_\Delta^\pm, \tilde{f}_\Delta^\pm] = B_\Delta[\tilde{f}_\Delta^\pm, \tilde{f}_\Delta^\pm] \tag{90}$$

so that, by (89),

$$B_\Delta[\tilde{f}_\Delta^\pm, \tilde{f}_\Delta^\pm] = \tilde{f}_\Delta^\pm \tag{91}$$

This, however, is equivalent to the original fixed-point equation. Thus, by uniqueness of solutions, $\tilde{f}_\Delta^\pm = f_\Delta^\pm$, as claimed. ∎

Thus, we have shown that out of the continuum of solutions $\mathscr{J}_0^m$ of arbitrary mean which satisfy the recursion relation in the scaling limit,

there are exactly two solutions, corresponding to means $\pm m^*$, that can bifurcate into new solutions for nonzero Δ. The fact that the origin is a saddle point in each case shows that indeed these functions do bifurcate.

6. MULTICRITICAL POINT

The multicritical point (p_G, λ_N) is the point on the phase diagram (Fig. 1) where the paramagnetic phase boundaries for the ferromagnet and the spin glass meet. From the point of view of critical phenomena, multicritical points often exhibit particularly striking behavior. Intermediate phases and crossover effects in the scaling behavior can be observed. Multicritical points also have rich behavior from the point of view of dynamical systems. At a regular critical point (like the spin-glass or ferromagnetic transitions previously analyzed) there is only one degree of freedom, leading to a codimension-one bifurcation. At a multicritical point, there will be two or more degrees of freedom, leading to a higher-order bifurcation.

It is interesting to note that the Nishimori line,[25],10 $p = 2\lambda - 1$, intersects the phase diagram at the multicritical point, and that where the Nishimori line is in the paramagnetic phase, no magnetized phase exists below it (i.e., for $\lambda < \lambda_N$). In finite dimensions, Nishimori showed that this should be the case, and certain exact results are known along this line. Recently, using an exact renormalization group approach, Le Doussal and Georges obtained the corresponding results for certain hierarchical lattices.[26] Using local gauge invariance, Le Doussal and Harris showed that the multicritical point should lie on the Nishimori line.[27]

This section is organized as follows. In Section 6.1 we perform a simple moment analysis to determine when the symmetric spin-glass solution is linearly unstable to perturbations in the mean. This instability coincides with the phase boundary separating the spin-glass from the magnetized spin-glass phase in Fig. 1. In Section 6.2 we perform a bifurcation analysis at the multicritical point. Here the recursion relation exhibits a twofold instability yielding a codimension-two bifurcation. This analysis shows that a pair of magnetized solutions emerge at the spin glass–MSG phase boundary. Because the phase boundary bends away from a vertical line toward $\lambda = 1$, the spin-glass phase is reentrant, as observed in many experimental spin glasses. On the other hand, we find that in the neighbor-

---

[10] Recall that the Nishimori line, defined by $P(-J_{ij})/P(J_{i,j}) = \exp(-2\beta J_{ij})$, where $P(J_{ij})$ is the probability distribution over the random bonds, is a special line in the phase diagram along which certain exact results, e.g., an expression for the quenched internal energy, can be obtained.

hood of the multicritical point there is no sharp change in $\rho(X)$ at the ferromagnet to magnetized spin-glass transition. Consequently, in the linear stability and bifurcation analyses we will speak of a magnetized solution, since we cannot distinguish between the ferromagnet and magnetized spin glass.

6.1. The MSG-SG Phase Boundary

In Section 3, we determined the lines along which the paramagnetic solution $\rho(x) = \delta(x)$ becomes unstable to perturbations in the width and mean, corresponding to the (potential) onset of spin-glass and ferromagnetic order. (The proof of existence of these phases required the full bifurcation analyses of Sections 4 and 5.) In this section, we do a moment analysis to determine the line along which the symmetric spin-glass solution becomes unstable to perturbations in the mean. While this argument does not prove the existence of a stable asymmetric distribution, it is simple, and it yields the phase boundary separating the spin-glass from the magnetized spin-glass phase.

Proposition 10. Let $\Delta = p - p_G \gtrsim 0$ and $\zeta(\Delta) = \Delta^{-1}(\lambda - \lambda_N) \equiv \zeta_0 + \zeta_1 \Delta$. Then, for asymptotically small Δ, the symmetric spin-glass solution is linearly stable with respect to perturbations in the mean when $\zeta(\Delta) < p_G \Delta$.

Remark. The limiting case of equality

$$|\lambda - \lambda_N|^{1/2} = p_G^{1/2} |p - p_G| \tag{92}$$

determines the asymptotic form of the phase boundary between the spin glass and magnetized spin glass, illustrated in Fig. 1. Note that because the coefficient of $|p - p_G|$ in (92) is positive, the spin-glass phase boundary is reentrant.

Proof. The method of proof is similar to moment analysis; however, here we calculate the leading behavior of the moments of *our solution*. Because we calculate the moments of this particular solution, rather than obtaining general bounds, we avoid large overestimates of the higher-order terms in moment expansions. Explicitly, we use the following two facts from our bifurcation analysis. First, because our spin-glass solution is symmetric, we can ignore all odd moments. Second, we use the fact that $t_n \equiv E(Y^4) = O(q_n^2)$, which allows us to neglect certain terms.

In Section 4.3 our results from the bifurcation analysis indicate that to leading order in Δ,

$$q = \frac{\Delta}{p_G \mu_G^2} \tag{93}$$

This can also be seen directly from the following moment calculation. Squaring the recursion relation (12), which is the (unrescaled) recursion relation used in the bifurcation theory, we obtain

$$X^2 = \frac{p^2(Y^2 + Z^2 + 2YZ)}{(1 + \mu^2 YZ)^2} = F^2(Y, Z; \theta) \tag{94}$$

Expanding the denominator yields

$$X^2 = p^2(Y^2 + Z^2 + 2YZ)(1 - 2\mu^2 YZ + 3\mu^4 Y^2 Z^2 - 4\mu^6 Y^3 Z^3)$$
$$+ (5\mu^8 Y^4 Z^4 + 6\mu^{10} Y^5 Z^5) F^2(Y, Z; \theta) \tag{95}$$

Taking the expectation gives us

$$q_{n+1} = 2p^2 q_n + 2p^2 m_n^2 - 4p^2 \mu^2 q_n^2 - 4p^2 \mu^2 m_n r_n + 6p^2 \mu^4 q_n t_n + 6p^2 \mu^4 r_n^2$$
$$- 8p^2 \mu^6 r_n s_n - 8p^2 \mu^6 t_n^2 + E[(5\mu^8 Y^4 Z^4 + 6\mu^{10} Y^5 Z^5) F^2(Y, Z; \theta)] \tag{96}$$

where $r_n = E(Y^3)$, $t_n = E(Y^4)$, $s_n = E(Y^5)$, and the last term is $O(q_n t_n^2)$. To obtain q for our spin-glass solution, we solve this equation self-consistently (set $q_{n+1} = q_n = q$), and set all odd moments equal to zero. Near the transition the leading-order terms are given by

$$q = 2p^2 q - 4p^2 \mu^2 q^2 + O(qt) \tag{97}$$

where similar expansions of X^4 give $t = 3q^2 + O(\Delta^4)$, so that $qt = O(q^3)$. Therefore, to leading order, q is given by Eq. (93). To obtain q to order Δ^2, we simply retain terms of order Δ^3,

$$q = 2p^2 q - 4p^2 \mu^2 q^2 + 6p^2 \mu^4 qt + O(t^2) \tag{98}$$

From this, and the leading behavior of t cited above, we obtain q to quadratic order,

$$q = \frac{\Delta}{p_G \mu_G^2} + \frac{\Delta^2(6\mu_G^2 p_G - 2)}{\mu_G^4 p_G} + O(\Delta^3) \tag{99}$$

Using this information, we will now look for an instability with respect to perturbations in the mean. To do this, we assume that the distribution has some infinitesimal mean m_n on the nth level. Instability is associated with growth of the mean m upon iteration. We begin by expanding the recursion relation

$$X = p\theta(Y + Z)(1 - \mu^2 YZ + \mu^4 Y^2 Z^2 - \mu^6 Y^3 Z^3) + \mu^8 Y^4 Z^4 F(Y, Z; \theta) \tag{100}$$

and taking the expectation

$$m_{n+1} = 2p(2\lambda - 1)[m_n - \mu^2 m_n q_n + \mu^4 q_n r_n - \mu^6 r_n t_n] + \mu^4 E(Y^2 Z^2 F(Y, Z; \theta))$$

(101)

where the last term is $O(m_n q_n^2)$. A similar expansion shows that $r_n = 3m_n q_n + O(m_n q_n^2)$.

Our spin-glass solution is unstable if the coefficient of m_n is greater than unity. We claim that marginal stability occurs when $\zeta = O(\varDelta)$. To see this, let us substitute into (101) the values of the even moments obtained above for our solution. Using the leading behavior of r_n and keeping terms of order $\varDelta^2$ in the coefficient of m_n, we obtain

$$m_{n+1} = 2p(2\lambda - 1)[1 - \mu^2 q + 3\mu^4 q^2] \, m_n + O(\varDelta^3 m_n)$$

(102)

Substituting the expansion (99) for q yields

$$m_{n+1} = [1 + 4p_G \zeta \varDelta - 2\varDelta^2] \, m_n + O(\varDelta^3 m_n)$$

(103)

We observe that the coefficient is less than unity when to leading order $\zeta < p_G \varDelta$, indicating that in this case small perturbations in the mean are suppressed. On the other hand, when $\zeta > p_G \varDelta$ to leading order, the coefficient of m_n is greater than unity, implying instability. The limiting case of equality determines the asymptotic form of the phase boundary. ∎

6.2. Multicritical Point: A Bifurcation Analysis

In this section we use bifurcation theory to determine the densities of single-site magnetization $\rho(X)$ which satisfy the full nonlinear recursion relation (4) in the neighborhood of the multicritical point, $p = p_G$, $\lambda = \lambda_N$. At this point there is a twofold instability [associated with the width and mean of $\rho(X)$], which reflects the fact that both the symmetric spin-glass and magnetized phases can be reached. Here we speak generally of the magnetized phases because the bifurcation analysis does not distinguish between the magnetized spin glass and ferromagnet: in the neighborhood of the multicritical point there is no sharp change in $\rho(X)$ at the transition. The asymptotic form of the phase boundary between the spin glass and magnetized spin glass (Fig. 1) discussed in the previous section coincides with the emergence of magnetized solutions.

Both the spin-glass and magnetized phases exist in an arbitrarily small neighborhood of the multicritical point, so that the nature of the existing solutions will depend on the direction in which one moves at the transition. Entering the spin-glass phase, the only solution which bifurcates from

the unstable paramagnetic solution is the symmetric spin-glass solution which was encountered previously in Section 4.3. The spin-glass solution continues to exist whenever $2p^2 > 1$; however, in the magnetized phases two additional solutions emerge, corresponding to the $\pm m$ magnetized ferromagnetic or MSG states. Consequently, for certain ranges of p and λ, three solutions will bifurcate. This situation is illustrated in Fig. 13a.

For the spin-glass and ferromagnetic transitions, the bifurcation analysis began with a look at the scaling solutions along the phase boundary (Sections 4.2 and 5.1). As in those cases, we define $\Delta = p - p_G > 0$. We rescale the random variables $X \rightarrow X^* = X/\sqrt{\Delta}$, and at $\Delta = 0$ we retrieve the linear scaling form of the recursion relation (40). At the multicritical point our results from the analysis of the spin-glass transition continue to hold. The scaling solution is again a Gaussian $\mathscr{G}_0^\sigma(X^*)$ of some arbitrary finite width. It is interesting to note that at the multicritical point asymmetric magnetized solutions bifurcate from a symmetric scaling solution. This occurs because, in terms of the original variables, asymptotically m approaches zero faster than $\sqrt{\Delta}$ near the multicritical point. In our analysis we find that both of the magnetized solutions bifurcate from the same Gaussian (these solutions differ only in the sign of the odd moments; the even moments are the same), while generally [i.e., when $\zeta(0) > 0$] the symmetric spin-glass solution bifurcates from a Gaussian with a different width. (See Fig. 13b.)

We apply the center manifold theorem (see Section 4.3) to show how new solutions bifurcate from some of the scaling solutions. At the multi-
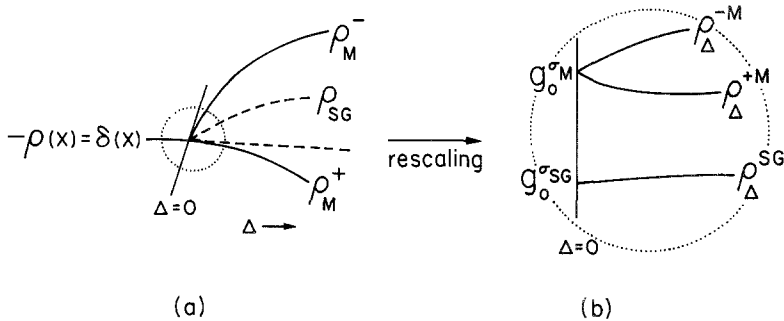

(a)   (b)

Fig. 13. (a) At the multicritical point, for certain ranges of Δ and ζ, three new solutions emerge from the unstable paramagnetic density; one is the unstable spin-glass solution, and the other two are stable magnetized solutions, related by a change in sign of the magnetization. (b) The two magnetized solutions bifurcate from the same Gaussian scaling solution, while typically the symmetric spin-glass solution bifurcates from a Gaussian of a different width. However, the three solutions merge at the phase boundary between the spin-glass and magnetized phases.

critical point the eigenfunctions of the linear operator [Eq. (32)] are the Hermite functions multiplied by Gaussians, $\mathscr{G}_n^\sigma(x) = H_n(x/\sigma) \, \mathscr{G}_0^\sigma(x)$, where σ^2 is the variance of the Gaussian $\mathscr{G}_0^\sigma$, as was the case along the spin-glass critical line. The associated eigenvalues are given in Eq. (35), and the point spectrum is illustrated in Fig. 9. Along the spin-glass phase boundary, the even eigenvalues, which depend only on p, remain fixed. The bifurcation analysis reveals that the evn eigenfunctions (which are symmetric in x) are the only relevant ones in the spin-glass phase, since the spin-glass density is symmetric. On the other hand, the eigenvalues of the odd (antisymmetric) eigenfunctions do vary as we move along the spin-glass phase boundary. When the bond distribution is symmetric ($\lambda = 1/2$), all of the odd eigenfunctions have eigenvalue -1, whereas at the multicritical point, each odd eigenvalue ν_{2n-1} becomes degenerate with an even eigenvalue ν_{2n}. In particular, at the multicritical point (and only at this point) there are two zero modes $\mathscr{G}_1^\sigma$ and $\mathscr{G}_2^\sigma$. It is here that the odd eigenfunctions play an important role: there are two unstable manifolds in the function space, giving rise to a codimension-two bifurcation.

Theorem 11. Define $\Delta = p - p_G > 0$ and $\zeta(\Delta) = \Delta^{-1}(\lambda - \lambda_N)$, and let $\mathscr{R}_\Delta$ be as given in Eq. (30). Then for positive Δ sufficiently small, there exists at least one one-parameter family of densities $\rho_\Delta \in L^2$ satisfying

$$\mathscr{R}_\Delta(\rho_\Delta) = 0$$

One particular family corresponds to a symmetric spin-glass solution, and has the property that

$$\lim_{\Delta \to 0} \rho_\Delta = \mathscr{G}_0^{\sigma_G}$$

where $\mathscr{G}_0^\sigma$ is a normalized Gaussian of width σ:

$$\mathscr{G}_0^\sigma = (\pi \sigma^2)^{-1} \exp(-x^2/\sigma^2)$$

and $(\sigma_G)^2 = 2/[p_G(2p_G - 1)]$. Furthermore, this solution is unique if $\lim_{\Delta \to 0} \zeta(\Delta)/\Delta < p_G$. However, if $\lim_{\Delta \to 0} \zeta(\Delta)/\Delta > p_G$, exactly two additional asymmetric families of solutions exist. These solutions are related by a change in sign of the odd moments and have the property that

$$\lim_{\Delta \to 0} \rho_\Delta = \mathscr{G}_0^{\sigma_M}$$

where $(\sigma_M)^2 = 2[2\zeta(0) + 1]/[p_G(2p_G - 1)]$.

Remark. Because the eigenfunctions are the same as the spin-glass eigenfunctions, a proof of the bifurcation of the spin-glass solution at any point along the phase boundary is contained in the proof we give below.

We work in the Banach space $L^2(\cosh x \, dx)$, which is spanned by the eigenfunctions $\{\mathscr{G}_n^\sigma\}$ (see Appendix D). As stated previously, at the multi-critical point both $\mathscr{G}_1^\sigma$ and $\mathscr{G}_2^\sigma$ have eigenvalue zero. Together they comprise the kernel and the cokernel of the linear operator $(\partial \mathscr{R}_0/\partial \rho)$. By the center manifold theorem we are guaranteed the existence of the functions g, h_1, h_2 which satisfy

$$\mathscr{R}_\varDelta(\mathscr{G}_0^\sigma + \varepsilon_1 \mathscr{G}_1^\sigma + \varepsilon_2 \mathscr{G}_2^\sigma + g(\varepsilon_1, \varepsilon_2, \varDelta; \zeta))$$
$$= h_1(\varepsilon_1, \varepsilon_2, \varDelta; \zeta) \, \mathscr{G}_1^\sigma + h_2(\varepsilon_1, \varepsilon_2, \varDelta; \zeta) \, \mathscr{G}_2^\sigma \qquad (104)$$

Fixed points of the recursion relation are zeros of $R_\varDelta$. We begin by expanding both sides of Eq. (104) for small ε_1, ε_2, and $\varDelta$. The nonlinearities in the functional expansion determine particular curves $\varepsilon_1(\varDelta)$ and $\varepsilon_2(\varDelta)$ for which the right-hand side vanishes. These are the coefficients of $\mathscr{G}_1^\sigma$ and $\mathscr{G}_2^\sigma$, respectively, in the expansion of the fixed point in terms of the eigenfunctions. For convenience, we choose σ to be the width of the bifurcating Gaussian. When $\zeta(0) > 0$, the symmetric spin-glass solution and the magnetized solutions bifurcate from different Gaussians, so we can treat the bifurcations separately. [In this case, if for some reason we chose to look at the bifurcation of the spin-glass solution using the width appropriate to the magnetized state, we would find that the spin-glass solution bifurcated from a point other than the origin, with $\varepsilon_1(0) = \varDelta = 0$, but $\varepsilon_2(0) \neq 0$.] When $\lim_{\varDelta \downarrow 0} \zeta(\varDelta)/\varDelta < p_G$, only the symmetric spin-glass solution bifurcates. The most interesting case occurs in the intermediate regime, where $\zeta(0) = 0$ and $\lim_{\varDelta \downarrow 0} \zeta(\varDelta)/\varDelta \geqslant p_G$. In this case all three solutions bifurcate from the same Gaussian, but are distinguished by three different sets of curves $\varepsilon_1(\varDelta)$ and $\varepsilon_2(\varDelta)$. To all orders in perturbation theory, the symmetric spin-glass solution has $\varepsilon_1(\varDelta) = 0$, whereas the pair of magnetized solutions are related by $\varepsilon_1^-(\varDelta) = -\varepsilon_1^+(\varDelta)$. At the phase boundary, $\lim_{\varDelta \downarrow 0} \zeta(\varDelta)/\varDelta = p_G$, the curves for the three solutions coalesce.

The proof is contained in two lemmas, analogous to the lemmas used at the ferromagnetic transition (Section 5.2.2). The main difference between our analysis at the multicritical point and our previous analysis is that at the ferromagnetic and spin-glass transitions we had a one-parameter family of scaling solutions, and one unstable manifold in the function space. Moving in the direction of the zero mode corresponded to moving from one scaling solution to another. [See Eqs. (36) and (60).] At the multicritical point we again have a one-parameter family of scaling solutions, but now we have two unstable manifolds in function space. At the multi-

critical point one of the zero modes, $\mathscr{G}_2^\sigma$, corresponds to moving from one scaling solution to another. The other one, $\mathscr{G}_1^\sigma$, corresponds to an unstable direction which is orthogonal to $\mathscr{G}_0^\sigma$ and $\mathscr{G}_2^\sigma$.

In the first lemma we primarily examine properties of $g(\varepsilon_1, \varepsilon_2, \Delta; \zeta)$, and in the second we explicitly determine the leading behavior of the functions $h_1(\varepsilon_1, \varepsilon_2, \Delta; \zeta)$ and $h_2(\varepsilon_1, \varepsilon_2, \Delta; \zeta)$ in the neighborhood of the transition. It follows from the center manifold theorem that $g(\varepsilon_1, \varepsilon_2, \Delta; \zeta) \in L^2(\cosh x \, dx) \backslash \{\mathscr{G}_1^\sigma, \mathscr{G}_2^\sigma\}$. In the first lemma we obtain some stronger results.

Lemma 12. Let $g(\varepsilon_1, \varepsilon_2, \Delta; \zeta)$ be the function defined in the center manifold theorem, such that $g(\varepsilon_1, \varepsilon_2, \Delta; \zeta)$ satisfies Eq. (104). Then at $\Delta = 0$:

1. $g(\varepsilon_1, \varepsilon_2, 0; \zeta)$ has no component along $\mathscr{G}_0^\sigma$, $\mathscr{G}_1^\sigma$, or $\mathscr{G}_2^\sigma$.

2. $\|g(\varepsilon_1, \varepsilon_2, 0; \zeta)\| = O(\varepsilon_1 \varepsilon_2) + O(\varepsilon_2^2)$.

3. $h_1(\varepsilon_1, \varepsilon_2, 0; \zeta) = 0$ and $h_2(\varepsilon_1, \varepsilon_2, 0; \zeta) = \varepsilon_1^2 p_G^2$ for ε_1 and ε_2 sufficiently small.

Proof. From the center manifold theorem, we know that $g(\varepsilon_1, \varepsilon_2, 0; \zeta)$ has no component along $\mathscr{G}_1^\sigma$ or $\mathscr{G}_2^\sigma$. We are also guaranteed that

$$\mathscr{R}_0(\mathscr{G}_0^\sigma + \varepsilon_1 \mathscr{G}_1^\sigma + \varepsilon_2 \mathscr{G}_2^\sigma + g(\varepsilon_1, \varepsilon_2, 0; \zeta))$$
$$= h_1(\varepsilon_1, \varepsilon_2, 0; \zeta) \mathscr{G}_1^\sigma + h_2(\varepsilon_1, \varepsilon_2, 0; \zeta) \mathscr{G}_2^\sigma \qquad (105)$$

The uniqueness clause of the center manifold theorem says that if we can find a $g(\varepsilon_1, \varepsilon_2, 0; \zeta)$ such that (105) is satisfied for *any* h_1 and h_2, then this must be the only such function g. As an ansatz, we can try the functions h_1 and h_2 in statement 3 of the lemma: i.e., if we can find a g which satisfies

$$\mathscr{R}_0(\mathscr{G}_0^\sigma + \varepsilon_1 \mathscr{G}_1^\sigma + \varepsilon_2 \mathscr{G}_2^\sigma + g(\varepsilon_1, \varepsilon_2, 0; \zeta)) = \varepsilon_1^2 p_G^2 \mathscr{G}_2^\sigma \qquad (106)$$

then we will have verified statement 3. If, in addition, we can show that this $g(\varepsilon_1, \varepsilon_2, 0; \zeta)$ has no component along $\mathscr{G}_0^\sigma$ and that it satisfies condition 2, then we will be done. To this end, let us explicitly compute the $g(\varepsilon_1, \varepsilon_2, 0; \zeta)$ satisfying Eq. (106). We see that $g(\varepsilon_1, \varepsilon_2, 0; \zeta)$ begins at $\mathscr{G}_3^\sigma$, and the first few terms are given by

$$g(\varepsilon_1, \varepsilon_2, 0; \zeta)) = \varepsilon_1 \varepsilon_2 \mathscr{G}_3^\sigma + \left(\frac{\varepsilon_2^2}{2} + \varepsilon_1^2 \varepsilon_2 \right) \mathscr{G}_4^\sigma + \left(\frac{\varepsilon_1 \varepsilon_2^2}{2} + \frac{\varepsilon_1^3 \varepsilon_2}{3} \right) \mathscr{G}_5^\sigma + \cdots \qquad (107)$$

The center manifold theorem implies that $g(\varepsilon_1, \varepsilon_2, 0; \zeta) \in L^2(\cosh x \, dx)$, so that, by the results in Appendix D, g must have an eigenfunction expansion

which can be determined by the small-k behavior. Therefore, the expansion (107) must converge for ε_1 and ε_2 sufficiently small. This verifies statements 1–3 of the lemma. ∎

Remark. Comparing Lemma 12 to our previous analysis of the bifurcations of the ferromagnetic (Section 5.2.2) and spin-glass solutions,[2] we see that in those cases the function $h(\varepsilon, \Delta)$ vanished at $\Delta = 0$. This implied that the argument of $\mathscr{R}_0$ in (105) was simply the scaing solution $\mathscr{G}_0^\sigma$ (or $\mathscr{J}_0^m$ for the ferromagnet) at a different value of the width (or mean)—see, e.g., Eq. (64). However, in general, $h_i(\varepsilon_1, \varepsilon_2, 0; \zeta)$ need not vanish. Indeed, in the above lemma, we have $h_2(\varepsilon_1, \varepsilon_2, 0; \zeta) \neq 0$ for $\varepsilon_1 \neq 0$, indicating that the argument of $\mathscr{R}_0$ at $\varepsilon_1 \neq 0$ is not simply a Gaussian of a different width. In hindsight, this should come as no surprise, since $\mathscr{G}_1^\sigma$ is an odd function. Finally, note that when $\varepsilon_1 = 0$, the problem reduces to the bifurcation of the symmetric spin-glass solution (Theorem I.5 of Section 4.3.2).

Now, using the information from the previous lemma, we expand the left-hand side of (104) for small ε_1, ε_2, and Δ. The expansion for small Δ involves straightforward differentiation of the nonlinear operator (30). The expansion for small ε_1 and ε_2 involves functional derivatives of the operator evaluated along the zero modes. Because the bifurcation is higher order, to extract meaningful results we must expand $\mathscr{R}_\Delta$ to higher order, resulting in intricate computations. After enormous labor, we extract the coefficients of $\mathscr{G}_1^\sigma$ and $\mathscr{G}_2^\sigma$ in these expansions to explicitly determine $h_1(\varepsilon_1, \varepsilon_2, \Delta; \zeta)$ and $h_2(\varepsilon_1, \varepsilon_2, \Delta; \zeta)$. In addition, we determine particular curves $\varepsilon_1(\Delta)$ and $\varepsilon_2(\Delta)$ along which h_1 and h_2 are zero, which proves the existence of the desired solutions.

Lemma 13. Define $\Delta = p - p_G > 0$ and $\zeta(\Delta) = \Delta^{-1}(\lambda_N - \lambda)$. Let $h_1(\varepsilon_1, \varepsilon_2, \Delta; \zeta)$ and $h_2(\varepsilon_1, \varepsilon_2, \Delta; \zeta)$ be the functions described in Lemma 12. We distinguish several cases:

1. Suppose $\zeta(0) > 0$. If the variance is chosen according to

$$\sigma^2 = \frac{2[1 + 2\zeta(0)]}{\mu_G^2 p_G} \equiv \sigma_M^2 \tag{108}$$

then there is a nontrivial parametric curve $(\varepsilon_1(s), \varepsilon_2(s), \Delta(s))$ passing through the origin along which the functions h_1 and h_2 vanish simultaneously. On the other hand, if we choose

$$\sigma^2 = \frac{2}{\mu_G^2 p_G} \equiv \sigma_G^2 \tag{109}$$

then there is a nontrivial curve in the (ε_2, Δ) plane, emanating from the origin, along which h_1 and h_2 simultaneously vanish.

The two halves of the first curve corresponding to $\varepsilon_1(s) > 0$ and $\varepsilon_1(s) < 0$ represent the positively and negatively magnetized solutions, while the second curve represents the (here, linearly unstable) symmetric spin-glass solution. If we choose $\sigma = \sigma_M$, then the magnetized solutions emanate from the origin and the spin glass bifurcates from a different point, while if we choose $\sigma = \sigma_G$, then the spin glass emanates from the origin, and the magnetized solutions branch from a different point.

2. Suppose $\zeta(0) = 0$. Then there exist curves along which h_1 and h_2 simultaneously vanish only for $\sigma = \sigma_G$.

(a) If $\lim_{\Delta \downarrow 0} \zeta(\Delta)/\Delta > p_G$, then both magnetized and symmetric spin-glass curves exist, and both emanate from the origin.

(b) If $\lim_{\Delta \downarrow 0} \zeta(\Delta)/\Delta = p_G$, then the magnetized and symmetric spin-glass curves both emanate from the origin, and agree to leading order in Δ.

(c) If $\lim^{\Delta \downarrow 0} \zeta(\Delta)/\Delta < p_G$, only the symmetric spin-glass curve exists, here corresponding to a linearly stable solution.

Proof. As previously mentioned, h_1 and h_2 can be identified with the coefficients of $\mathscr{G}_1^\sigma$ and $\mathscr{G}_2^\sigma$, respectively, in the expansion of $\mathscr{R}_\Delta(\mathscr{G}_0^\sigma + \varepsilon_1 \mathscr{G}_1^\sigma + \varepsilon_2 \mathscr{G}_2^\sigma + g(\varepsilon_1, \varepsilon_2, \Delta; \zeta))$ in the neighborhood of the origin $(\Delta = \varepsilon_1 = \varepsilon_2 = 0)$. Expanding the operator $\mathscr{R}_\Delta$ to quadratic order in Δ yields

$$\mathscr{R}_\Delta = \mathscr{R}_0 + \Delta \partial \mathscr{R}_0 + \frac{\Delta^2}{2} \partial^2 \mathscr{R}_0 + O(\Delta^3) \tag{110}$$

where $\partial \mathscr{R}_0 \equiv (\partial \mathscr{R}_\Delta / \partial \Delta)_{\Delta = 0}$ and $\partial^2 \mathscr{R}_0 \equiv (\partial^2 \mathscr{R}_\Delta / \partial \Delta^2)_{\Delta = 0}$. Each term on the right-hand side of (110) can be thought of as an operator which acts on a pair of functions. At this stage in the expansion, these functions are both equal to the argument of $\mathscr{R}_\Delta$ in (104). To obtain the expansion for small ε_1 and ε_2 we calculate the Frechet derivative $\partial \mathscr{R}_\Delta / \partial \rho$ evaluated at the known solution. Furthermore, we need only keep track of terms which have nonzero components along $\mathscr{G}_1^\sigma$ and $\mathscr{G}_2^\sigma$. In terms of the bilinear operator $B_0[f, g]$ given in Eq. (37), we obtain

$$\mathscr{R}_\Delta(\mathscr{G}_0^\sigma + \varepsilon_1 \mathscr{G}_1^\sigma + \varepsilon_2 \mathscr{G}_2^\sigma + g(\varepsilon_1, \varepsilon_2, \Delta; \zeta))$$
$$= B_0[\mathscr{G}_0^\sigma, \mathscr{G}_0^\sigma] - \mathscr{G}_0^\sigma$$
$$+ 2\varepsilon_1 B_0[\mathscr{G}_0^\sigma, \mathscr{G}_1^\sigma] - \varepsilon_1 \mathscr{G}_1^\sigma + 2\varepsilon_2 B_0[\mathscr{G}_0^\sigma, \mathscr{G}_2^\sigma] - \varepsilon_2 \mathscr{G}_2^\sigma + \varepsilon_1^2 B_0[\mathscr{G}_1^\sigma, \mathscr{G}_1^\sigma]$$
$$+ \Delta \partial \mathscr{R}_0[\mathscr{G}_0^\sigma, \mathscr{G}_0^\sigma] + 2\varepsilon_1 \Delta \partial \mathscr{R}_0[\mathscr{G}_0^\sigma, \mathscr{G}_1^\sigma] + 2\varepsilon_2 \Delta \partial \mathscr{R}_0[\mathscr{G}_0^\sigma, \mathscr{G}_2^\sigma]$$
$$+ \varepsilon_1^2 \Delta \partial \mathscr{R}_0[\mathscr{G}_1^\sigma, \mathscr{G}_1^\sigma] + 2\varepsilon_1 \varepsilon_2 \Delta \partial \mathscr{R}_0[\mathscr{G}_1^\sigma, \mathscr{G}_2^\sigma] + \varepsilon_2^2 \Delta \partial \mathscr{R}_0[\mathscr{G}_2^\sigma, \mathscr{G}_2^\sigma]$$
$$+ \tfrac{1}{2} \Delta^2 \partial^2 \mathscr{R}_0[\mathscr{G}_0^\sigma, \mathscr{G}_0^\sigma] + \varepsilon_1 \Delta^2 \partial^2 \mathscr{R}_0[\mathscr{G}_0^\sigma, \mathscr{G}_1^\sigma] + O(\varepsilon_2 \Delta^2) + O(\varepsilon_1^2 \Delta^2)$$
$$+ O(\varepsilon_1 \Delta^3) \tag{111}$$

From our results in the previous lemma, we deduce that the terms in this expansion which come from $g(\varepsilon_1, \varepsilon_2, \Delta; \zeta)$ will not contribute to this order.

Next we determine the $\mathscr{G}_1^\sigma$ and $\mathscr{G}_2^\sigma$ components of this expansion term by term. The first seven terms in the above expansion are written explicitly in terms of the bilinear operator B_0 and the identity. The only nonzero contribution from this group of terms comes from the last term $\varepsilon_1^2 B_0[\mathscr{G}_1^\tau, \mathscr{G}_1^\tau]$. From (38) it follows that the projection of this term onto the cokernel is given by

$$\varepsilon_1^2 B_0[\mathscr{G}_1^\sigma, \mathscr{G}_1^\sigma] \circ \{\mathscr{G}_1^\sigma, \mathscr{G}_2^\sigma\} = \varepsilon_1^2 p_G^2 \mathscr{G}_2^\sigma \tag{112}$$

The operators $\partial\mathscr{R}_0$ and $\partial^2\mathscr{R}_0$ can also be expanded in terms of the bilinear operator $B_0[f, g]$ and a related function. We begin with $\partial\mathscr{R}_0$. This operator is very similar to the operator $C_0[f, g]$ which we studied previously in our analysis of the ferromagnet [Eq. (80)]. Now, however, λ and p both depend on Δ, which gives rise to an additional term. For the ferromagnet (where only p depends on Δ), the operator C_0 is written in terms of B_0 operating on the eigenfunctions $\mathscr{J}_0^m$ and $\mathscr{J}_1^m$ and their derivatives in Eq. (81). To obtain the operator in this more general case, we include the additional term which arises because $\lambda = \lambda(\Delta) = \lambda_N + \zeta(\Delta)\,\Delta$, and we replace $\mathscr{J}_0^m$ and $\mathscr{J}_1^m$ with f and g, respectively, in Eq. (81). We write the resulting equation in terms of the Fourier transforms of the functions, where we recall that $\zeta(\Delta) = \zeta_0 + \zeta_1\Delta + O(\Delta^2)$,

$$\partial\mathscr{R}_0[\hat{f}(k), \hat{g}(k)] = \zeta_0[\hat{f}(p_G k)\,\hat{g}(p_G k) - \hat{f}(-p_G k)\,\hat{g}(-p_G k)] - \frac{1}{p_G} B_0[\hat{f}, \hat{g}]$$

$$- 2\mu_G^2 B_0[\hat{f}', \hat{g}'] - \mu_G^2 B_0[\hat{f}, \hat{g}''] + \frac{1}{p_G} B_0[(k\hat{f}), \hat{g}']$$

$$+ \frac{1}{p_G} B_0[(k\hat{f})', \hat{g}] + \mu_G^2 B_0[(k\hat{f})', \hat{g}''] + \mu_G^2 B_0[(k\hat{f})'', \hat{g}'] \tag{113}$$

The individual integrals are evaluated using the small-k expansions. From this we obtain the projection onto the cokernel $\{\mathscr{G}_1^\sigma, \mathscr{G}_2^\sigma\}$ for the relevant terms in (111),

$$\partial\mathscr{R}_0[\mathscr{G}_0^\sigma, \mathscr{G}_0^\sigma] \circ \{\mathscr{G}_1^\sigma, \mathscr{G}_2^\sigma\} = \left(p_G - \frac{\mu_G^2 p_G^2 \sigma^2}{2}\right)\mathscr{G}_2^\sigma$$

$$\partial\mathscr{R}_0[\mathscr{G}_0^\sigma, \mathscr{G}_1^\sigma] \circ \{\mathscr{G}_1^\sigma, \mathscr{G}_2^\sigma\} = \left(2p_G\zeta_0 + \frac{1}{2p_G} - \frac{\mu_G^2\sigma^2}{4}\right)\mathscr{G}_1^\sigma \tag{114}$$

$$\partial\mathscr{R}_0[\mathscr{G}_0^\sigma, \mathscr{G}_2^\sigma] \circ \{\mathscr{G}_1^\sigma, \mathscr{G}_2^\sigma\} = 2p_G(1 - p_G\mu_G^2\sigma^2)\,\mathscr{G}_2^\sigma$$

$$\partial\mathscr{R}_0[\mathscr{G}_1^\sigma, \mathscr{G}_2^\sigma] \circ \{\mathscr{G}_1^\sigma, \mathscr{G}_2^\sigma\} = -\mu_G^2\sigma^2\mathscr{G}_1^\sigma$$

A similar (and far more gruesome) calculation yields an expression for $\partial^2 \mathcal{R}_0$ in terms of B_0 and a related function. The following results are the only ones which will be necessary to proceed with our calculation:

$$\partial^2 \mathcal{R}_0[\mathcal{G}_0^\sigma, \mathcal{G}_1^\sigma] \circ \{\mathcal{G}_1^\sigma, \mathcal{G}_2^\sigma\}$$

$$= [4\zeta_0 + 4p_G\zeta_1 - p_G\mu_G^2\sigma^2(1 + 2\zeta_0) - \sigma^2 + \tfrac{3}{4}\mu_G^4\sigma^4] \mathcal{G}_1^\sigma \quad (115)$$

and

$$\partial^2 \mathcal{R}_0[\mathcal{G}_0^\sigma, \mathcal{G}_0^\sigma] \circ \{\mathcal{G}_1^\sigma, \mathcal{G}_2^\sigma\} = 2[1/2 - p_G\mu_G^2\sigma^2 - p_G^2\sigma^2 + \tfrac{9}{16}\mu_G^4\sigma^4] \mathcal{G}_2^\sigma \quad (116)$$

From the above expressions we obtain the functions h_1 and h_2 in the neighborhood of the origin,

$$h_1 = \left[4p_G\zeta_0 + \frac{1}{p_G} - \frac{\sigma^2\mu_G^2}{2} \right] \varepsilon_1 \Delta - 2\mu_G^2\sigma^2\varepsilon_1\varepsilon_2\Delta$$

$$+ \left[4\zeta_0 + 4p_G\zeta_1 - \sigma^2 - p_G\mu_G^2\sigma^2(1 + 2\zeta_0) + \frac{3\mu_G^4\sigma^4}{4} \right] \varepsilon_1 \Delta^2$$

$$+ O(\varepsilon_1\Delta^3) + O(\varepsilon_1\varepsilon_2\Delta^2)$$

$$h_2 = p_G^2\varepsilon_1^2 + \left[p_G - \frac{\mu_G^2 p_G^2 \sigma^2}{2} \right] \Delta + [4p_G - 4p_G^2\mu_G^2\sigma^2] \varepsilon_2 \Delta$$

$$+ \left[1/2 - p_G\mu_G^2\sigma^2 - p_G^2\sigma^2 + \frac{9}{16}\mu_G^4\sigma^4 \right] \Delta^2$$

$$+ O(\varepsilon_1^2\Delta) + O(\varepsilon_2^2\Delta) + O(\varepsilon_2\Delta^2) + O(\Delta^3)$$

$$(117)$$

A solution of the recursion relation for $\Delta > 0$ must have $h_1(\varepsilon_1, \varepsilon_2, \Delta; \zeta) = h_2(\varepsilon_1, \varepsilon_2, \Delta; \zeta) = 0$. First, consider the case $\zeta_0 > 0$. The leading order $[O(\varepsilon_1\Delta)]$ contribution to h_1 will be zero for $\varepsilon_1 \neq 0$ only when the variance of the Gaussian has the special value

$$\sigma_M^2 = \frac{2(2\zeta_0 + 1)}{\mu_G^2 p_G} \quad (118)$$

Consequently, for this value of the variance, the origin is a critical point for the magnetized solution. On the other hand, if $\varepsilon_1 = 0$, from the leading contribution $[O(\Delta)]$ to h_2, we find that the origin is a critical point for the symmetric solution when $\sigma = \sigma_G$, where

$$\sigma_G^2 = \frac{2}{\mu_G^2 p_G} \quad (119)$$

Let us focus on the magnetized solution: $\varepsilon_1 \neq 0$. We choose $\sigma = \sigma_M$. The condition $h_2 = 0$ is satisfied to $O(\Delta)$ when

$$\varepsilon_1(\Delta) = \pm \left(\frac{2\zeta_0 \Delta}{p_G} \right)^{1/2} \tag{120}$$

to leading order, which defines the surface of a symmetric *trough* resting on the ε_2 axis in the three-dimensional space defined by $\varepsilon_1, \varepsilon_2$, and Δ. Similarly, the condition $h_1 = 0$ is satisfied to $O(\Delta^2)$ when

$$\varepsilon_2(\Delta) = \frac{4\zeta_0 + 4p_G\zeta_1 - \sigma_M^2 - p_G\mu_G^2\sigma_M^2(1 + 2\zeta_0) + 3\mu_G^4\sigma_M^4/4}{2\mu_G^2\sigma_M^2} \Delta$$

$$= \left[\frac{\zeta_1}{2(2\zeta_0 + 1)} - \frac{1}{2\mu_G^2} + p_G(2\zeta_0 + 1) \right] \Delta \tag{121}$$

to leading order. Equation (121) defines a *plane* in $(\varepsilon_1, \varepsilon_2, \Delta)$ space which intersects the ε_1 axis at a finite angle, and which, consequently, *must* intersect the trough [Eq. (121)] in two distinct curves, which yield our magnetized solutions. This calculation proves that the scaling solution at the origin bifurcates when $\sigma = \sigma_M$, since we have explicitly determined nontrivial curves along which $h_1 = h_2 = 0$. Because $\varepsilon_1 = O(\sqrt{\Delta})$ and $\varepsilon_2 = O(\Delta)$, direct examination of (117) verifies that the additional terms which contribute to h_1 and h_2 are indeed higher order. Note that when $\varepsilon_1 = 0$, we retrieve the spin-glass solution, where the corresponding equation for $\varepsilon_2(\Delta)$ is given by setting $\zeta_0 = \zeta_1 = 0$ in (121).

Next we examine the case $\zeta_0 = 0$. By inspection of Eqs. (118) and (119), we see that $\sigma_M = \sigma_G$, so that magnetized and symmetric solutions must bifurcate from the same Gaussian. We consider the magnetized solution ($\varepsilon_1 \neq 0$). (Analysis of the symmetric spin-glass solution follows exactly as before.) As in the previous case, the plane $\varepsilon_2(\Delta)$ along which the solutions must lie is determined by the condition $h_2 = 0$, and is given by (121) with $\zeta_0 = 0$:

$$\varepsilon_2(\Delta) = \frac{\zeta_1}{2} - \frac{1}{2\mu_G^2} + p_G \tag{122}$$

to leading order. Similarly, the condition $h_2 = 0$ determines $\varepsilon_1(\Delta)$ for the magnetized solution. When $\sigma = \sigma_G, h_2 = 0$ on a surface given to leading order by

$$\varepsilon_1^2(\Delta, \varepsilon_2) = -\frac{1}{p_G^2} \left[(4p_G - 4p_G^2\mu_G^2\sigma_G^2) \varepsilon_2 \Delta \right.$$

$$\left. + \left(\frac{1}{2} - p_G\mu_G^2\sigma_G^2 - p_G^2\sigma_G^2 + \frac{9}{16}\mu_G^4\sigma_G^4 \right) \Delta^2 \right]$$

$$= 2\Delta \left[4p_G\varepsilon_2 - \left(\frac{3 - 2p_G}{\mu_G^2} \right) \Delta \right] \tag{123}$$

Substituting $\varepsilon_2(\Delta)$ from (122) into (123), we obtain $\varepsilon_1(\Delta)$ for the bifurcating magnetized solutions. It is important to note that in order for these solutions to exist, we must have $\varepsilon_1^2 \geqslant 0$, and hence

$$\varepsilon_2 \geqslant \left(\frac{3}{2} p_G - \frac{1}{2\mu_G^2} \right) \Delta \qquad (124)$$

From Eq. (122) we see that this is satisfied when $\zeta_1 \geqslant p_G$, where in the limiting case of equality, $\varepsilon_1 = 0$ to leading order, so that the symmetric spin-glass and magnetized solutions agree to order Δ. When $\zeta_1 < p_G$ the only solution is the symmetric spin-glass solution.

To determine the stability of the symmetric and magnetized solutions, we must calculate the leading corrections to the marginal eigenvalues v_1 and v_2 for each of the solutions. These are obtained by diagonalizing the operator $\mathcal{R}_\Delta$ to order Δ^2. This procedure is straightforward, and makes use of the integrals (114)–(116), which we have already evaluated. For the magnetized solution, we find that when $\zeta_0 > 0$

$$
\begin{aligned}
v_1(\Delta) &= -8\zeta_0 \Delta/p_G + O(\Delta^2) \\
v_2(\Delta) &= -2(1 + 2\zeta_0) \, \Delta/p_G + O(\Delta^2)
\end{aligned}
\qquad (125)
$$

whereas when $\zeta_0 = 0$ and $\zeta_1 \geqslant p_G$,

$$
\begin{aligned}
v_1(\Delta) &= -2\Delta^2(4p_G\zeta_1 - 2) + O(\Delta^3) \\
v_2(\Delta) &= -2\Delta/p_G + O(\Delta^2)
\end{aligned}
\qquad (126)
$$

In each case, for the magnetized solution, the leading corrections are seen to be negative. Thus we may conclude that when the magnetized solution exists, it is linearly stable. Similarly, we compute the corrections to the eigenvalues for the symmetric spin-glass solution. These are given by

$$
\begin{aligned}
v_1(\Delta) &= 4p_G\zeta_0\Delta + 4p_G\zeta_1\Delta^2 + O(\Delta^3) \\
v_2(\Delta) &= -2\Delta/p_G + O(\Delta^2)
\end{aligned}
\qquad (127)
$$

Because $v_1(\Delta) > 0$ in the magnetized phase, the symmetric spin-glass solution is unstable. ∎

The eigenfunction $\mathscr{G}_1^\sigma$ is associated with the mean, and the small-k expansion is given by $\hat{\mathscr{G}}_1^\sigma = i\sigma k + O(k^2)$. The coefficient ε_1 multiplied by the variance of the bifurcating Gaussian is the mean of the rescaled density in the neighborhood of the transition. From this we extract the scaling behavior of the unrescaled magnetization of our solution in the neighborhood of the multicritical point.

Corollary. Define $\Delta = p - p_G$ and $\zeta(\Delta) = \Delta^{-1}(\lambda - \lambda_N)$. Near the multicritical point (for small Δ), the mean of the magnetized solution determined in Theorem 11 is given by

$$m = \pm 2\Delta \left[\frac{2\zeta(1 + 2\zeta)}{\mu_G^2} \right]^{1/2} + O(\Delta^2)$$

when $\Delta > 0$ and $\lim_{\Delta \to 0} \zeta/\Delta > p_G$. If either $\Delta < 0$ or $\lim_{\Delta \to 0} \zeta/\Delta < p_G$, then $m = 0$.

Finally, we note that the magnetization as well as all the other moments of $\rho(X)$ are smooth in the neighborhood of the multicritical point throughout the magnetized phase(s). There are no sharp changes which could signal the existence of an intermediate phase. Nonetheless, in the companion paper (ref. 1, Section 2), we verify the existence of a magnetized spin-glass phase by calculating the Edwards–Anderson susceptibility.

APPENDIX A. DERIVATION OF THE MAGNETIC RECURSION RELATIONS

In this Appendix we give a derivation of a set of three coupled recursion relations for two coupled replicas of the lattice in an external field (Theorem A.3). All recursion relations used in this paper can be obtained as special cases. Since the formulas in Theorem A.3 are quite complicated, we begin with a derivation of the simple recursion relation, introduced in Section 2, for a single copy of the half-space Bethe lattice with forward branching ratio two:

$$X = \frac{p(\theta_y Y + \theta_z Z)}{1 + p^2 \theta_y \theta_z YZ} \tag{A1}$$

Equation (A1) was derived rigorously in ref. 2; however, here we present a much simpler derivation. Once (A1) has been derived, the methods are easily extended to the more general case for which we present an abbreviated derivation.

Theorem A.1. Let X be the magnetization of the origin. Then

$$X = \frac{p(\theta_y Y + \theta_z Z)}{1 + p^2 \theta_y \theta_z YZ} \tag{A2}$$

where Y and Z are the magnetization sites y and z would have if they were disconnected from x, $p = \tanh(J/kT)$, and θ_y and θ_z are the signs of the bonds joining sites y and z, respectively, to site x.

Proof. Consider the left subtree, which starts at site y. Let $\mathscr{A}_y$ be the partition function for that subtree, given $\sigma_y = +1$, and let $\mathscr{B}_y$ be the partion function for that subtree, given $\sigma_y = -1$. Define $\mathscr{A}_z$ and $\mathscr{B}_z$ to be the corresponding quantities for the subtree starting at site z. We can write the corresponding conditional partition functions for the half-space lattice (starting at x) in terms of these quantities:

$$\mathscr{A}_x = \mathscr{A}_y \mathscr{A}_z e^{\beta(\theta_y + \theta_z)J} + \mathscr{A}_y \mathscr{B}_z e^{\beta(\theta_y - \theta_z)J} + \mathscr{B}_y \mathscr{A}_z e^{-\beta(\theta_y - \theta_z)J}$$
$$+ \mathscr{B}_y \mathscr{B}_z e^{-\beta(\theta_y + \theta_z)J} \tag{A3}$$
$$= (\mathscr{A}_y e^{\beta\theta_y J} + \mathscr{B}_y e^{-\beta\theta_y J})(\mathscr{A}_z e^{\beta\theta_z J} + \mathscr{B}_z e^{-\beta\theta_z J})$$

Similarly,

$$\mathscr{B}_x = (\mathscr{A}_y e^{-\beta\theta_y J} + \mathscr{B}_y e^{\beta\theta_y J})(\mathscr{A}_z e^{-\beta\theta_z J} + \mathscr{B}_z e^{\beta\theta_z J}) \tag{A4}$$

The partition function and the magnetization are easily expressed in terms of these variables; for example,

$$\mathscr{Z}_y = \mathscr{A}_y + \mathscr{B}_y \tag{A5}$$

and

$$Y = \frac{\mathscr{A}_y - \mathscr{B}_y}{\mathscr{A}_y + \mathscr{B}_y} \tag{A6}$$

From this we deduce that

$$\mathscr{A}_y = \tfrac{1}{2}\mathscr{Z}_y(1 + Y)$$
$$\mathscr{B}_y = \tfrac{1}{2}\mathscr{Z}_y(1 - Y) \tag{A7}$$

Therefore

$$\mathscr{A}_y e^{\beta\theta_y J} + \mathscr{B}_y e^{-\beta\theta_y J} = \mathscr{Z}_y \cosh \beta J(1 + p\theta_y Y) \tag{A8}$$

Hence the magnetization of the origin is given by

$$X = \frac{\mathscr{A}_x - \mathscr{B}_x}{\mathscr{A}_x + \mathscr{B}_x} = \frac{p(\theta_y Y + \theta_z Z)}{1 + p^2 \theta_y \theta_z YZ} \tag{A9}$$

Finally, it is worth noting that this proof is easily extended to general branching ratio K, where we obtain[11]

$$X = \frac{\prod_{i=1}^{K}(1 + p\theta_i Y_i) - \prod_{i=1}^{K}(1 - p\theta_i Y_i)}{\prod_{i=1}^{K}(1 + p\theta_i Y_i) + \prod_{i=1}^{K}(1 - p\theta_i Y_i)} \quad \blacksquare \tag{A10}$$

Note that once the half-space lattices have settled down to the fixed point (i.e., after a sufficient number of iterations of the recursion relation), the same type of procedure can be used to join two half-space lattices and obtain the full-space quantities (e.g., the magnetization) in terms of the corresponding half-space quantities. Here we simply state the result; the proof is given in ref. 2 and also follows by the same type of method used above.

Proposition A.2. Let m_L be the half-space magnetization of the origin x_L for the left half-space lattice. Similarly, let m_R be the half-space magnetization of the origin x_R for the right half-space lattice. Let θ be the sign of the bond joining sites x_L and x_R. Then the full-space magnetization $\underline{m}_L$ of the site x_L is given by

$$\underline{m}_L = \frac{m_L + p\theta m_R}{1 + p\theta m_L m_R} \tag{A11}$$

where $p = \tanh(\beta J)$.

The same method applied to two coupled replicas of the lattice in a nonzero external field yields the set of coupled recursion relations discussed in Sections 2 and 3 of the companion paper.

Theorem A.3. Consider a system of two coupled copies of the same quench of the lattice. Let σ_x^U denote the spin at site x on the upper lattice, and let σ_x^L denote the spin at site x on the lower lattice. Let R be the ferromagnetic coupling strength of each site on the upper lattice to the corresponding site on the lower lattice. At each site we define the following quantities:

$$\begin{aligned} Q_x &= \langle \sigma_x^U \sigma_x^L \rangle \\ S_x &= \langle \sigma_x^U \rangle + \langle \sigma_x^L \rangle \\ D_x &= \langle \sigma_x^U \rangle - \langle \sigma_x^L \rangle \end{aligned} \tag{A12}$$

In terms of these quantities we have the following set of coupled recursion relations:

$$Q_x = \frac{G_{yz} + rF_{yz} + h^2(F_{yz} + rG_{yz}) + h\phi_x(1 + r) N_{yz}^s}{F_{yz} + rG_{yz} + h^2(G_{yz} + rF_{yz}) + h\phi_x(1 + r) N_{yz}^s} \tag{A13}$$

$$S_x = \frac{(1 + r)[(1 + h^2) N_{yz}^s + 2h\phi_x E_{yz}]}{F_{yz} + rG_{yz} + h^2(G_{yz} + rF_{yz}) + h\phi_x(1 + r) N_{yz}^s} \tag{A14}$$

$$D_x = \frac{(1 - r)(1 - h^2) N_{yz}^d}{F_{yz} + rG_{yz} + h^2(G_{yz} + rF_{yz})} + h\phi_x(1 + r) N_{yz}^s \tag{A15}$$

where

$$G_{yz} = p^2[Q_y + Q_z + \tfrac{1}{2}\theta_y\theta_z(S_yS_z - D_yD_z)] \tag{A16}$$

$$F_{yz} = 1 + \tfrac{1}{2}p^2\theta_y\theta_z(S_yS_z + D_yD_z) + p^4Q_yQ_z \tag{A17}$$

$$N_{yz}^s = p[\theta_yS_y(1 + p^2Q_z) + \theta_zS_z(1 + p^2Q_y) \tag{A18}$$

$$N_{yz}^d = p[\theta_yD_y(1 - p^2Qz) + \theta_zD_z(1 - p^2Q_y) \tag{A19}$$

$$E_{yz} = p^2\theta_y\theta_zS_yS_z + (1 + p^2Q_y)(1 + p^2Q_z) \tag{A20}$$

and where $r = \tanh \beta R$, $p = \tanh \beta J$, $h = \tanh \beta H$, θ_y and θ_z are the signs of the bonds joining the origin x to sites y and z, respectively, and ϕ_x is the sign of the external field at site x.

Proof. The method used here is a straightforward generalization of the method used to prove Theorem A.1. However, because we have two lattices instead of one, and a nonzero external field, the algebra is a lot more complicated.

We define the following conditional partition functions for the subtree of the coupled lattice system beginning at site y:

$$\begin{aligned}
\mathcal{A}_y &= \mathcal{Z}_y^{++} \\
\mathcal{B}_y &= \mathcal{Z}_y^{--} \\
\mathcal{C}_y &= \mathcal{Z}_y^{+-} \\
\mathcal{D}_y &= \mathcal{Z}_y^{-+}
\end{aligned} \tag{A21}$$

where $\mathcal{Z}_y^{\sigma_y^U \sigma_y^L}$ is the partition function for the subtree given that the spin at site y on the upper lattice has spin σ_y^U, and the spin at site y on the lower lattice has spin σ_y^L. In the same way we define these quantities for the site z. The corresponding quantities at the site x can be written in terms of these as

$$\mathcal{A}_x = e^R e^{2H}[\mathcal{A}_y e^{2\beta\theta_y J} + \mathcal{B}_y e^{-2\beta\theta_y J} + \mathcal{C}_y + \mathcal{D}_y][\mathcal{A}_z e^{2\beta\theta_z J} + \mathcal{B}_z e^{-2\beta\theta_z J} + \mathcal{C}_z + \mathcal{D}_z]$$

$$\mathcal{B}_x = e^R e^{-2H}[\mathcal{A}_y e^{-2\beta\theta_y J} + \mathcal{B}_y e^{2\beta\theta_y J} + \mathcal{C}_y + \mathcal{D}_y][\mathcal{A}_z e^{-2\beta\theta_z J} + \mathcal{B}_z e^{2\beta\theta_z J} + \mathcal{C}_z + \mathcal{D}_z]$$

$$\mathcal{C}_x = e^{-R}[\mathcal{A}_y + \mathcal{B}_y + \mathcal{C}_y e^{2\beta\theta_y J} + \mathcal{D}_y e^{-2\beta\theta_y J}][\mathcal{A}_z + \mathcal{B}_z + \mathcal{C}_z e^{2\beta\theta_z J} + \mathcal{D}_z e^{-2\beta\theta_z J}]$$

$$\mathcal{D}_x = e^{-R}[\mathcal{A}_y + \mathcal{B}_y + \mathcal{C}_y e^{-2\beta\theta_y J} + \mathcal{D}_y e^{2\beta\theta_y J}][\mathcal{A}_z + \mathcal{B}_z + \mathcal{C}_z e^{-2\beta\theta_z J} + \mathcal{D}_z e^{2\beta\theta_z J}]$$

$$\tag{A22}$$

The natural variables Q_y, S_y, and D_y for the coupled lattice system are defined in Eq. (A12). We can write these and the full partition function in terms of the conditional partition functions

$$\mathcal{L}_y = \mathcal{A}_y + \mathcal{B}_y + \mathcal{C}_y + \mathcal{D}_y$$

$$\mathcal{L}_y Q_y = (\mathcal{A}_y + \mathcal{B}_y) - (\mathcal{C}_y + \mathcal{D}_y)$$

$$\mathcal{L}_y S_y = (\mathcal{A}_y - \mathcal{B}_y) \tag{A23}$$

$$\mathcal{L}_y D_y = (\mathcal{C}_y - \mathcal{D}_y)$$

From this we obtain

$$\mathcal{A}_y = \tfrac{1}{4}\mathcal{L}_y(1 + Q_y + 2S_y)$$

$$\mathcal{B}_y = \tfrac{1}{4}\mathcal{L}_y(1 + Q_y - 2S_y)$$

$$\mathcal{C}_y = \tfrac{1}{4}\mathcal{L}_y(1 - Q_y + 2D_y) \tag{A24}$$

$$\mathcal{D}_y = \tfrac{1}{4}\mathcal{L}_y(1 - Q_y - 2D_y)$$

Using these and basic trigonometric identities, we rewrite the conditional partition function $\mathcal{A}_x$ at level x as

$$\mathcal{A}_x = \frac{e^R e^{2H}}{4} \prod_{i=y,z} \mathcal{L}_i[(\cosh 2\beta J + 1) + Q_i(\cosh 2\beta J - 1) + 2\theta_i S_i \sinh 2\beta J]$$

$$= \frac{e^R e^{2H}}{4} \cosh^2 \beta J \prod_{i=y,z} \mathcal{L}_i[1 + p^2 Q_i + 2p\theta_i S_i] \tag{A25}$$

where $p = \tanh \beta J$. Similarly, we find that

$$\mathcal{B}_x = \frac{e^R e^{-2H}}{4} \cosh^2 \beta J \prod_{i=y,z} \mathcal{L}_i[1 + p^2 Q_i - 2p\theta_i S_i]$$

$$\mathcal{C}_x = \frac{e^{-R}}{4} \cosh^2 \beta J \prod_{i=y,z} \mathcal{L}_i[1 - p^2 Q_i + 2p\theta_i D_i] \tag{A26}$$

$$\mathcal{D}_x = \frac{e^{-R}}{4} \cosh^2 \beta J \prod_{i=y,z} \mathcal{L}_i[1 - p^2 Q_i - 2p\theta_i D_i]$$

Substituting these equations into the equations corresponding to (150) for the site x, we obtain the desired result. ∎

APPENDIX B. GLOBAL STABILITY OF THE PARAMAGNETIC FIXED POINT

In this Appendix we prove that the paramagnetic solution $\rho(X) = \delta(X)$ is the unique globally attracting fixed point in the paramagnetic region of the phase diagram (Fig. 1).

Theorem 2. The paramagnetic solution is globally stable when both of the following conditions hold:

1. $2p(2\lambda - 1) \leqslant 1$

2. $2p^2 \leqslant 1$

(B1)

To prove Theorem 2, it is sufficient to show that $q \equiv E(X^2) = 0$ is a globally stable fixed point of the recursion relation (11). To accomplish this task, we use the recursion relation to derive an iterative map which gives an upper bound for the second moment on the $(n+1)$th level q_{n+1} in terms of q_n and other moments. If there were a sufficiently robust bound for q_{n+1} simply in terms of q_n (as there is in the symmetric case), then the problem becomes analogous to a one-dimensional dynamical system (with the usual equalities replaced by inequalities)—a contraction mapping. However, in the asymmetric case the problem becomes more complicated because a sufficiently strong bound on q_{n+1} necessarily involves the first moment m_n (Lemma B.2). Consequently, we must also derive a map which gives an upper bound on the first moment. Fortunately, we can derive a good bound on m_{n+1} in terms of m_n and q_n alone, so that the resulting pair of maps for m_{n+1} and q_{n+1} can be used simultaneously and the problem is similar to a two-dimensional dynamical system (again, with inequalities).

By analogy to the one-dimensional system, the initial hope is that the $\{m, q\}$ will obey a strict two-dimensional contraction—i.e., for all p and λ in the specified range and for all initial m and q, one might hope that both m and q decrease on every iteration. However, were this the case, then the problem could have been treated by a simple one-dimensional map on q. Indeed, it is easy to construct initial conditions on m and q for which this is not the case.

Instead, we will employ the following device, which we call box contraction. We begin by considering a rectangular region (or box) in the q–$|m|$ quadrant, $B(\delta_n, \eta_n) = \{0 \leqslant |m_n| \leqslant \delta_n, 0 \leqslant q_n \leqslant \eta_n\}$ with one corner at the origin, and the opposite one at the upper bounds (δ_n, η_n). Our aim is to show that after one iteration of our bounds, this region maps into a strictly smaller region. It is important to note that it is not necessary for each point (a particular pair $|m_n|, q_n$) in the box to systematically flow toward the origin. Instead we show that the corner of the box contracts. Our proof involves showing that there is a *wedge* $W \in B(1, 1)$ from $(m, q) = (0, 0)$ to one or both of the boundaries $m = 1$, $q = 1$ with the following property. Let $(\delta_n, \eta_n) \in W$. Then the bounding map applied to the box $B(\delta_n, \eta_n)$ results in a new box $B(\delta_{n+1}, \eta_{n+1})$ with $\delta_{n+1} < \delta_n$ and $\eta_{n+1} < \eta_n$. If the corner $(\delta_{n+1}, \eta_{n+1})$ of the new box also lies in the wedge W, then the procedure may be safely repeated. On the other hand, it may

be that the corner of the new box is either below or above the wedge (see Fig. 14). In the former case, for example, we may safely replace δ_{n+1} by a larger value $\delta'_{n+1} < \delta_n$ such that $(\delta'_{n+1}, \eta_{n+1}) \in W$. As a result the new box $B(\delta'_{n+1}, \eta_{n+1})$ is contained strictly within the box $B(\delta_n, \eta_n)$ of the preceding iteration, and its corner is in the wedge. We can now apply the bounding map to $B(\delta'_{n+1}, \eta_{n+1})$.

We determine the "lower" and "upper" boundaries of the wedge in Lemmas B.3 and B.4. In Lemma B.5 we show that the "upper" boundary always lies above the "lower" boundary, i.e., that there is a wedge. Finally, in our proof of the theorem we verify that this is a sufficient condition for the initial maximal bounding box $B(1, 1)$ to systematically contract to $(0, 0)$.

As previously stated, we will begin by deriving an upper bound on the first moment. We give bounds for the absolute value, to avoid any ambiguity regarding sign.

Lemma B.1. Let q_n denote the second moment and $|m_n|$ denote the absolute value of the first moment of the distribution $\rho_n(Y)$ on the nth
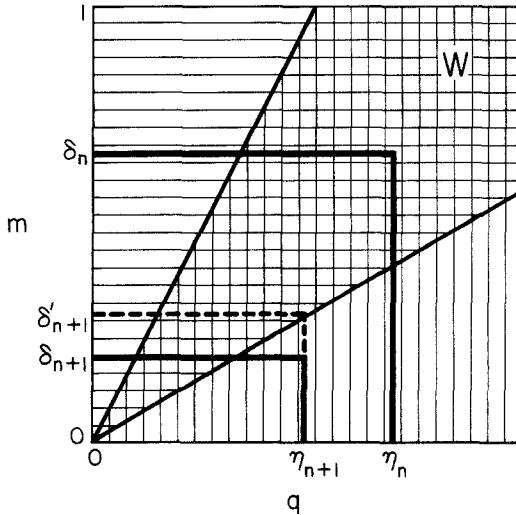

Fig. 14. Box contraction in the q–$|m|$ plane. Suppose $(|m_n|, q_n)$ lies in the bounding box $B(\delta_n, \eta_n)$. After an iteration of the recursion relation, Lemma B.3 shows that bound δ_n on the first moment contracts when $\delta_n < \eta_n L$ (the horizontally striped region), while Lemma B.4 shows that the bound η_n on the second moment contracts when $\delta_n < \eta_n U$ (the vertically striped region). When the corner (δ_n, η_n) lies in the wedge W, both bounds contract. As shown in the figure, if the new corner $(\delta_{n+1}, \eta_{n+1})$ lies below the wedge, the bound δ_{n+1} can be replaced by δ'_{n+1}, satisfying $\delta_{n+1} < \delta'_{n+1} < \delta_n$, such that $B(\delta'_{n+1}, \eta_{n+1})$ is strictly contained in the initial box $B(\delta_n, \eta_n)$, and $(\delta'_{n+1}, \eta_{n+1})$ lies in the wedge.

level. After a single iteration of the recursion relation (11) the absolute value of the first moment is bounded above by

$$|m_{n+1}| \leqslant 2p(2\lambda - 1)[|m_n| - \mu^2 q_n |m_n| + \kappa(p) \mu^4 q_n^2] + \mu^8 q_n^2 \equiv R(q_n, |m_n|) \tag{B2}$$

where

$$\kappa(p) = \begin{cases} 1, & p < 2/3 \\ 2/3, & p \geqslant 2/3 \end{cases} \tag{B3}$$

Proof. Making use of the identity

$$\frac{1}{1+x} = 1 - x + x^2 - x^3 + \frac{x^4}{1-x} \tag{B4}$$

which is valid for all $x \neq -1$, we expand the denominator of Eq. (11) to obtain

$$X = p(\theta_y Y + \theta_z Z)[1 - \mu^2 \theta_y \theta_z YZ + \mu^4 Y^2 Z^2 - \mu^6 \theta_y \theta_z Y^3 Z^3]$$
$$+ \mu^8 Y^4 Z^4 F(Y, Z; \theta_y, \theta_z) \tag{B5}$$

Taking the expectation and absolute value of both sides of this equation, we obtain

$$|m_{n+1}| \leqslant 2p(2\lambda - 1)[|m_n| - \mu^2 q_n |m_n| + \mu^4 q_n |r_n| - \mu^6 |r_n| t_n] + \mu^8 t_n^2 \tag{B6}$$

where $r_n \equiv E(Y^3)$ and $t_n \equiv E(Y^4)$. In arriving at Eq. (B6), we used the facts that $|F(Y, Z; \theta_y, \theta_z)| \leqslant 1$, $(1 - \mu^2 q_n) \geqslant 0$, and $(q_n - \mu^2 t_n) \geqslant 0$. In order to reduce this to a two-dimensional equation, we must replace r_n and t_n by some function of m_n and q_n. In the last term we replace t_n^2 with q_n^2 because $q_n \geqslant t_n$. Next we consider the pair of terms $\mu^4 |r_n| [q_n - \mu^2 t_n]$ together. We must consider two cases. If $p < 2/3$ and therefore $\mu^2 \equiv 2p - 1 < 1/3$, we replace $|r_n|$ by q_n in the first term, and drop the (negative) second term and the inequality still holds. If $p \geqslant 2/3$, and hence $\mu^2 \geqslant 1/3$, we need to get some mileage out of the second term. Making use of the moment inequality $E^2(Y^3) \leqslant E(Y^2) E(Y^4)$, we obtain

$$\mu^4 |r_n| [q_n - \mu^2 t_n] \leqslant \mu^4 (q_n t_n)^{1/2} [q_n - \mu^2 t_n] \tag{B7}$$

Because $\mu^2 \geqslant 1/3$ we obtain the inequality

$$\mu^4 |r_n| [q_n - \mu^2 t_n] \leqslant \mu^4 (q_n t_n)^{1/2} [q_n - \tfrac{1}{3} t_n] \tag{B8}$$

The usefulness of this substitution will become apparent in a moment. The simplest upper and lower bounds on t_n are given by

$$q_n \geqslant t_n \geqslant q_n^2 \tag{B9}$$

We want to choose t_n so that the upper bound takes its maximum value. This corresponds to maximizing the right-hand side of (B8). Differentiating the right-hand side of (B8) once with respect to t_n reveals that it is a monotonically increasing function of t_n for all t_n satisfying (B9). Hence the bound takes its maximum value when t_n is replaced by q_n, from which we obtain the bound (B2). ∎

Next we determine the corresponding upper bound on the second moment.

Lemma B.2. Using notation as in Lemma B.1, after a single iteration of the recursion relation (11), the second moment is bounded above by

$$q_{n+1} \leqslant 2p^2 q_n + 2p^2(2\lambda - 1)^2 m_n^2 + 4p^2\mu^2(2\lambda - 1)^2 |m_n| q_n$$
$$- [4p^2\mu^2 - 3\mu^4 - 2\mu^6(2\lambda - 1)^2] q_n^2$$
$$\equiv S(q_n, |m_n|) \tag{B10}$$

Proof. We begin by squaring the recursion relation

$$X^2 = \frac{p^2(Y^2 + Z^2 + 2\theta_y\theta_z YZ)}{(1 + \mu^2\theta_y\theta_z YZ)^2} \tag{B11}$$

This time we will make use of the identity

$$\frac{1}{(1+x)^2} = 1 - 2x + \frac{3x^2 + 2x^3}{(1+x)^2} \tag{B12}$$

which is valid for all $x \neq -1$. As before we expand the denominator, and obtain

$$X^2 = p^2(Y^2 + Z^2 + 2\theta_y\theta_z YZ)[1 - 2\mu^2\theta_y\theta_z YZ]$$
$$+ (3\mu^4 Y^2 Z^2 + 2\mu^6\theta_y\theta_z Y^3 Z^3) F^2(Y, Z; \theta_y, \theta_z) \tag{B13}$$

Taking the expectation, we obtain Eq. (B10), where we have replaced the absolute value of the third moment r_n with the upper bound q_n and chosen the positive sign of the cross term ($\propto |m_n| q_n$) corresponding to the maximum value of the right-hand side. ∎

Next we determine when the first moment individually contracts, which gives us the lower boundary of the wedge.

Lemma B.3. When $2p(2\lambda - 1) \leqslant 1$ and $2p^2 \leqslant 1$, if $|m_n| \leqslant \delta$ and $q_n \leqslant \eta$, then after an iteration,

$$|m_{n+1}| < 2p(2\lambda - 1)\,\delta \tag{B14}$$

for all δ, η satisfying

$$\delta > \eta L(p, \lambda) \tag{B15}$$

where

$$L(p, \lambda) = \kappa(p)\,\mu^2 + \frac{\mu^6}{2p(2\lambda - 1)} \tag{B16}$$

and $\kappa(p)$ is defined in Eq. (B3).

Proof. We determine the values of $|m_n|$ and q_n which maximize the bound [the right-hand side of Eq. (B2)] in the box (η, δ). Since $R(q_n, |m_n|)$ is a monotonically increasing function of $|m_n|$ for all $|m_n| \leqslant 1$, the right-hand side of Eq. (B2) takes its maximum value when $|m_n| = \delta$. However, because $R(q_n, |m_n|)$ is not a nondecreasing function of q_n, a simple substitution of η for q_n does not generally maximize eq. (B2). To avoid this complication, we formally replace $R_n(|m_n|, q_n)$ by a less restrictive bound,

$$
\begin{aligned}
|m_{n+1}| &< 2p(2\lambda - 1)\,\delta, &&\text{for } 0 < q_n < q^* \\
|m_{n+1}| &\leqslant R(q_n, \delta), &&\text{for } q^* \leqslant q_n \leqslant \eta
\end{aligned}
\tag{B17}
$$

where $q^* = \delta/L(p, \lambda)$ [note that $L(p, \lambda)$ is strictly positive], and we have used the facts that $q_n > 0$ and $\delta > 0$ to provide the strict inequality on the first line. This new function has the advantage that it is a nondecreasing function of both q_n and $|m_n|$ throughout the range of interest. Now if we define our box as specified in (B15), then $q_n \leqslant \eta < q^*$. Hence $|m_{n+1}| < 2p(2\lambda - 1)\,\delta$ as desired. ∎

Next we examine our bounds on the second moment to determine when it contracts.

Lemma B.4. When $2p^2 \leqslant 1$ and $2p(2\lambda - 1) \leqslant 1$, and η and δ are defined as in Lemma B.3, after an iteration of (B10),

$$q_{n+1} < 2p^2\eta \tag{B18}$$

for all δ, η satisfying

$$\delta < \eta U(p, \lambda) \tag{B19}$$

where

$$U(p, \lambda) = -\mu^2 + \{\mu^4 + [4p^2\mu^2 - 3\mu^4 - 2\mu^6(2\lambda - 1)^2]/[2p^2(2\lambda - 1)^2]\}^{1/2} \tag{B20}$$

Proof. Because the right-hand side of Eq. (B10) is a monotonically increasing function of both $|m_n|$ and q_n throughout the region of interest, it takes its maximum value when $|m_n| = \delta$ and $q_n = \eta$. Explicitly substituting these values, we obtain

$$q_{n+1} \leqslant 2p^2\eta + 2p^2(2\lambda - 1)^2\,\delta^2 + 4p^2\mu^2(2\lambda - 1)^2\,\delta\eta$$
$$- [4p^2\mu^2 - 3\mu^4 - 2\mu^6(2\lambda - 1)^2]\,\eta^2 \tag{B21}$$

From this we find that $q_{n+1} < 2p^2\eta$ when

$$\delta < \eta U(p, \lambda) \quad \blacksquare \tag{B22}$$

The existence of the contraction wedge W depends on the fact that $U(p, \lambda) > L(p, \lambda) > 0$. This key point is proved in the following lemma.

Lemma B.5.   When $2p^2 \leqslant 1$ and $2p(2\lambda - 1) \leqslant 1$, it is always the case that $L(p, \lambda) < U(p, \lambda)$, and $L(p, \lambda) > 0$, where these functions are defined in Eqs. (B19) and (B20).

Proof.   We verify that $U(p, \lambda) - L(p, \lambda) > 0$ for the ranges of p and λ stated in the lemma. It is equivalent to show that

$$\{\mu^4 + [4p^2\mu^2 - 3\mu^4 - 2\mu^6(2\lambda - 1)^2]/[2p^2(2\lambda - 1)^2]\}^{1/2}$$
$$> [1 + \kappa(p)]\,\mu^2 + \frac{\mu^6}{2p(2\lambda - 1)} \tag{B23}$$

Squaring both sides, it is sufficient to verify that

$$\mu^4 + \frac{4p^2\mu^2 - 3\mu^4 - 2\mu^6(2\lambda - 1)^2}{2p^2(2\lambda - 1)^2}$$
$$> [1 + \kappa(p)]^2\,\mu^4 + \frac{2[1 + \kappa(p)]\,\mu^8}{2p(2\lambda - 1)} + \frac{\mu^{12}}{4p^2(2\lambda - 1)^2} \tag{B24}$$

Bringing all the terms to the left-hand side, letting $\omega = 2p(2\lambda - 1)$, and multiplying the whole equation by $\omega^2 > 0$, we find that this is equivalent to

$$2[4p^2\mu^2 - 3\mu^4 - \mu^6\omega^2/2p^2]$$
$$- \omega^2\kappa(p)[2 + \kappa(p)]\,\mu^4 - 2\omega[1 + \kappa(p)]\,\mu^8 - \mu^{12} > 0 \qquad \text{(B25)}$$

We see that (B25) is a monotonically decreasing function of ω. Hence it is sufficient to verify the equation in the worst case scenario $\omega = 1$. In addition, recalling that $\mu^2 = 2p - 1$, we minimize the right-hand side of (B25) with respect to p. We find that the rhs is strictly positive for all p in the allowed range, taking its minimum value as $p \to 2/3$ from below. This proves the lemma. ∎

Armed with these results, we are ready to give the proof of Theorem 2.

Proof of Theorem 2. Let p and λ satisfy the conditions stated in the theorem. Consider an initial box $B(\eta, \delta)$ whose corner $(\eta \leqslant 1, \delta \leqslant 1)$ lies in the wedge $L(p, \lambda)\,\eta < \delta < U(p, \lambda)\,\eta$. Lemmas B.3 and B.4 indicate that after a single iteration, this box maps into a smaller box strictly contained in $B(2p^2\eta, 2p(2\lambda - 1)\,\delta)$. If the new corner does not lie in the wedge, we can always define a slightly larger box, still contained in the initial box $B(\eta, \delta)$, whose corner does lie in the wedge. If the wedge includes the point $\eta = 1$, $\delta = 1$, then our proof is complete. This corresponds to the case $L(p, \lambda) \leqslant 1$ and $U(p, \lambda) \geqslant 1$. However, there are two other possible cases. If $U(p, \lambda) < 1$, then we first consider boxes of the form $(1, \delta)$, where $L(p, \lambda) \leqslant \delta \leqslant 1$, and apply our argument for the contraction of the first moment, independent of the second, to show that after a finite number of iterations, the first moment is bounded above by $|m_n| < L(p, \lambda)$, which is contained in a box with corner in the wedge. Similarly, if $L(p, \lambda) > 1$, we first apply our argument for the contraction of the second moment, independent of the first, to show that boxes of the form $(\eta, 1)$, where $1/U(p, \lambda) \leqslant \eta \leqslant 1$, contract into the wedge.

If the given values of p and λ do not lie on a phase boundary, then convergence to the paramagnetic solution is exponential: i.e., if we let $C = \max(2p^2, 2p(2\lambda - 1))$, we find that after n iterations in the wedge our initial box maps into a box contained in the region $B(C^n\eta, C^n\delta)$. Even along the phase boundaries (i.e., $C = 1$), the strict inequalities of Lemmas B.3 and B.4 imply that the box converges to the origin, although here we do not obtain an estimate on the rate. In either case, we may conclude that the paramagnetic solution is globally stable. ∎

APPENDIX C.   BOUNDS ON THE EDWARDS–ANDERSON ORDER PARAMETER IN THE SPIN-GLASS PHASE

In this Appendix we prove Theorem I.3 of Section 4.1, which gives an upper bound on the Edwards–Anderson order parameter q_{EA}, as illustrated in Fig. 6. The proof is divided into two parts. First we use moment analysis to obtain upper and lower bounds which hold whenever $1/2 \leqslant \lambda < \lambda_N$ and $p \geqslant p_G$. The proof of the lower bound (Proposition C.1) is rather straightforward. For the upper bound (Proposition C.2), we must use a two-dimensional moment analysis (m and q), similar to the method used to prove global stability of the paramagnetic solution in Appendix B.

Although the results of Propositions C.1 and C.2 do establish that, as $p \to p_G$, q_{EA} scales linearly with $|p - p_G|$, they do not give the same coefficients of linear scaling. This is due to the fact that our bounds on q_{n+1} [e.g., Eq. (B10)] involve odd moments, for example, the magnetization $m_n = E(Y)$, which cannot be *a priori* ignored in the asymmetric case. However, our bifurcation results in Section 4.2 indicate that these odd moments should vanish in the (nonmagnetized) spin-glass phase. In Proposition C.5 we use a relatively simple functional analysis argument to show that whenever $\lambda < 3/4$, the fixed-point density must be symmetric. Consequently, when $\lambda < 3/4$, odd moments can be ignored, and we can borrow the results of moment analysis in the symmetric case[2] to obtain the exact coefficient of linear scaling. We expect that an analogue of Proposition C.5 should hold for all $\lambda < \lambda_N$. In fact, this turns out to be related to questions of global stability which we are currently investigating.

First we give a simple lower bound on the Edwards–Anderson order parameter in the spin-glass phase.

Proposition C.1.   In a finite neighborhood of the phase boundary, $p \gtrsim p_G = 1/\sqrt{2}$ and $1/2 \leqslant \lambda < \lambda_N$, iterates of the second moment are eventually bounded below by

$$q_L = \frac{2p^2 - 1}{2p^2\mu^2[2 + \mu^2(2\lambda - 1)^2]} \tag{C1}$$

Proof.   Squaring the recursion relation (11), we obtain

$$X^2 = \frac{p^2(Y^2 + Z^2 + 2\theta_y\theta_z YZ)}{(1 + \mu^2\theta_y\theta_z YZ)^2} \equiv F^2(Y, Z; \theta_y\theta_z) \tag{C2}$$

Making use of the fact

$$\frac{1}{(1 + x)^2} = 1 - 2x + \frac{3x^2 + 2x^3}{(1 + x)^2} \tag{C3}$$

we expand the denominator of (C2),

$$X^2 = p^2(Y^2 + Z^2 + 2\theta_y\theta_z YZ)[1 - 2\mu^2\theta_y\theta_z YZ]$$
$$+ (3\mu^4 Y^2 Z^2 + 2\mu^6\theta_y\theta_z Y^3 Z^3) F^2(Y, Z; \theta_y\theta_z) \qquad \text{(C4)}$$

Taking the expectation and noting that $F^2(Y, Z; \theta_y\theta_z) \geqslant 0$ yields the lower bound on $q_{n+1} = E(X^2)$:

$$q_{n+1} \geqslant 2p^2 q_n + 2p^2(2\lambda - 1)^2 m_n^2 - 4p^2\mu^2(2\lambda - 1)^2 m_n r_n - 4p^2\mu^2 q_n^2 \qquad \text{(C5)}$$

where $m_n = E(Y)$, $q_n = E(Y^2)$, and $r_n = E(Y^3)$. Next we simplify our bound on q_{n+1}, so that the right-hand side of Eq. (C5) is replaced by a function of q_n alone. To maintain the inequality in Eq. (C5), we want to minimize the right-hand side with respect to m_n and r_n. Because the term proportional to r_n is negative, we can replace r_n with the upper bound $q_n \geqslant r_n$. To minimize the right-hand side with respect to m_n, we note that for any given value of q_n, the terms containing m_n (after r_n is replaced by q_n) are

$$f_{q_n}(m_n) = 2p^2(2\lambda - 1)^2 m_n^2 - 4p^2\mu^2(2\lambda - 1)^2 m_n q_n \qquad \text{(C6)}$$

which will have a minimum value when $m_n = \mu^2 q_n$ for any q_n. Hence, substituting this for m_n in (C5), we obtain

$$q_{n+1} \geqslant 2p^2 q_n - 2p^2\mu^2[2 + \mu^2(2\lambda - 1)^2] q_n^2 \equiv D(q_n) \qquad \text{(C7)}$$

Note that $D(q_n)$ is quadratic in q_n, with a maximum at $q_n = q^* = p^2/2p^2\mu^2[2 + \mu^2(2\lambda - 1)^2]$.

Let q_L be defined as in the statement of the proposition. [Note that q_L may be obtained by solving Eq. (C7) self-consistently.] It is easily verified that in a neighborhood of the phase boundary

$$q_L = O(\Delta) \ll q^* < 1 \qquad \text{(C8)}$$

and

$$D(q_L) < D(1) \qquad \text{(C9)}$$

From (C8) and (C9) and the fact that $D(q)$ is quadratic, it follows that for $\Delta \ll 1$, (C7) can be replaced by

$$q_{n+1} \geqslant \tilde{D}(q_n) \qquad \text{(C10)}$$

where

$$\tilde{D}(q_n) = \begin{cases} D(q_n), & q_n < q_L \\ q_L, & q_L < q_n \leqslant 1 \end{cases} \qquad \text{(C11)}$$

Note that $\tilde{D}(q_n)$ is monotonically increasing, and hence that the equation $\tilde{D}(q) = q$ has only one stable fixed point at $q = q_L$. Thus, (C10) implies that for $\Delta \ll 1$, q_n converges exponentially to q_L. ∎

The lower bound on q proves that a phase transition occurs crossing the spin-glass phase boundary. However, from a lower bound alone we cannot determine the order of the transition or the associated critical exponents. The next proposition gives an upper bound on q. Because this bound approaches zero at the phase boundary, we can conclude that the transition is second order. Furthermore, because both the upper and lower bounds have the same limiting power law behavior at the phase transition, we can determine the critical exponent $\beta = 1$.

Proposition C.2. In a finite neighborhood of the phase boundary, $p \gtrsim p_G = 1/\sqrt{2}$ and $1/2 < \lambda < \lambda_N$, iterates of the second moment are eventually bounded above by

$$
\begin{aligned}
q_U = (2p^2 - 1) \\
\times \{ 4p^2\mu^2 - [3 + (32/9)\, p^2(2\lambda - 1)^2]\, \mu^4 \\
- 2\mu^6(2\lambda - 1)^2 - (10/3)\, p(2\lambda - 1)\, \mu^8 - \mu^{12}/2 \}^{-1} \quad \text{(C12)}
\end{aligned}
$$

Remark. The above bound is valid in a finite neighborhood of $\Delta = 0$. However, for each value of λ, the bound q_U eventually reaches the limiting value of 1 as p increases (T decreases). This defines a smooth curve $p(\lambda)$ in the spin-glass phase. Below this curve we replace the above bound by the trivial bound $q_U = 1$. In addition, our results break down when $2p(2\lambda - 1) > 1$. Usually the curve $2p(2\lambda - 1) = 1$ lies below the curve $p(\lambda)$ (defined by $q_U = 1$) which was discussed previously, and consequently we do not have to worry about it. However, in a small region near the multicritical point, $2p(2\lambda - 1) = 1$ lies above $p(\lambda)$, in which case we set $q_U = 1$ when $2p(2\lambda - 1) = 1$. In Lemma C.4 we show that it is always the case that q_U is of the form specified in (C12) in a neighborhood of the phase boundary, so that the leading behavior is $q_U \propto 2p^2 - 1 \propto |p - p_G|$.

The proof of the proposition makes use of several lemmas. The first three of these were used earlier to prove global stability of the paramagnetic solution in Appendix B. In Lemmas B.1 and B.2 we determined upper bounds on the first and second moments after $n + 1$ iterations, m_{n+1} and q_{n+1}, in terms of m_n and q_n. The resulting equations (B2) and (B10) comprise the analogue of a two-dimensional dynamical system. Our goal is to determine a range of q and m which is globally stable with respect to iteration of these equations. As in Appendix B, we begin by considering a general box in the q–m plane, with one corner at the origin

$q = m = 0$, say $0 \leqslant q_n \leqslant \eta$ and $0 \leqslant |m_n| \leqslant \delta$, where η and δ are less than or equal to 1. We refer to the coordinates (η, δ) as the corner of the box, and the limiting box has corner at (q_U, m_U). Our aim is to show that any box with corner outside the limiting box will after a sufficient number of iterations lead to a box which has its corner at $q \leqslant q_U$ and $m \leqslant m_U$. In Lemma B.3 we determined the conditions under which our upper bound on the first moment contracts after a single iteration. In Lemma C.3 of this section we determine the corresponding conditions under which the bound on the second moment contracts. In Lemma C.4 we show that in the neighborhood of the phase transition these two regions overlap in a manner such that there is a continuous strip connected to a point $m = m_U$ and $q = q_U$ along which the bounds on q and m simultaneously contract. Finally, in our proof of the proposition we verify that this is a sufficient condition for the initial maximal bounding box $(\eta = 1, \delta = 1)$ to systematically contract to (q_U, m_U). This determines the upper bound q_U, as well as the corresponding bound m_U. For simplicity we assume $\lambda > 1/2$ throughout the proof. An analogous result was proved for $\lambda = 1/2$ in ref. 2.

Lemma C.3. Let $2p^2 \geqslant 1$ and $1/2 < \lambda < \lambda_N$, and let η and δ be defined as in Lemma B.3. After one iteration of (B10),

$$q_{n+1} < \eta \qquad \qquad (C13)$$

for all δ, η satisfying

$$\delta < f(\eta; p, \lambda) \qquad \qquad (C14)$$

where

$f(\eta; p, \lambda)$

$$= -\mu^2 \eta + \sqrt{\left\{ \mu^4 \eta^2 + \frac{[4p^2\mu^2 - 3\mu^4 - 2\mu^6(2\lambda - 1)^2]\,\eta^2 - (2p^2 - 1)\,\eta}{2p^2(2\lambda - 1)^2} \right\}^{1/2}}$$

$$(C15)$$

Proof. Because the right-hand side of Eq. (B10) is a monotonically increasing function of both $|m_n|$ and q_n throughout the region of interest, it takes its maximum value when $|m_n| = \delta$ and $q_n = \eta$. Explicitly substituting these values, we obtain

$$q_{n+1} \leqslant 2p^2\eta + 2p^2(2\lambda - 1)^2\,\delta^2 + 4p^2\mu^2(2\lambda - 1)^2\,\delta\eta$$
$$- [4p^2\mu^2 - 3\mu^4 - 2\mu^6(2\lambda - 1)^2]\,\eta^2 \qquad (C16)$$

From this we find that $q_{n+1} < \eta$ when $\delta < f(\eta; p, \lambda)$. ∎

The region of the q–m plane for which this argument holds is illustrated in Fig. 15 for particular values of p and λ. Any box with its corner (η, δ) lying below the curve $m = f(q; p, \lambda)$ will be mapped into a box with $q_{n+1} < \eta$. Furthermore, the boundary δ contracts for any box with its corner lying above the line $m = qL(p, \lambda)$, where $L(p, \lambda)$ is given in (B19).

In order to obtain the desired upper bounds m_U and q_U, we need to prove three more things. First, the two curves $m = qL(p, \lambda)$ and $m = f(q; p, \lambda)$ must intersect in a point $m = m_U$ and $q = q_U$. Second, $q_U \leqslant 1$ in a neighborhood of the phase boundary. Finally, for $m > m_U$ and $q > q_U$, when $q_U < 1$ the curve $m = qL(p, \lambda)$ must lie below $m = f(q; p, \lambda)$. This ensures that we have the situation illustrated in Fig. 15, and allows us to prove the proposition.

Lemma C.4. Let $f(\eta; p, \lambda)$ be defined as in Eq. (C15), and $L(p, \lambda)$ be as defined in Eq. (B19). When $2p^2 \geqslant 1$ and $1/2 < \lambda < \lambda_N$, the two curves $m = qL(p, \lambda)$ and $m = f(q; p, \lambda)$ intersect in a point $m = m_U$ and $q = q_U$, where $q_U < 1$ in a neighborhood of the spin-glass phase boundary. Furthermore, when $m > m_U$ and $q > q_U$, $qL(p, \lambda) < f(q; p, \lambda)$.

Proof. First we determine the point of intersection (q_U, m_U) given by

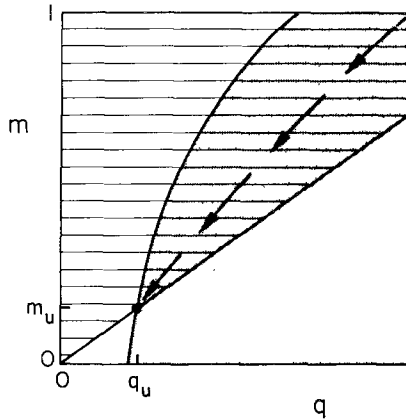$$m_U = q_U L(p, \lambda) = f(q_U; p, \lambda) \tag{C17}$$

Fig. 15. Upper bound on q_{EA} in the spin-glass phase. We use the same method to obtain this bound as was used to prove global stability of $\rho(X) = \delta(X)$ in the paramagnetic phase. The bound η on the first moment contracts after one iteration if the corner of the bounding box (η, δ) lies in the striped region, while the bound δ on the second moment contracts if (η, δ) lies in the shaded region. In the neighborhood of the transition, these regions overlap as shown, leading to upper bounds m_U and q_U on the first and second moments.

Solving second equality for q_U, we obtain (C12), as given in the statement of the proposition. Combining this with the first equality in Eq. (C17) yields the corresponding bound m_U.

We find that $q_U = 1$ along a curve in the spin-glass phase which is not connected to the phase boundary. The fact that $q_U < 1$ near the phase boundary is obtained by checking the leading behavior of q_U when $p = p_G + \Delta$ for Δ small. Because $(2\lambda - 1)$ always appears with a negative sign in the denominator of (C12), at a fixed value of p, q_U takes its maximum value in the neighborhood of the spin-glass phase boundary when $\lambda \lesssim \lambda_N$. Near the multicritical point, we find

$$q_U = \frac{2p_G \Delta}{2\mu_G^2 - (35/9)\,\mu_G^4 - \mu_G^6 - (5/3)\,\mu_G^8 - \mu_G^{12}/2} + O(\Delta^2) \qquad \text{(C18)}$$

where the denominator in the first term is strictly positive. Hence $q_U \propto \Delta$ near the phase boundary.

It remains to be shown that for $m > m_U$ and $q > q_U$ the curve $m = qL(p, \lambda)$ lies below $m = f(q; p, \lambda)$. Proving this requires some uninspiring but straightforward algebra as in Lemma B.5 of Appendix B. We leave it to the reader to verify this. We note that the worst case is encountered at the multicritical point, where at $\eta = 1$ we find $L(p_G, \lambda_N) \approx 0.35$ and $f(1; p_G, \lambda_N) \approx 0.4$. ∎

This situation is illustrated in Fig. 15. It corresponds to having a continuous strip from the boundary $m = 1$ or $q = 1$ connected to $q = q_U$ and $m = m_U$ along which both q and $|m|$ contract. Armed with these results, we are ready to give the proof of the proposition.

Proof of Proposition C.2. Consider an initial box whose corner is given by (η, δ) with $\eta < q_U$ and $\delta > m_U$. Suppose the corner lies in the strip $\eta L(p, \lambda) < \delta < f(\eta; p, \lambda)$.

Lemmas B.3 and C.3 indicate that after a single iteration, this box maps into a smaller box contained in $(\eta, 2p(2\lambda - 1)\,\delta)$. If the new corner does not lie in the strip, we can always define a slightly larger box, still contained in the initial box, whose corner does lie in the strip.

If the strip includes the point $\eta = 1$, $\delta = 1$, then our proof is complete. However, there are two other possible cases. As in the paramagnetic phase, one corresponds to q contracting first, until we reach the strip, while the other corresponds to m contracting first. In either of these cases, the proof is given by a straightforward generalization of this case. ∎

Finally, we show that for $\lambda < 3/4$, the fixed-point density must be symmetric.

Proposition C.5. Let $\rho(x)$ denote a probability density supported on $[-1, +1]$. Using ρ as the initial density, denote by ρ_n the density obtained from ρ under n iterations of (11). Then, provided $\lambda < 3/4$, any limit of the sequence (ρ_n) is symmetric.

Remark. With a little caution, the above result may be generalized to the case in which the initial distribution cannot be expressed as a density.

Proof. Let ρ_n be defined as in the statement of the proposition. We may decompose ρ_n into symmetric and antisymmetric pieces: $\rho_n = s_n + a_n$, where $s_n = \frac{1}{2}[\rho_n(x) + \rho_n(-x)]$ and $a_n = \frac{1}{2}[\rho_n(x) - \rho_n(-x)]$. Observe that $\int \rho_n = \int s_n = 1$ and that s_n is a.e. nonnegative.

By definition, ρ_{n+1} is obtained from ρ_n according to $\rho_{n+1} = B_{\lambda, p}[\rho_n, \rho_n]$, where $B_{\lambda, p}$ is an unrescaled bilinear operator, analogous to the rescaled operator defined in Eq. (26):

$$B_{\lambda, p}[f, g] = \int_{-1}^{1} \int_{-1}^{1} f_A(y) \, g_A(z) \, E_{\theta_y \theta_z}[\delta(x - F^*(y, z; \theta_y, \theta_z))] \, dy \, dz \tag{C19}$$

Thus

$$\rho_{n+1} = B_{\lambda, p}[s_n, s_n] + B_{\lambda, p}[a_n, a_n] + 2B_{\lambda, p}[a_n, s_n] \tag{C20}$$

Next we note that each of the terms above may be expressed in terms of the symmetric bilinear operator $B_{1/2, p}[\cdot, \cdot] \equiv B_p[\cdot, \cdot]$. Indeed, we clearly have

$$B_{\lambda, p}[s_n, s_n] = B_p[s_n, s_n] \tag{C21}$$

while

$$B_{\lambda, p}[s_n, a_n] = \lambda^2 B_p[s_n(y), a_n(z)] + (1 - \lambda)^2 B_p[s_n(y), a_n(-z)]$$
$$+ \lambda(1 - \lambda)[B_p[s_n(y), a_n(z)] + B_p[s_n(y), a_n(-z)]] \tag{C22}$$

etc. Using the antisymmetry of a_n and the symmetr of B_p under exchange of its arguments, we find that Eq. (C20) reduces to

$$\rho_{n+1} = B_p[s_n, s_n] + (2\lambda - 1)^2 B_p[a_n, a_n] + 2(2\lambda - 1) B_p[s_n, a_n] \tag{C23}$$

Furthermore, it is seen that s_{n+1} is given by the first two terms of (C23), while a_{n+1} is given by the last term. Finally, we note that the inequality

$$|B_{\lambda, p}[f, g]| \leqslant B_{\lambda, p}[|f|, |g|] \tag{C24}$$

holds pointwise (a.e.). Using (27) and (C24), as well as the observations $\int s_n = 1$ and $s_n \geqslant 0$ a.e., we obtain

$$\|a_{n+1}\|_1 \leqslant 2(2\lambda - 1) \|a_n\|_1 \tag{C25}$$

Hence, as $n \to \infty$, $a_n \to 0$ whenever $2(2\lambda - 1) < 1$, i.e., $\lambda < 3/4$. ∎

Corollary. In a finite neighborhood of the phase boundary, $p \gtrsim p_G = 1/\sqrt{2}$ and $1/2 < \lambda < 3/4$, the iterates q_n of the second moment eventually obey the bounds

$$q_L \equiv \frac{2p^2 - 1}{4p^2\mu^2} \leqslant q_n \leqslant \frac{2p^2 - 1}{4p^2\mu^2(1 - 3/2\mu^2)} \equiv q_U \tag{C26}$$

Proof. By Proposition C.5, for n sufficiently large, we may ignore all factors of m_n (and other odd moments) in our upper and lower bounds on q_n. This reduces our bounds to those obtained in the symmetric case ($\lambda = 1/2$) in ref. 2, where the forms of q_L and q_U are given in Propositions 3.7 and 3.8. ∎

Proof of Theorem 3. Proposition C.1 and C.2 and the corollary to Proposition C.5 clearly give bounds on q_{EA} of the desired form. In particular, for $\lambda < 3/4$, the functions $V(p, \lambda)$ and $W(p, \lambda)$ are independent of λ and are obtained from the bounds in the corollary, while for $3/4 \leqslant \lambda < \lambda_N$, $V(p, \lambda)$ and $W(p, \lambda)$ are obtained from Propositions C.1 and C.2, respectively. ∎

APPENDIX D. COMPLETENESS OF THE FERROMAGNETIC EIGENFUNCTIONS

In this Appendix we begin with a general result (Theorem D.1) on $L^2(dx)$ completeness of a set of functions, consisting of a function $\mathscr{S}_0 = S(x)$, which satisfies certain conditions, and its derivatives $\mathscr{S}_n = d^n S(x)/dx^n$. We work in L^2 because it is convenient; however, a similar theorem should hold in any L^P space. Although this theorem can be verified for many well-known sets of functions (e.g., Hermite and other orthogonal functions), it is obviously most useful when the explicit form of the function $S(x)$ is not known.

This first result is not directly applicable to the eigenfunctions of the ferromagnet, $\{\mathscr{I}_n\}$, which we recall are not given simply by the derivatives of $\mathscr{I}_0$, but rather by

$$\mathscr{I}_n = \begin{cases} \dfrac{d^n \mathscr{I}_0}{dx^n}, & n \text{ even} \\[2mm] \dfrac{d^n(x\mathscr{I}_0)}{dx^n}, & n \text{ odd} \end{cases} \tag{D1}$$

Consequently, in Theorem D.2, we extend the general result to the case in which even and odd eigenfunctions are generated by derivatives of different functions.

Finally, we restrict to the specific case of the $\{\mathscr{J}_n\}$. In Corollary D.3 we verify that these satisfy the conditions of Theorem D.2, and hence are complete in $L^2(dx)$. Then, in Corollary D.4 we restrict to the space $L^2(\cosh dx)$, and show that the remaining "good" functions are complete in this more restrictive space. We conclude this Appendix with a technical lemma which allows us to approximate the $\hat{\mathscr{J}}_n(k)$ by their small-k expansions.

Theorem D.1. Let $S \in L^2(dx)$. Suppose that the Fourier transform $\hat{S}$ vanishes only on sets of zero measure, and that $\hat{S}$ decays faster than exponentially at high frequencies, e.g.,

$$\hat{S}(k) \leqslant c_1 e^{-c_2 |k|^a}$$

where c_1 and c_2 are constants, and $a > 1$. The set of functions defined by

$$\mathscr{S}_0 = S(x)$$

$$\mathscr{S}_n(x) = \frac{d^n S(x)}{dx^n}$$

form a complete set in $L^2(dx)$.

Proof. Let M denote the L^2 closure of span$\{\mathscr{S}_n\}$. We want to show that $M = L^2(dx)$. To this end, let us define a convolution operator $\mathbf{S}$ on $L^2(dx)$ according to

$$\mathbf{S}(\phi) = \int S(x - y)\, \phi(y)\, dy \tag{D2}$$

for $\phi \in L^2(dx)$. First we claim that $\mathbf{S}: L^2(dx) \to L^2(dx)$. Indeed, using the transform operator $\hat{\mathbf{S}}$ (which is, of course, simply a multiplication operator), it is easy to see that $\mathbf{S}$ is bounded in L^2:

$$\|\mathbf{S}(\phi)\|_2 = \|\mathbf{S}(\phi)\|_2 = \|\hat{S}(k)\, \hat{\phi}(k)\|_2 \leqslant c_1 \|\hat{\phi}(k)\|_2 \tag{D3}$$

where $c_1 < \infty$ is the constant in the statement of the theorem.

Next we claim that

$$\text{(a)} \quad \overline{\text{Ran}(\mathbf{S})} = L^2(dx)$$

and

$$\text{(b)} \quad \text{Ran}(\mathbf{S}) \subset M$$

which, together with the fact that M is closed, imply that $M = L^2(dx)$, the desired result. (Here the overbar denotes the L^2 closure.)

It remains to establish (a) and (b). Take $\phi \in L^2(dx)$ and $\varepsilon > 0$. To prove (a), it suffices to show that there exists $\phi_\varepsilon \in \text{Ran}(S)$ such that $\|\phi - \phi_\varepsilon\|_2 < O(\varepsilon)$. To this end, we define $\hat{g}_\varepsilon(k)$ in the domain of S according to

$$\hat{g}_\varepsilon(k) = \begin{cases} \hat{\phi}(k)/\hat{S}(k) & \text{if} \quad |\hat{S}(k)| > \varepsilon \\ 0 & \text{otherwise} \end{cases} \tag{D4}$$

and

$$\hat{\phi}_\varepsilon(k) = \begin{cases} \hat{\phi}(k) & \text{if} \quad |\hat{S}(k)| > \varepsilon \\ 0 & \text{otherwise} \end{cases} \tag{D5}$$

Using that fact that $\hat{S}(k)$ vanishes only on sets of zero measure, it is easy to see that $\hat{\phi}_\varepsilon(k)$ defines a function with the required properties. In particular

$$S(\hat{g}_\varepsilon) = \hat{\phi}_\varepsilon \tag{D6}$$

Next we show that $\text{Ran}(S) \subset \bar{M}$, which, since M is closed, implies (b). Since C_0^∞ is dense in L^2, we may consider $\phi \in C_0^\infty$. We write

$$\hat{\phi}(k) = \sum \phi_n k^n \tag{D7}$$

where the coefficients are bounded by

$$|\phi_n| \leqslant C \frac{e^{Dn}}{n!} \tag{D8}$$

for some constants C and D (as usual for C_0^∞ functions). Now if we write

$$S(\phi) = \sum_{n=0}^\infty \phi_n k^n \hat{S}(k) \equiv \sum_{n=0}^\infty \phi_n \mathscr{S}_n(k) \tag{D9}$$

then we have apparently expanded $S(\phi)$ in terms of the functions $\{\mathscr{S}_n\}$. However, we must verify that the rhs of (D9) is well defined, i.e., that this expansion is well behaved. Thus it is sufficient to show that

$$\lim_{N \to \infty} \left\| \sum_{n > N} \phi_n \mathscr{S}_n(k) \right\| = 0 \tag{D10}$$

From the triangle inequality,

$$\left\| \sum_{n > N} \phi_n \mathscr{S}_n(k) \right\|_2 \leqslant \sum_{n > N} |\phi_n| \, \|\mathscr{S}_n(k)\|_2 \tag{D11}$$

so that (D10) follows immediately from our assumptions of the decay of $\hat{S}(k)$. This establishes (b), and hence completeness. ∎

We now generalize this result to the case which applies to the ferromagnetic eigenfunctions (D1).

Theorem D.2. Let $S(x)$, $T(x) \in L^2(dx)$. Suppose that the transform functions $\hat{S}$ and $\hat{T}$ decay faster than exponentially at height frequencies (e.g., $\hat{S}$ and $\hat{T}$ obey bounds like those stated in Theorem D.1). Define the real-valued functions $\hat{R}(k)$, $\hat{I}(k)$, $\hat{P}(k)$, and $\hat{Q}(k)$ in terms of $\hat{S}(k)$ and $\hat{T}(k)$ according to

$$\hat{S}(k) = \hat{R}(k) + i\hat{I}(k) \tag{D12}$$

$$\hat{T}(k) = \hat{P}(k) + i\hat{Q}(k) \tag{D13}$$

and suppose that $\hat{A} \equiv \hat{Q}\hat{I} + \hat{R}\hat{P}$ vanishes only on sets of zero measure. Then the set of functions $\{\mathscr{S}_{2n}, \mathscr{T}_{2n+1}\}$ defined by

$$\mathscr{S}_{2n} = \frac{d^{2n}S(x)}{dx^{2n}}$$

$$\mathscr{T}_{2n+1} = \frac{d^{2n+1}T(x)}{dx^{2n+1}} \tag{D14}$$

form a complete set in $L^2(dx)$.

Proof. The structure of the proof is almost identical to that of the previous theorem. Here we take M to be the L^2 closure of span$\{\mathscr{S}_{2n}, \mathscr{T}_{2n+1}\}$ and show that $M = L^2$. Again we do this by introducing an operator which maps L^2 to L^2 and establishing properties of the range of the operator.

Let $\mathbb{P}_e$ and $\mathbb{P}_o$ denote the projection operators onto even and odd subspaces of $L^2(dx)$, respectively. (Thus, in k space, $\mathbb{P}_e$ and $\mathbb{P}_0$ annihilate the imaginary and real parts, respectively, of the transform of a real-valued function.) Let $\mathbf{S}$ and $\mathbf{T}$ be convolution operators on $L^2(dx)$, as in (D2) with S replaced by our functions S or T, respectively. From these, we may construct an operator $\mathbf{C}$ on $L^2(dx)$ defined by

$$\mathbf{C}(\phi) \equiv \mathbb{P}e\mathbf{S}(\phi) + \mathbb{P}_0\mathbf{T}(\phi) \tag{D15}$$

for $\phi \in L^2(dx)$. Note that $\|\mathbf{C}\|_2 \leqslant \|\mathbf{S}\|_2 + \|\mathbf{T}\|_2$ immediately implies $\mathbf{C}: L^2 \to L^2$.

Just as in the proof of Theorem D.1, it suffices to show

$$\text{(a)} \quad \overline{\text{Ran}(\mathbf{C})} = L^2$$

and

$$\text{(b)} \quad \text{Ran}(\mathbf{C}) \subset M$$

The proof of (b) is strictly analogous to that in the previous theorem, so we do not repeat it here.

It thus suffices to establish (a). As before, we take $\phi \in L^2(dx)$ and $\varepsilon > 0$, and show that there exists $\phi_\varepsilon \in \text{Ran}(\mathbf{C})$ such that $\|\phi - \phi_\varepsilon\|_2 < O(\varepsilon)$. We begin by writing the transform $\hat{\phi}$ in the form

$$\hat{\phi}(k) = \hat{\xi}(k) + i\hat{\eta}(k) \tag{D16}$$

By analogy to Eq. (D6), we are looking for functions $\hat{a}_\varepsilon(k)$ and $\hat{b}_\varepsilon(k)$ with $\hat{g}_\varepsilon(k) = \hat{a}_\varepsilon(k) + i\hat{b}_\varepsilon(k)$ such that

$$\begin{aligned}
\hat{R}\hat{a}_\varepsilon - \hat{I}\hat{b}_\varepsilon &= \hat{\xi} \\
\hat{Q}\hat{a}_\varepsilon + \hat{P}\hat{b}_\varepsilon &= \hat{\eta}
\end{aligned} \tag{D17}$$

on a set of large measure. Defining $\hat{\Delta}$ as in the statement of the theorem, the solution of these equations is simply

$$\hat{a}_\varepsilon = \frac{1}{\hat{\Delta}} (\hat{P}\hat{\xi} + \hat{I}\hat{\eta})$$

$$\hat{b}_\varepsilon = \frac{1}{\hat{\Delta}} (\hat{R}\hat{\psi} - \hat{Q}\hat{\phi}) \tag{D18}$$

Therefore, by analogy with Eq. (D4) we define

$$\hat{g}_\varepsilon = \begin{cases} \hat{a}_\varepsilon + i\hat{b}_\varepsilon & \text{if } \hat{\Delta} > \varepsilon \\ 0 & \text{otherwise} \end{cases} \tag{D19}$$

and by analogy with Eq. (D5)

$$\hat{\phi}_\varepsilon = \begin{cases} \phi & \text{if } \hat{\Delta} > \varepsilon \\ 0 & \text{otherwise} \end{cases} \tag{D20}$$

Therefore $\hat{\mathbf{C}}(\hat{g}_\varepsilon) = \hat{\phi}_\varepsilon$, and ϕ_ε is a function of the desired form. ∎

Next we verify that Theorem D.2 indeed applies to the ferromagnetic eigenfunctions $\{\mathscr{J}_n\}$.

Corollary D.3. The set of functions $\{\mathscr{J}_n(x)\}$ defined in (D1) are complete in $L^2(dx)$.

Proof.   Using the notation of Theorem D.2, we set $S(x) = \mathcal{J}_0(x)$ and $T(x) = x\mathcal{J}_0(x)$. That $\hat{S}$ and $\hat{T}$ have sufficient decay properties was demonstrated in Eq. (49). Thus, in order to apply the theorem, we must verify that

$$\hat{I}\hat{Q} + \hat{P}\hat{R} \neq 0 \tag{D21}$$

for almost every k, where

$$\hat{I}\hat{Q} + \hat{P}\hat{R} = \frac{1}{2}\frac{d}{dk}(\hat{R}^2 + \hat{I}^2) \tag{D22}$$

which can only vanish at isolated points, since $\hat{\mathcal{J}}_0(k)$ is analytic.   ∎

Because $L^2(\cosh x\, dx) \subset L^2(dx)$ and because our functions $\{\mathcal{J}_n\}$ decay faster than exponentially (implying that they are elements of the more restrictive space), we also have the following corollary.

Corollary D.4.   The eigenfunctions $\{\mathcal{J}_n\}$ defined by (D1) are complete in $L^2(\cosh x\, dx)$.

In Section 5 we use the more restrictive space $L^2(\cosh x\, dx)$ since this allows us to discard the "undesirable" generalized eigenfunctions of the linear operator; in k space these are

$$\hat{\mathcal{U}}_n(k) = \begin{cases} \operatorname{sign}(k)\,|k^n|\,\hat{\mathcal{J}}_0'(k), & n \text{ even} \\ |k^n|\,\hat{\mathcal{J}}_0(k), & n \text{ odd} \end{cases} \tag{D23}$$

It is clear that the singular behavior of the $\{\hat{\mathcal{U}}_n(k)\}$ near $k = 0$ prevents the transforms of these functions from being summable in $L^2(\cosh x\, dx)$. Of course, there is nothing special about our choice of $L^2(\cosh x\, dx)$ beyond the fact that functions in this space must fall off sufficiently rapidly.

Given Corollary D.4, we can express the transform $\hat{f}$ of a function $f \in L^2(\cosh x\, dx)$ in an eigenfunction expansion:

$$\hat{f}(k) = \sum_{n=0}^{\infty} d_n \hat{\mathcal{J}}_n(k) \tag{D24}$$

However, in order to do computations in Section 5, it is necessary for us to express $\hat{f}(k)$ in a Taylor expansion about $k = 0$:

$$\hat{f}(k) = \sum_{n=0}^{\infty} c_n k^n \tag{D25}$$

The following lemma shows that the coefficients d_n of the eigenfunction expansion (D24) can be deduced from the coefficients c_n of the Taylor

expansion (D25) and the Taylor coefficients in the expansion of the (analytic) functions $\hat{\mathscr{J}}_n(k)$.

Lemma D.5. Let $f \in L^2(\cosh x \, dx)$. Suppose that f has the eigenfunction expansion (D24) and the Taylor expansion (D25). Then c_n is uniquely determined by the $\{d_m \mid m \leqslant n\}$ and the Taylor coefficients in the low-momentum expansions of the analytic functions $\{\hat{\mathscr{J}}_m(k) \mid m \leqslant n\}$.

Remark. This lemma shows that, as one would expect, the c_n can be derived simply by equating coefficients of k^n in the term-by-term expansions.

Proof. Here we will use $\|\cdot\|_p$ to denote the $L^p(dx)$ norm, $\|\cdot\|_{P(\mathrm{ch})}$ to denote the $L^p(\cosh x \, dx)$ norm, and $\|\cdot\|_{P(1/\mathrm{ch})}$ to denote the $L^p((1/\cosh x) \, dx)$ norm. We first claim that if $g_n \in L^2(\cosh x \, dx)$ is a general sequence of functions with $\|g_n\|_{2(\mathrm{ch})} \to 0$, then the Fourier transforms $\hat{g}_n(k) \to 0$ uniformly in k. To show this, we begin by noting that

$$\sup_k \hat{g}(k) \leqslant \frac{1}{(2\pi)^{1/2}} \|g\|_1 \tag{D26}$$

which follows simply from the definition of Fourier transform. Next, we note that

$$\|g(x)\|_{2(\mathrm{ch})} = \|g(x) \cosh x\|_{2(1/\mathrm{ch})} \tag{D27}$$

Furthermore, convergence in $L^2((1/\cosh x) \, dx)$ implies convergence in $L^1((1/\cosh x) \, dx)$, since $dx/\cosh x$ is a finite measure.

Now suppose $\|g_n\|_{2(\mathrm{ch})} \to 0$. Then, using the properties noted above, we have

$$0 = \lim_{n \to \infty} \|g_n(x)\|_{2(\mathrm{ch})} = \lim_{n \to \infty} \|g_n(x) \cosh x\|_{2(1/\mathrm{ch})}$$

$$\Rightarrow 0 = \lim_{n \to \infty} \|g_n(x) \cosh x\|_{1(1/\mathrm{ch})} = \lim_{n \to \infty} \|g_n(x)\|_1 \tag{D28}$$

This, together with (D26), shows that

$$\lim_{n \to \infty} \sup_k \hat{g}_n(k) = 0 \tag{D29}$$

as claimed.

Now suppose $f \in L^2(\cosh x \, dx)$ has the eigenfunction expansion (D24). Defining the partial sums

$$\hat{f}_N(k) = \sum_{n=0}^{N} d_n \hat{\mathscr{J}}_n(k) \tag{D30}$$

it is clear that $\lim_{N \to \infty} \|f_N\|_{2(\text{ch})} \to 0$. Then, applying the uniform convergence (D29) established above, it is clear that we may use the Taylor expansions of the $\hat{\mathscr{J}}_n(k)$ about $k = 0$, as well as (D25), and equate coefficients term by term to get the coefficients d_n. ∎

ACKNOWLEDGMENTS

REFERENCES

1. J. M. Carlson, J. T. Chayes, J. P. Sethna, and D. J. Thouless, *J. Stat. Phys.*, this issue.
2. J. T. Chayes, L. Chayes, J. P. Sethna, and D. J. Thouless, *Commun. Math. Phys.* **106**:41 (1986).
3. K. Binder and A. P. Young, *Rev. Mod. Phys.* **58**:801 (1986).
4. S. F. Edwards and P. W. Anderson, *J. Phys. F* **5**:965 (1975).
5. D. Sherrington and S. Kirkpatrick, *Phys. Rev. Lett.* **35**:1792 (1975).
6. J. R. L. de Almeida and D. J. Thouless, *J. Phys. A* **11**:983 (1978).
7. G. Parisi, *Phys. Rev. Lett.* **43**:1754 (1979).
8. F. Matsubara and M. Sakata, *Prog. Theor. Phys.* **55**:672 (1976); S. Katsura, S. Fujiki, and S. Inawashiro, *J. Phys. C* **12**:2839 (1979); S. Katsura, *Physica* **104A**:333 (1980); S. Fujiki, Y. Abe, and S. Katsura, *Comput. Phys. Comun.* **25**:119 (1982).
9. Y. Ueno and T. Oguchi, *J. Phys. Soc. Japan* **40**:1513 (1976); T. Oguchi and Y. Ueno, *J. Phys. Soc. Japan* **41**:1123 (1976); T. Oguchi and Y. Ueno, *Prog. Theor. Phys.* **57**:683 (1977); T. Oguchi and T. Takano, *J. Mag. Mag. Mat.* **31–34**:1301 (1983).
10. D. R. Bowman and K. Levin, *Phys. Rev. B* **25**:3438 (1982).
11. D. J. Thouless, *Phys. Rev. Lett.* **56**:1082 (1986).
12. J. M. Carlson, J. T. Chayes, L. Chayes, J. P. Sethna, and D. J. Thouless, *Europhys. Lett.* **5**:355 (1988).
13. C. Kwon and D. J. Thouless, *Phys. Rev. B* **37**:7649 (1988).
14. H. Maletta and P. Convert, *Phys. Rev. Lett.* **42**:108 (1979).
15. H. Maletta and W. Felsch, *Z. Phys. B* **37**:55 (1980).
16. K. Westerholt and H. Bach, *J. Phys. F* **12**:1227 (1982).
17. H. Yoshizawa, S. Mitsuda, H. Aruga, and A. Ito, *Phys. Rev. Lett.* **59**:2364 (1987).
18. R. Hoogerbeets, W. L. Luo, and R. Orbach, N. Bontemps, and H. Maletta, *J. Mag. Mag. Mat.* **54/7**:177 (1986).
19. P. Monod and H. Bouchiat, *J. Phys. Lett.* (Paris) **43**:L-45 (1982).
20. H. Bouchiat, *J. Phys.* (Paris) **47**:71 (1986).

21. J. M. Carlson, Ph.D. Thesis, Cornell University (1988).
22. C. M. Fortuin, P. W. Kasteleyn, and J. Ginibre, *Commun. Math. Phys.* **22**:89 (1981).
23. M. S. Berger, Nonlinearity and functional analysis, in *Lectures on Nonlinear Problems in Mathematical Analysis* (Academic Press, New York, 1977), Chapter 4.1.
24. M. Reed and B. Simon, *Methods of Mathematical Physics*, Vol. II (Academic Press, New York, 1975), pp. 145, 205.
25. H. Nishimori, Rigorous results on random spin systems with competing interactions, Thesis, Department of Physics, University of Tokyo (1981).
26. P. Le Doussal and A. Georges, Yale University Report YCTP-P1-88 (1988).
27. P. Le Doussal and A. B. Harris, *Phys. Rev. Lett.* **61**:625 (1988).